

Copyright

by

Qian Susan Chi

2000

# **Oxidative Degradation of Monoethanolamine**

by

Qian Susan Chi, B.S.

Thesis

Presented to the Faculty of the Graduate School

of The University of Texas at Austin

in Partial Fulfillment

of the Requirements

for the Degree of

**Master of Science in Engineering**

The University of Texas at Austin

December, 2000

## **Oxidative Degradation of Monoethanolamine**

APPROVED BY

SUPERVISING COMMITTEE:

---

Gary T. Rochelle, Supervisor

---

R. Bruce Eldridge

To BeBe

## **Acknowledgements**

I would like to thank Dr. Rochelle for all the great ideas and unending support he has offered throughout the entire project. He has made this a rewarding experience and a proud achievement in my life.

Special thanks to Dr. Eldridge for his assistance. Thanks to my fellow research group members: Hongyi Dang, Sanjay Bishnoi, Norman Yeh, Sharmi Roy, and Eric Chen for being there for me.

Most of all, I want to thank the person who made all this possible, Nicholas Nguyen. Without his unconditional love and support, I would have given up. Thanks for constantly pushing me to be the strongest person who never admits defeat. He has taught me everything I know, and everything I am is because of him.

Lastly, I would like to thank God for the destiny he has chosen for me. He directs me through this world. I am lucky to have him by my side every step of the way.

I dedicate this work to my best friend Danny Lee who passed away in January 2000. I hope I made you proud.

December 8, 2000

# **Oxidative Degradation of Monoethanolamine**

by

Susan Chi, M.S.E.

The University of Texas at Austin, 2000

SUPERVISOR: Gary T. Rochelle

Aqueous monoethanolamine (MEA) is used to remove CO<sub>2</sub> from flue gas. MEA degrades in service in the presence of oxygen and CO<sub>2</sub> resulting in extensive amine loss and equipment corrosion as well as generating environmental impacts.

Oxidative degradation of MEA was studied under typical absorber conditions 55°C. The rate of evolution of a degradation product NH<sub>3</sub>, which was indicative of the overall rate of degradation, was measured continuously in a batch MEA solvent system. The effects of CO<sub>2</sub> loading, iron concentration, and MEA concentration on the rate of NH<sub>3</sub> production were quantified. Several additives were studied; these include possible inhibitors such as ethylenediaminetetraacetic acid (EDTA), N,N-Bis (2-hydroxyethyl) glycine or bicine, and tertiary amines like N,N-diethylethanolamine as well as possible catalysts such as KMnO<sub>4</sub>, formaldehyde, and H<sub>2</sub>O<sub>2</sub>.

Iron ranging in concentration from 0.0001 mM to 1 mM yields oxidation rates ranging from 0.37 to 2 mM/hr in CO<sub>2</sub> loaded MEA solutions in the presence of oxygen. The rates can be correlated with the total iron (Fe<sup>+2</sup> and Fe<sup>+3</sup>) concentration in solution. Additives such as EDTA and bicine effectively decrease the rate of oxidation in CO<sub>2</sub> loaded MEA in the presence of iron by 40 to 50%.

Ferrous ion caused oxidation in unloaded MEA with stoichiometry ranging from 0.1 to 0.33. Ferrous concentration from 0.0001 to 3.2 mM yields rates from 0.12 to 1.1 mM/hr. These rates can also be correlated to the total ferrous concentration in solution. Ferric iron did not appear to catalyze oxidation in unloaded MEA.

The oxidation rate was three times faster in CO<sub>2</sub> loaded MEA than in unloaded MEA with no additional iron. The same concentration of iron can catalyze oxidation in 0.4 CO<sub>2</sub> loading MEA 6 to 8 times faster than in unloaded MEA.

Oxidation rate increased a factor of two over the MEA concentration of 2.5 to 12 m.

## Table of Contents

List of Tables .....	xi
List of Figures .....	xii
Chapter One: Introduction .....	1
1.1 Acid Gas Treating .....	1
1.2 Process Flow Diagram .....	1
1.3 Alkanolamines .....	3
1.4 Degradation .....	4
1.5 Scope of this Work .....	5
Chapter Two: Expected Mechanisms and Results .....	6
2.1 Mechanism .....	6
2.1.1 Amine Oxidation Mechanism and Products .....	6
2.1.2 Aldehydes .....	7
2.1.3 Metal Ions .....	9
2.1.4 Role of Ferrous Ion .....	10
2.1.5 Role of Copper .....	12
2.1.6 Autooxidation .....	12
2.1.7 Data on Reaction Rates .....	13
2.2 Navy Studies .....	16
2.2.1 Girdler Studies (1950) .....	16
2.2.2 Blachly and Ravner (1964) .....	19
2.2.3 Rooney, Dupart, and Bacon (1998) .....	21
Chapter Three: Experimental Methods and Procedures .....	25
3.1 Overall Flow Diagram .....	25
3.2 Sparged Reactor .....	26
3.3 Supporting Equipment .....	28



3.4 Source Gases.....	29
3.5 Reagent Preparation, Storage, and Disposal.....	30
3.6 Batch Mode Operation.....	31
3.7 Analytical Methods.....	33
3.7.1 Gas Phase Analysis by FT-IR Spectroscopy .....	33
3.7.2 CO <sub>2</sub> Infrared Analyzer .....	37
3.8 Data Reduction and Analysis.....	37
3.8.1 Unsteady State Model.....	37
3.8.2 Raw Data Manipulation .....	39
3.8.3 Extrapolation of Steady State Rates.....	41
3.8.4 Extrapolation of Stiochiometry.....	43
Chapter Four: Experimental Results and Discussion .....	45
4.1 Experimental Conditions .....	45
4.2 Raw Experimental Data.....	46
4.3 Rate Data.....	47
4.4 Effect of Iron.....	52
4.4.1 Rates in CO <sub>2</sub> Loaded and Acidified MEA.....	53
4.4.2. Rates in Unloaded MEA.....	54
4.4.3 Ferrous Stiochiometry in Unloaded MEA.....	55
4.5 Effect of CO <sub>2</sub> Loading .....	58
4.6 Effect of EDTA.....	60
4.7 Effect of Bicine.....	62
4.8 Effect of KMnO <sub>4</sub> .....	63
4.9 Other Additives.....	64
4.10 Effect of MEA Concentration.....	66
4.11 Comparison with Other Studies.....	66
Chapter Five: Conclusions and Recommendations .....	69

5.1 Conclusions.....	69
5.1.1 Effect of CO <sub>2</sub> Loading .....	69
5.1.2 Iron in Loaded MEA.....	69
5.1.3 Iron in Unloaded MEA .....	70
5.1.4 Oxidants Other than Oxygen .....	70
5.1.5 Oxidation Inhibitors.....	71
5.2 Application to Acid Gas Treating.....	71
5.3 Recommendations.....	71
Appendix A: Analytical Methods & Equipment Operating Procedures.....	73
Appendix B: Experimental Data.....	81
Reference Cited.....	102
Vita.....	106

## List of Tables

Table 2-1	Second Order Rate Constants for Free Radical Reactions .....	13
Table 2-2	Accelerated Oxidation Rates of Amines (Girdler,1950) .....	17
Table 3-1	Gas Cylinders Used for Experimental Data Collection.....	29
Table 3-2	Calibration Data for Mass Flow Meters and Controller.....	30
Table 3-3	Assays for LCI MEA.....	31
Table 3-4	Reagent Specifications .....	31
Table 3-5	Multiple Steady-state Rates with 0.4 mole CO <sub>2</sub> /mole MEA.....	42
Table 3-6	Multiple Steady-state Rates in Unloaded MEA .....	43
Table 3-7	Ferrous Stoichiometry with Unloaded MEA.....	44
Table 4-1	Experimental Conditions .....	45
Table 4-2	Experiments at 55°C.....	48
Table 4-3	Oxidation Studies 20 wt % MEA with 0.25 mole CO <sub>2</sub> /mole MEA....	60
Table 4-4	Effect of EDTA in Unloaded 5 m MEA with No Additional Iron.....	61
Table 4-5	Rate Comparison .....	67
Table A-1	NH <sub>3</sub> Calibration.....	77

## List of Figures

Figure 1-1	Typical Absorption/Stripping System.....	2
Figure 1-2	Structural Formulas for Commonly Used Alkanolamines.....	3
Figure 2-1	Oxidation of MEA .....	6
Figure 2-2	Reaction of Formaldehyde with Monoethanolamine.....	8
Figure 2-3	Reaction of Formaldehyde with $\text{Fe}(\text{CN})_6^{3-}$ at High pH .....	8
Figure 2-4	Reaction of Aldehyde with Peroxyacid and Oxygen .....	9
Figure 2-5	Reaction Rates of Amines with Chlorine Dioxide at 25°C.....	15
Figure 2-6	Degradation Prediction Based on Chemical Structures (Girdler,1950) .....	18
Figure 2-7	Effect of Bicine in the Presence of Metals (Blachly and Ravner, 1964) .....	21
Figure 2-8	Comparison of Total Anions Measured for Unloaded Amines (Rooney, 1998) .....	22
Figure 2-9	Comparison of Total Anion Measured for 0.25 mole $\text{CO}_2$ /mole amine (Rooney, 1998) .....	23
Figure 2-10	Oxidation of MEA (Rooney, 1998) .....	24
Figure 3-1	Experimental Flow Diagram for MEA Oxidation .....	25
Figure 3-2	Reactor Schematic Diagram.....	26
Figure 3-3	Reactor and Condenser Dimensions.....	27
Figure 3-4	Reactor Top Plate Configuration and Dimensions .....	28
Figure 3-5	FT-IR Spectrum for Ammonia.....	34
Figure 3-6	FT-IR Spectrum for 7 m MEA with 0.4 mole $\text{CO}_2$ /mole MEA.....	35
Figure 3-7	Ammonia Calibration Curve and Equation.....	36
Figure 3-8	FT-IR Raw Data.....	39
Figure 3-9	Experiment 71700 Data for Unloaded 5 m MEA .....	40

Figure 3-10 Multiple Steady States with Increasing Ferric Concentrations in 7 m MEA with 0.4 mole CO <sub>2</sub> /mole MEA .....	41
Figure 3-11 Multiple Steady States with Increasing Ferrous Concentrations in 7 m Unloaded MEA.....	42
Figure 3-12 Area of Integration for Determining Reaction Stoichiometry .....	43
Figure 4-1 Oxidation of Unloaded 5 m MEA.....	50
Figure 4-2 Injection Times for Experiment 092200: Oxidation in 7 m MEA with 0.4 mole CO <sub>2</sub> /mole MEA with Air .....	51
Figure 4-3 Steady-state Rates for Experiment 092200.....	51
Figure 4-4 Effect of Iron in 7 m MEA at 55°C.....	52
Figure 4-5 Steady-state Rates in Experiment 71700 .....	54
Figure 4-6 Rate Dependence on Total Ferrous Concentration in Unloaded MEA .....	55
Figure 4-7 Integration for Experiment 71700.....	56
Figure 4-8 Ferrous Stoichiometry in Unloaded MEA .....	57
Figure 4-9 Oxidation of 7 m MEA, 0 CO <sub>2</sub> Loading with N <sub>2</sub> .....	58
Figure 4-10 Effect of EDTA in 7 m MEA with 0.4 CO <sub>2</sub> /mole MEA.....	61
Figure 4-11 Effect of EDTA in Unloaded MEA with 1 mM Fe <sup>+3</sup> .....	62
Figure 4-12 Effect of Bicine in 7m MEA with 1 mM Fe <sup>+2/+3</sup> .....	63
Figure 4-13 Effect of KMnO <sub>4</sub> in Unloaded 5 m MEA with N <sub>2</sub> .....	64
Figure 4-14 Effect of MEA Concentration .....	66
Figure A-1 NH <sub>3</sub> Calibration Raw Data.....	76
Figure A-2 NH <sub>3</sub> Calibration Curve.....	76
Figure B-1 Experiment 62700A .....	82
Figure B-2 Experiment 62700B.....	83
Figure B-3 Experiment 70700 .....	84
Figure B-4 Experiment 71300 .....	85

Figure B-5 Experiment 71700 .....	86
Figure B-6 Experiment 71800 .....	87
Figure B-7 Experiment 72000 .....	88
Figure B-8 Experiment 72600 .....	89
Figure B-9 Experiment 81500 .....	90
Figure B-10 Experiment 81600 .....	91
Figure B-11 Experiment 90800 .....	92
Figure B-12 Experiment 90900 .....	93
Figure B-13 Experiment 91000 .....	94
Figure B-14 Experiment 91300 .....	95
Figure B-15 Experiment 91400 .....	96
Figure B-16 Experiment 91600 .....	97
Figure B-17 Experiment 92000 .....	98
Figure B-18 Experiment 92200 .....	99
Figure B-19 Experiment 100200 .....	100
Figure B-20 Experiment 100300 .....	101

## **Chapter One**

### **Introduction**

#### **1.1 Acid Gas Treating**

Acid gases, mainly  $\text{H}_2\text{S}$  and  $\text{CO}_2$ , are components in a variety of gas mixtures including natural gas, synthesis gas, flue gas, and refinery streams.  $\text{H}_2\text{S}$  needs to be completely removed from gas streams due to its toxicity and corrosiveness in refinery operations. Carbon dioxide removal from flue gas is a necessary means of combating global warming. Carbon dioxide is also removed from natural gas because it acts as a diluent, increasing transportation costs and reducing the heating value of the gas. The process of separating acid gases from source gases is referred to as acid gas treating.

#### **1.2 Process Flow Diagram**

Various acid gas treating technologies have been studied and applied in industry. Adsorption, membrane separation, and reactive absorption are common processes for removing acid gas.

Absorption/stripping with aqueous alkanolamine solutions is the dominant technology used by gas processing industries to remove acid gases such as carbon dioxide and hydrogen sulfide. An ideal solvent should have a high capacity for absorbing acid gases through reversible chemical reaction. Increasing the temperature and/or reducing the pressure should also reverse the chemical reaction between the acid gases and the amine in order to permit regeneration of the original amine. Monoethanolamine (MEA) in water is the current solvent of choice for  $\text{CO}_2$  removal from flue gas. The basic schematic

flow diagram of an absorber/stripper system with monoethanolamine as the solvent is illustrated in Figure 1.1..

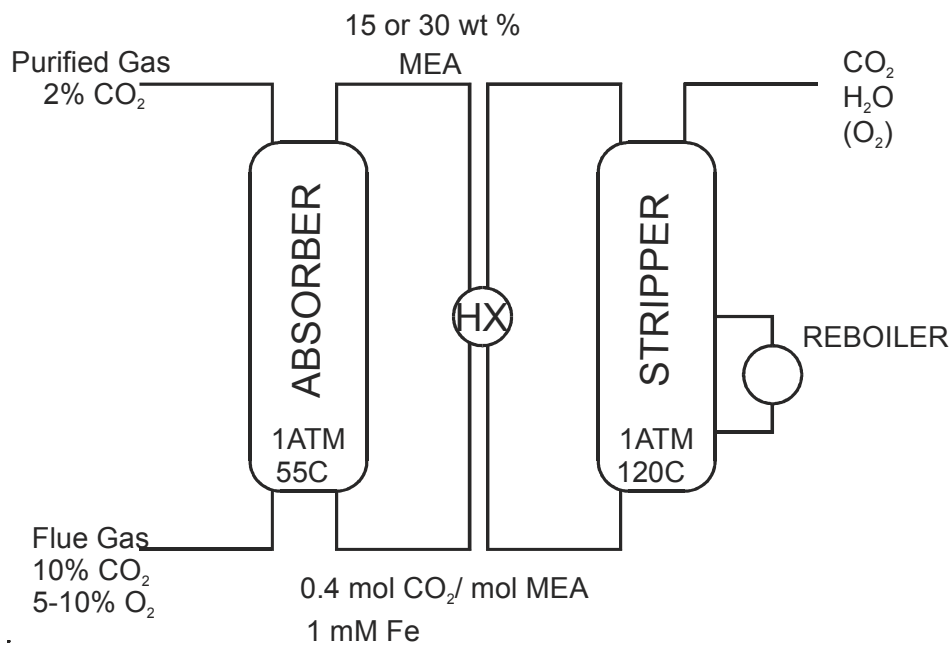


**Figure 1.1** Typical Absorption/Stripping System for the Removal of CO<sub>2</sub> by Monoethanolamine

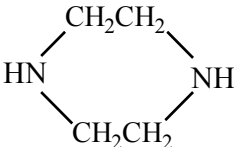
In a typical absorber / stripper system, a flue gas stream with 10% CO<sub>2</sub>, and 5% - 10% O<sub>2</sub> enters the bottom of the absorber operating at 55 °C and 1 atmosphere and is countercurrently contacted with 15 to 30 wt % lean MEA. The MEA solution selectively absorbs the CO<sub>2</sub> from the flue gas. The rich MEA with about 0.4 mole CO<sub>2</sub>/mole amine leaves the bottom of the absorber while the purified gas containing only 0.5 - 2% CO<sub>2</sub> exits at the top. The rich MEA is pumped through a cross heat exchanger where its temperature is raised. It is then introduced into the top of the stripper, where it countercurrently contacts steam at 120 °C and 1 atmosphere. The steam, produced in a reboiler, provides the necessary energy to reverse the reaction of the amine with CO<sub>2</sub> and strips the acid gas from the amine solution. After the CO<sub>2</sub>, H<sub>2</sub>O and O<sub>2</sub> are stripped, the lean



MEA is cooled down in the heat exchanger before recycling back to the absorber. Both trayed and packed towers can be used for gas treating.

### 1.3 Alkanolamines

Aqueous solutions of alkanolamine are used in absorption/stripping systems to remove acid gases from flue gas. The commonly used alkanolamines are monoethanolamine, diethanolamine, triethanolamine, diglycolamine® (B,B'-hydroxyaminoethyl ether), methyldiethanolamine, and piperazine (Figure 1.2)

Monoethanolamine (MEA)	Diglycolamine® (DGA®)
$\text{H}_2\text{NCH}_2\text{CH}_2\text{OH}$	$\text{H}_2\text{NCH}_2\text{CH}_2\text{OCH}_2\text{CH}_2\text{OH}$
Diethanolamine (DEA)	Methyldiethanolamine (DMEA)
$\text{HN}(\text{CH}_2\text{CH}_2\text{OH})_2$	$\text{CH}_3\text{N}(\text{CH}_2\text{CH}_2\text{OH})_2$
Triethanolamine (TEA)	Piperazine
$\text{N}(\text{CH}_2\text{CH}_2\text{OH})_3$	

**Figure 1.2** Structural Formulas for Commonly Used Alkanolamines

Alkanolamines are classified into three main categories: primary, secondary, and tertiary depending on the number of carbon-nitrogen bonds. For instance, MDEA is a tertiary amine whereas MEA is a primary amine.

MEA is used in the current state of the art technology for CO<sub>2</sub> removal from flue gas. MEA is inexpensive to produce and is very reactive and thus able

to effect high volume acid gas removal at a fast rate. Tertiary amines like MDEA are less reactive and therefore mostly used in the selective removal of  $\text{H}_2\text{S}$ . However, the less reactive MDEA is characterized by lower stripping energy requirement than MEA or DEA. Recently, research attention has been focused on the use of amine blends to maximize the desirable qualities of individual amines.

#### **1.4 Degradation**

Studies made over the years have shown that amines such as DEA and MEA degrade in service. Degradation is an irreversible chemical transformation of alkanolamines into undesirable compounds resulting in its diminished ability to absorb acid gases. Degradation is undesirable and leads to substantial amine loss, impaired process efficiency and throughput, and equipment fouling and corrosion. The degradation products generate environmental impacts such as gaseous pollutants and liquid wastes. The direct and indirect costs resulting from amine degradation are considerable thus mandating further studies on the chemistry, mechanisms and kinetics of amine degradation.

Degradation in a typical absorber / stripper system shown in Figure 1.1 can be divided into three types depending on its products, mechanisms, and conditions.

1. Carbamate polymerization is the most common degradation mechanism. It requires carbon dioxide and high temperature. Since only primary and secondary alkanolamines form carbamates with  $\text{CO}_2$ , tertiary amines do not undergo this type of degradation reaction. The degradation products resulting from carbamate polymerization are usually of high molecular weight. Carbamate polymerization is expected to occur at the higher temperature of the stripper.

2. Oxidative degradation requires the presence of oxygen and is catalyzed by iron. The degradation products are typically oxidized fragments of the solvent. For MEA, oxidation products include heat stable salts such as acetates, formates, and glycolates; ammonia is also produced as major degradation product. Since flue gas contains 5 to 10% O<sub>2</sub>, oxidative degradation can be significant. Neither CO<sub>2</sub> nor high temperature is required in this case. Oxidative degradation is expected to occur in the presence of dissolved O<sub>2</sub> in the liquid holdup at the bottom of the absorber. It may also occur in the absence of O<sub>2</sub> at the higher temperature of the stripper by reaction with oxidized states of dissolved metals such as Fe<sup>+3</sup>.
3. Thermal degradation is not commonly encountered since it involves temperatures higher than 205 °C; therefore, it is the least well studied.

### **1.5 Scope of this Work**

This work focuses on the oxidative degradation of monoethanolamine used in CO<sub>2</sub> capture from flue gas. The rate of NH<sub>3</sub> production, which is indicative of the overall rate of degradation, is measured in a batch system. All of the oxidation experiments were performed at 55°C, 1atm, which corresponds to typical operating conditions of the absorber. The effects of MEA, CO<sub>2</sub> loading, and dissolved iron (both Fe<sup>+2</sup> and Fe<sup>+3</sup>) on the rate of NH<sub>3</sub> production were quantified. This study also investigates the effect of additives including chelating agents, free radical inhibitors, and catalyst.

## Chapter Two

### Expected Mechanisms and Results

#### 2.1 Mechanism

##### 2.1.1 Amine Oxidation Mechanism and Products

Studies at Edgewood Arsenal have quantified the oxidation of amines by chlorine dioxide and other single electron oxidants (Rosenblatt et al., 1963, 1967a, 1968; Dennis et al., 1967, Davis et al., 1968; Hull et al., 1967, 1969a, 1969b, 1969c). A number of papers by Lindsay Smith et al. (Audeh and Lindsay Smith, 1970, Lindsay Smith and Mead, 1973, 1967) have quantified the oxidation of tertiary amines by hexacyanoferrate ( $\text{Fe}(\text{CN})_6^{-3}$ ). Since  $\text{Fe}^{+3}$  is most likely the catalyst/reactant in our system, these results with single electron oxidants are highly relevant.

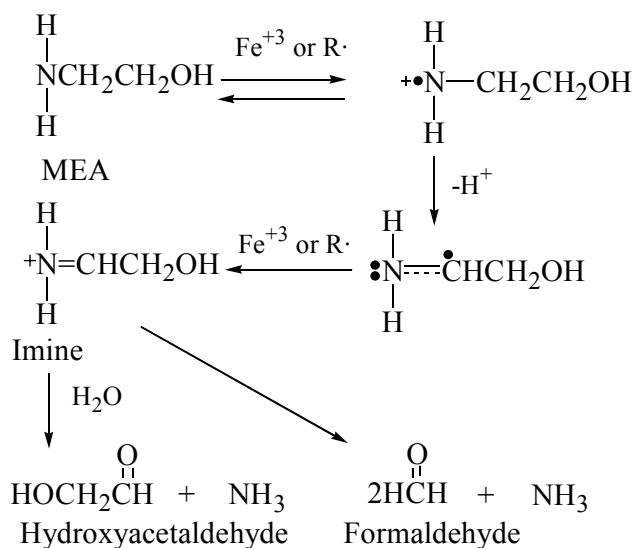


**Figure 2.1** Oxidation of MEA

The mechanism for MEA oxidation according to the general scheme proposed by these researchers is shown in Figure 2.1 (Hull et al., 1969a). A reactive free radical, such as  $\text{ClO}_2$  or  $\text{Fe}^{+3}$ , extracts an electron from the nitrogen of an unprotonated MEA molecule to form an aminium cation radical. This is usually the rate-limiting step. The cation radical loses a proton to form the imine radical where the radical is delocalized between the nitrogen and the carbon. Imine radical is attacked by another free radical or  $\text{Fe}^{+3}$  to produce an imine. Imine can either hydrolyze to form hydroxyacetaldehyde and  $\text{NH}_3$  resulting from the C-N bond cleavage, or it can form 2 moles of formaldehyde and  $\text{NH}_3$  resulting from the C-C bond cleavage. The latter mechanism is often referred to as oxidative fragmentation (Dennis et al., 1967).

Rosenblatt et al. (1968) recognized that the oxidation of some amines could also be initiated by the extraction of a proton from the  $\alpha$ -carbon giving the imine radical directly without forming the aminium cation radical. However, most of the evidence with aliphatic amines suggests that electron extraction is the dominant mechanism.

### 2.1.2 Aldehydes

Aldehydes react with water; in aqueous solution 99% of formaldehyde is hydrated (Singh et al., 1969). Aldehydes also react readily with primary amines. These reactions would not be significant with tertiary amines. In aqueous solution of monoethanolamine, formaldehyde will be present as an equilibrium mixture primarily in the form of imine with some hydrated aldehyde, carbinolamine, and aминаl (Figure 2.2). Similar reactions can occur with other aldehydes such as hydroxyacetaldehyde.

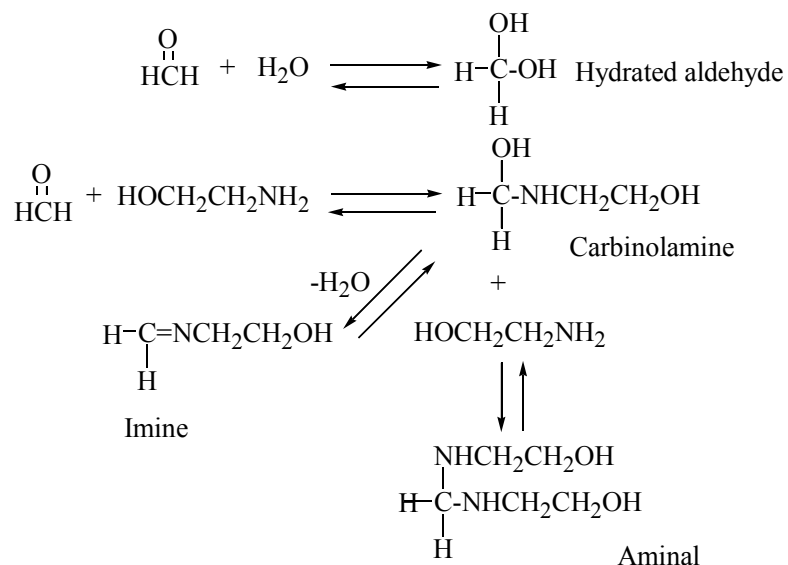


**Figure 2.2** Reaction of Formaldehyde with Monoethanolamine

At high pH formaldehyde is oxidized by  $\text{Fe}(\text{CN})_6^{3-}$  (Singh et al., 1969) and probably by other similar single electron oxidants. The reaction requires hydroxide to get the ionized hydrated formaldehyde, which is then attacked by  $\text{Fe}^{+3}$ . The resulting radical loses a proton to another  $\text{Fe}^{+3}$  and the oxidation results in formate ion.

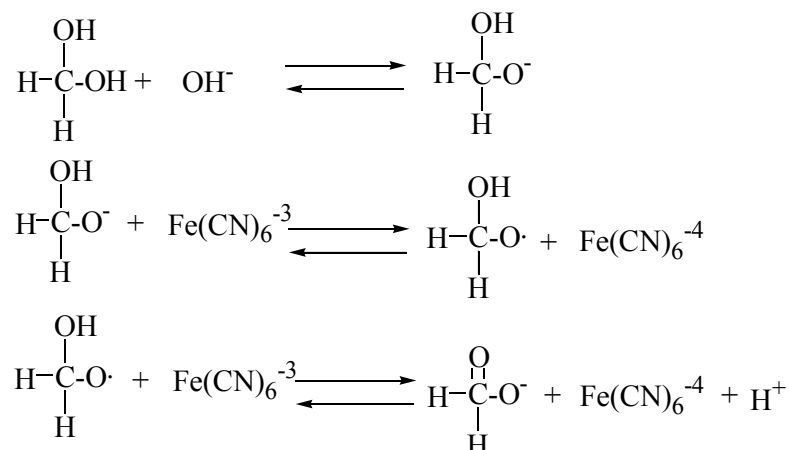


**Figure 2.3** Reaction of Formaldehyde with  $\text{Fe}(\text{CN})_6^{3-}$  at High pH

The imine formed from primary or secondary amines such as MEA may be subject to similar attack by radical oxidants. The presence of formaldehyde may also facilitate the oxidation of the amine molecule.

Other less easily hydrated aldehydes, such as acetaldehyde and hydroxyacetaldehyde, react at room temperature with oxygen to produce the corresponding organic acid (Denisov et al., 1977; Sajus and Seree De Roch, 1980). The oxidation usually takes place by a free radical chain mechanism. An initiator extracts a H from the  $\alpha$  carbon to produce a free radical. The radical reacts with  $O_2$  to produce a peroxyacid radical. The peroxyacid radical reacts with aldehyde to propagate the reaction with the production of the aldehyde radical and a peroxyacid. The reaction terminates with the reaction of two free radicals to produce molecules. The reaction may be accelerated by the decomposition of the peroxyacid to produce two free radicals. Such a decomposition could be catalyzed by  $Fe^{+2}$ .

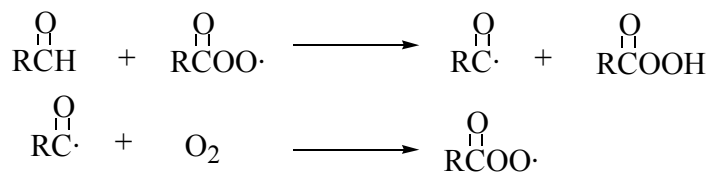


**Figure 2.4** Reaction of Aldehyde with Peroxyacid and Oxygen

Ultimately the degradation products determined in studies of commercial solutions have included no aldehyde or ketones, most likely because they readily oxidize to formic acid, glycolic acid, and oxalic acid.

### 2.1.3 Metal Ions

Because of corrosion, dissolved iron is usually present at high levels. Other possible metal catalysts include  $Mn^{+2}/Mn^{+4}$  and components of stainless

steel such as Cr, Ni, and Mo. Vanadium ( $V^{+3}$ ) can also be introduced with ash for oil combustion.  $Cu^{+2}$  is a patented corrosion inhibitor that may be added to these systems (Pearce et al., 1984, Faucher, 1989, Wolcott et al., 1986). Ferris et al. (1968) showed that  $Cu^{+2}$  and  $V^{+3}$  have catalytic properties similar to  $Fe^{+2}$ .

#### 2.1.4 Role of Ferrous Ion

Dissolved iron is the most probable catalyst. It will be a corrosion product in systems constructed of carbon steel. It can be present in fresh alkanolamine and make up water. It can leach from residual fly ash that may enter the system. In many systems it may be present at its solubility limit. With degradation products that chelate iron, as much as 160 ppm of dissolved iron has been observed in amine systems (Hall and Barron, 1981). The Girdler studies (Kindrick et al. 1950a) measured 25 to 60 ppm of dissolved iron in routine amine solutions in contact with carbon steel coupons.

Ulrich (1983) found that as little as 1 ppm of iron was effective in catalyzing oxidation of sulfite at pH 6. He observed that the catalytic effect was more pronounced at greater pH. Lee and Rochelle (1988) suggested that  $Fe^{+2}$  reacts with the "peroxide", peroxymonosulfate ( $SO_5^-$ ), to produce two free radicals as the initiating step of oxidation.

It is probable that any organic peroxides produced by alkanolamine oxidation would be decomposed by  $Fe^{+2}$  to produce free radicals in this branching reaction, which would then catalyze further oxidation (Russell, 1960):



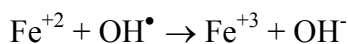
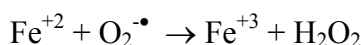
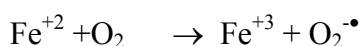
The  $Fe^{+2}$  is regenerated without losing any free radicals by another parallel reaction with the peroxide:





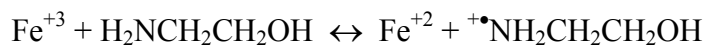
The two organic free radicals produced by this sequence can initiate another series of oxidation reactions. This reaction is analogous to that occurring with Fenton's reagent ( $\text{H}_2\text{O}_2$ ,  $\text{Fe}^{+2}$ ).

The direct reaction of  $\text{Fe}^{+2}$  with  $\text{O}_2$  may be an important source of free radicals ( $\text{Fe}^{+3}$ ) and a way of getting  $\text{O}_2$  into the oxidation mechanism. In water  $\text{Fe}^{+2}$  appears to react with  $\text{O}_2$  with intermediates such as hydroperoxy radical ( $\text{HOO}^\bullet$ ), oxygen radical ( $\text{O}_2^\bullet$ ) and hydrogen peroxide (Stumm and Lee, 1961).



At pH 6 - 7.5 the rate of oxidation is second order in hydroxide ion concentration and first order in  $\text{Fe}^{+2}$  and oxygen. Anions such as sulfate (Tamura et al., 1976) and chelating agents such as EDTA (ethylenediamine tetraacetic acid) and NTA (nitrilotriacetic acid) do not appear to modify the oxidation significantly (Sada et al., 1987). In a working solution, the free radicals  $\text{O}_2^\bullet$  and  $\text{OH}^\bullet$  and  $\text{H}_2\text{O}_2$  could react directly with the amine.

The  $\text{Fe}^{+3} / \text{Fe}^{+2}$  couple reacts reversibly with amines/aminium radicals (Ferris et al., 1967, 1968). Figure 2.1 shows the reaction with MEA.



MEA

Aminium radical

$\text{Fe}^{+3}$  also reacts directly with the aminium radical to make the corresponding imine:



Imine

In the case of tertiary amines, rapid hydrolysis of the imine to aldehyde and secondary amine would mean that there is never the possibility of an  $\alpha$  H prone to free radical or oxygen attack. The net effect of oxidation of a tertiary amine is simply the production of one mole of aldehyde and a secondary amine with the consumption of two moles of  $\text{Fe}^{+3}$ . In contrast, the oxidation of a secondary or primary amine gives more stable imines or enamines that are subject to oxidation at  $\alpha$  H's.

#### **2.1.5 Role of Copper**

Several patents assigned to Dow Chemical address the use of cupric salts as corrosion inhibitors in alkanolamine system, especially in the presence of  $\text{O}_2$  (Wolcott et al., 1968; Pearce et al., 1984; Pearce, 1984; Cringle et al., 1987). Ferris et al. (1968) showed that  $\text{Cu}^{+2}$  and  $\text{V}^{+3}$  have catalytic properties similar to  $\text{Fe}^{+2}$ .

#### **2.1.6 Autooxidation**

Oxygen may enter the reaction as peroxides. Most autooxidations show reactions of  $\text{O}_2$  with a free radical on a carbon. A possible route for oxidation is the extraction of H or loss of  $\text{H}^+$  on a  $\alpha$  (next to nitrogen) or  $\beta$  carbon. Molecular oxygen reacts with the carbon-centered radical to make a peroxy radical. The peroxy radical could react with  $\text{Fe}^{+2}$  or  $\text{Fe}^{+3}$  to produce additional radicals in a branching reaction. Such a mechanism would not be applicable if the carbon adjacent to the nitrogen or  $\alpha$  carbon were tertiary.

## 2.1.7 Data on Reaction Rates

A number of fundamental studies of free radical reaction kinetics have been compiled (Neta et al., 1988; Anbar and Neta, 1967; Howard and Scaiano, 1984; Asmus and Bonifacic, 1984). Rate constants for reactions of several radicals with a number of amines and other substrates are summarized in Table 2.1. The sulfate radical can be present in our systems with S(IV). It might also be representative of other highly reactive radicals such as  $\text{OH}^\bullet$ . The carbonate radical is less reactive and could be a dominant radical in a loaded system. Bicarbonate reacts with sulfate radical at a rate that is comparable to the alcohols.

**Table 2.1** Second Order Rate Constants ( $\text{L mol}^{-1} \text{s}^{-1}$ ) for Free Radical Reactions, Neta et al (1988), Anbar and Neta (1967), Howard and Scaiano (1984), Asmus and Bonifacic (1984)

Radical	$\text{CO}_3^{\bullet-}$	$\text{SO}_4^\bullet$	$(\text{CH}_3)_3\text{COO}^\bullet$	$(\text{CH}_3)_3\text{CO}^\bullet$	$\text{ClO}_2^\bullet$	$\text{OH}^\bullet$
<i>Inorganic</i>						
$\text{CO}_3^=$						2e8
$\text{HCO}_3^=$		9.1e6				1e7
$\text{Fe}^{+2}$		9.9e8				2.5e8
$\text{Fe}(\text{CN})_6^{-4}$					7.4e7	8.1e9
$\text{Mn}^{+2}$	1.5e7	2.0e7				8.6e9
$\text{NH}_3$		1.4e7				
$\text{NH}_4^+$		3e5				
$\text{SO}_3^=$	1.3e7	2e9			7.8e5	3.0e9
$\text{S}_2\text{O}_3^=$		1e9				
<i>Primary Alcohols</i>						
Methanol	5e3	3.2e6		1.3e5		6.1e8
Ethanol	1.5e4	1.6e7		1.1e6		1.1e9
1-propanol	1.9e4	5.8e7				1.1e9
<i>Secondary Alcohols</i>						
2-methyl-2-propanol	<2e2	4e5				2.1e9
2-propanol	5e4	3.2e7	9e-3	1.8e6		1.3e9
<i>Primary Amines</i>						
Methylamine, high pH						1.4e9
Isopropylamine	5e5					
Isobutylamine	4e5					
N-propylamine				1.7e7		
Butylamine	4e5					
Tert-butylamine	5.4e4			3.3e6		

Radical	CO <sub>3</sub> <sup>•-</sup>	SO <sub>4</sub> <sup>•-</sup>	(CH <sub>3</sub> ) <sub>3</sub> COO <sup>•</sup>	(CH <sub>3</sub> ) <sub>3</sub> CO <sup>•</sup>	ClO <sub>2</sub> <sup>•</sup>	OH <sup>•</sup>
Cyclohexylamine	7.2e5					
Ethylenediamine					2e-1	3.5e7
Monoethanolamine					1.4e-2	
<i>Secondary Amines</i>						
Dipropylamine	4.5e6					
Piperidine	3.3e6		47.5	7.9e7	2.4e3	
Dibutylamine	5e6					
Diisopropylamine					3.5e2	
Piperazine					4e3	
Diethylamine	3.8e6				1e3	
<i>Tertiary Amines</i>						
Trimethylamine				1.1e8	1e5	
Triethanolamine					1e4	
Triethylamine	6.4e6			1.8e8	2e5	
N,N-Dimethyl-tert-butylamine	3e6				2.3e5	
Triethylenediamine			0.3	2.8e7		
<i>Carboxylate Ions</i>						
Acetate	6e2	5e6				
<i>Amino Acids</i>						
Glycine		9e6				1.2e9
Alanine	<1e3	1e7			<<1e2	3.4e9
Arginine	9e4					
<i>Aldehydes/Ketones</i>						
Formaldehyde						2e9
1-propionaldehyde			61.6			
Acetone						4.3e7

With radicals where systematic data are available, tertiary amines react faster than primary amines. Hull et al. (1969) correlated the rate constants for reaction of amines and ClO<sub>2</sub> with the pK<sub>a</sub> of the amines (Figure 2.5). They found that the rate constant is inversely proportional to the K<sub>a</sub> of the amine and that the rates of tertiary/secondary/ primary amines were in the ratio of 10<sup>7</sup>/10<sup>4</sup>/1. The rate constant for MEA at 25°C was 1.4×10<sup>-2</sup> M<sup>-1</sup>s<sup>-1</sup>. For TEA the rate constant was 1×10<sup>4</sup> M<sup>-1</sup>s<sup>-1</sup>. Reactions of other radicals have confirmed that tertiary amines react much faster than primary amines.

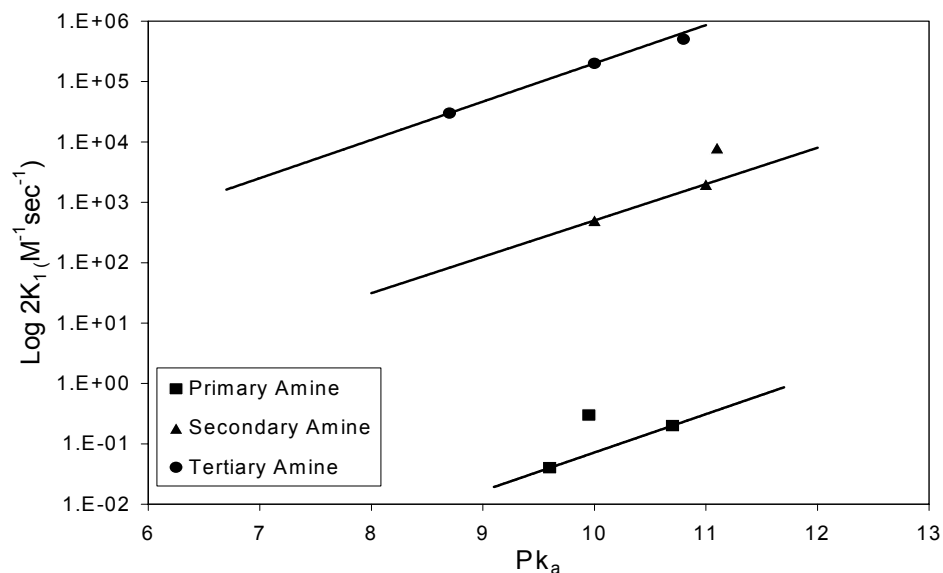


**Figure 2.5** Reaction Rates of Amines with Chlorine Dioxide at 25°C (Hull et al., 1969b)

Alkanolamines react with  $\text{Fe}^{+3}$  five to ten times faster than with the corresponding alkyl amines. Lindsay Smith et al. (1976) found that the rate of reaction of dimethylmonoethanolamine with  $\text{Fe}(\text{CN})_6^{-3}$  in 0.5 M KOH was  $0.038 \text{ M}^{-1}\text{s}^{-1}$  at 25 °C. With 1 mM  $\text{Fe}^{+3}$  and 1 M amine, this corresponds to a rate of 137 mM/hr, substantially greater than expected in commercial systems. This rate was five times faster than the corresponding dimethylmonopropanolamine. The rate for N,N-dimethyl-n-butylamine was  $0.0045 \text{ M}^{-1}\text{s}^{-1}$  (Audeh and Lindsay Smith, 1976). Therefore, in basic media the alcohol on the  $\beta$  carbon increases the rate of oxidation.

## **2.2 Navy Studies**

Oxygen is known to be present in streams such as flue gas or in CO<sub>2</sub> contaminated air in submarines. The efforts of the U.S. Navy to clean up CO<sub>2</sub> contaminated air in nuclear powered submarines drove the earliest work on oxidative degradation of alkanolamines.

### **2.2.1 Girdler Studies (1950)**

The goal of one study (Kindrick et al., 1950a) was to test the relative resistance to oxidative degradation of possible CO<sub>2</sub> absorbents that are to be used in the presence of oxygen. Thirty-nine amines and eleven mixtures of amines were tested for relative resistance to oxidation. Selected results are given in Table 2.2.

The accelerated oxidation test used in this study involved contacting a gas mixture consisting of 50% CO<sub>2</sub> and 50% O<sub>2</sub> at a rate of 100 cc/min for 166 hrs with 100 ml of 2.5 N amine solution at 80°C. These experiments were performed with 25 - 60 ppm (0.5 - 1 mM) of dissolved iron in solution. The analytical methods involve determining the free amine concentration by titration. Total organic N<sub>2</sub> was determined using the Micro Kjeldahl method. Ammonia is condensed into ammonium carbonate. The equivalents of ammonia are determined to close the N<sub>2</sub> balance.

The loss of alkalinity from primary amines (MEA and DGA) was about 5 mM/hr. Secondary amines such as DEA oxidize about twice as fast (10 mM/hr). The hindered primary amines (AMP and isobutanolamine), the tertiary amines (MDEA), the K<sup>+</sup> salt of alanine, and mixtures of MDEA with other amines (and

diethylaminopropylamine) degrade at rates less than 1 mM/hr, approaching the detection limit of the experiment.

An additional series of long-term tests were performed with 13 selected amines that showed low rates of degradation in the accelerated tests (Kindrick et al., 1950 b). The tests included isobutanolamine, AMP, MDEA, K<sup>+</sup> alanine, and diethylaminopropylamine. The prolonged tests were conducted with 100 ml of 2.5 N amine using 100 cc/min of 5% CO<sub>2</sub> in air at 30°C for forty days. The solutions were analyzed before and after the tests. Dissolved iron was present at 0.5 to 1 mM concentrations throughout all the tests. The maximum rate of degradation was 0.13 mM/hr by alkalinity loss (diethylaminoethanol), 0.07 mM/hr by total organic nitrogen (triethanolamine), and 0.04 mM/hr NH<sub>3</sub> evolution (K<sup>+</sup> alanine).

**Table 2.2** Accelerated Oxidation Rates of Amines, 80°C, 0.5 atm O<sub>2</sub>, 0.5 atm CO<sub>2</sub>, 2.5 N amine, 25-60 ppm Fe , Girdler 1950

Amine	Loss of titratable alkalinity (mM/hr)	Loss of organic nitrogen (mM/hr)	NH <sub>3</sub> production (mM/hr)
Monoethanolamine (MEA)	7	1.7	0.4
Diglycolamine (DGA)	5	1.5	0.7
2-amino-2-methyl-propanol(AMP)	0.6	0.7	1.0
Isobutanolamine	0.2	0	0.2
Diethanolamine (DEA)	9.3	2.4	1.0
Methyldiethanolamine (MDEA)	0.2	0.1	0
50%DEA/50%MDEA	0.9	0	0
50%MEA/50%MDEA	0.5	0.5	0
50%DGA/50%MDEA	0.2	0	0
75%DGA/25%MDEA	0.2		0
a-alanine, K <sup>+</sup> salt	0	0	0.2
Diethylaminopropylamine	0.1	0	0.1

From the primary alkanolamines tested in this study, three conclusions can be drawn about the nature of the chemical structure and the likelihood of oxidation. First, the rate of oxidation of an alkanolamine depends on the type of hydroxyl group present. Primary alcohol groups oxidize more readily than secondary alcohol groups which oxidize much more readily than tertiary alcohol groups. Tertiary alcohols are especially resistant to oxidation. Second, the rate of oxidation depends on the type of  $\alpha$  carbon adjacent to the amino group. Amines with primary and secondary  $\alpha$  carbons have hydrogen(s) that can be abstracted by free radicals; therefore, they exhibit higher oxidation rates than amines with a tertiary  $\alpha$  carbon. Lastly, amines with primary alcohol groups oxidize more readily than amines with primary  $\alpha$  carbons.

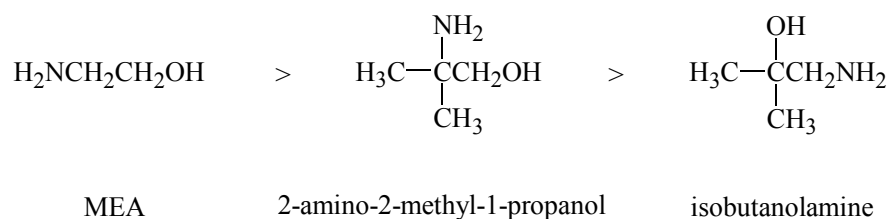


**Figure 2.6** Degradation Prediction Based on Chemical Structures (Girdler, 1950)

These three predictions can be seen from the analysis of the three alkanolamines in Figure 11. It is experimentally determined that MEA oxidizes the most, followed by 2-amino-2-methyl-1-propanol, followed by isobutanolamine. All three amines are primary amines, meaning that their amino group has only carbon substitution. MEA has a primary alcohol group and a primary  $\alpha$  carbon (the carbon adjacent to the amino group only has one carbon substitution). The second amine, 2-amino-2-methyl-1-propanol, has a primary alcohol group and a tertiary  $\alpha$  carbon. And lastly, isobutanolamine has a tertiary alcohol group and a primary  $\alpha$  carbon. Comparison of MEA with isobutanolamine verifies the



conclusion that primary alcohol groups oxidize more than tertiary alcohol groups. Comparison of the first two amines verifies the conclusion that tertiary  $\alpha$  carbon oxidizes less readily than primary  $\alpha$  carbon. Comparison of the last two amines verifies the conclusion that primary alcohol groups oxidize more readily than primary  $\alpha$  carbon.

The order of least resistance, as far as groups present in an alkanolamine, is as follows: 1) secondary amino groups, 2) primary alcohol groups, and (3) primary amino group attached to a primary  $\alpha$  carbon.

The failure of tertiary alkanolamines containing primary alcohol groups to undergo appreciable oxidation is unexpected and contrary to the above predictions. Therefore, it is suggested that tertiary amino groups have the unexpected property of slowing degradation of primary alcohol groups. Further experimental evidence is found in the blends of tertiary amines with primary and secondary amines. The results showed markedly reduced rates of oxidation of primary and secondary amines that are in the presence of tertiary amines.

### **2.2.2 Blachly and Ravner (1964)**

MEA is used as a regenerative absorbent in CO<sub>2</sub> scrubbers for atmosphere purification aboard nuclear-powered submarines. This study evaluates the effectiveness of additives in the stabilization of MEA solution in the presence of oxidation-catalyzing metals. Aeration oxidation experiments were performed at 55 °C with 4 M MEA. Air at a rate of 1cc. per ml of solution per minute was sparged into a 300 ml sample. All MEA used was redistilled and stored at 5 °C. Ammonia evolution was monitored by passing the effluent air through 2% boric acid solutions, which were periodically titrated with strong acid. Total nitrogen

was determined by conventional Kjeldahl analysis, and peroxide formation was measured by iodine-thiosulfate method.

The first important conclusion of this study was that in the absence of CO<sub>2</sub>, no degradation was observed. The addition of 1% CO<sub>2</sub> to the air stream simulating submarine atmospheric conditions resulted in almost instantaneous degradation characterized by the production of ammonia and peroxides. The rate of NH<sub>3</sub> evolution was 0.14 mM/hr with 100 ml of 4 N MEA solution.

With the addition of the compound, N,N-diethanolglycine or bicine at 1.5 wt %, no degradation was observed during a period of six weeks, indicating that the chelate was an efficient antioxidant.

This study tested the effect of bicine in the presence of metals, namely, chromium, nickel, iron, and copper. Bicine was found to be effective in stabilizing in the presence of Cr at 30 ppm, Fe<sup>+2</sup> and Fe<sup>+3</sup> at 30 ppm, and Ni<sup>+2</sup> at 37 ppm. However, it was not effective with Cu<sup>+2</sup> at concentrations higher than 1 ppm. With 30 ppm (0.5 mM) of ferric, the rate of NH<sub>3</sub> production was zero in bicine enhanced MEA, and with 30 ppm (0.5 mM) of ferrous, the rate was 0.04 mM/hr. See Figure 2.7.

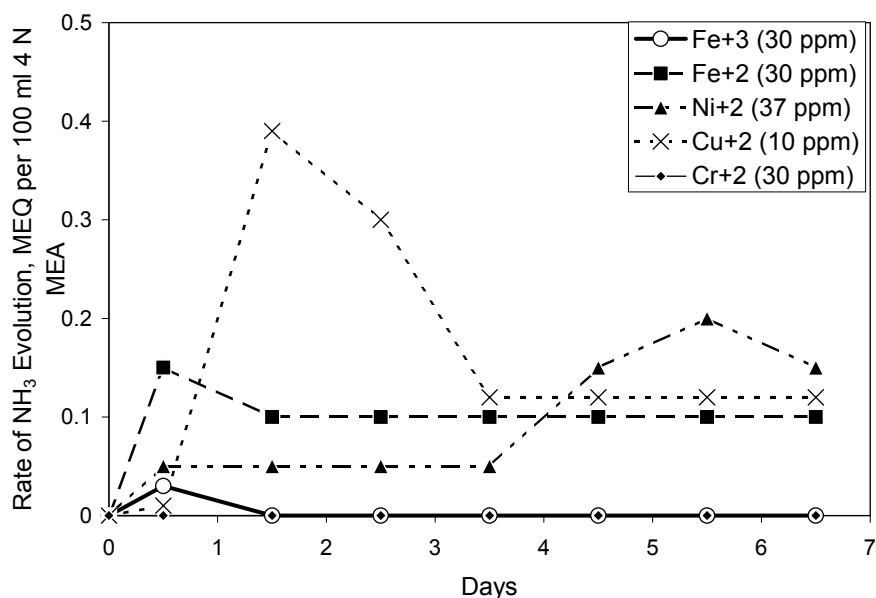


**Figure 2.7** Effect of Bicine in the Presence of Metals (Blachly and Ravner, 1964)

Oxidation with the additive ethylenediaminetetraacetate (EDTA) resulted in no  $\text{NH}_3$  production in a 1-week period with 30 ppm of  $\text{Cu}^{+2}$  present. The additive was less effective than bicine in the presence of metals other than  $\text{Cu}^{+2}$ .

The researchers hypothesized that the presence of peroxides in oxidized MEA solutions suggested that oxidation of amine was peroxide-auto-catalyzed. Both bicine and EDTA reacted with and destroyed peroxides and in turn were converted to amine oxides.

### 2.2.3 Rooney, Dupart, and Bacon (1998)

This work quantified the rate of oxidation of various alkanolamines in the presence of  $\text{O}_2$  with and without  $\text{CO}_2$  present. The degradation products used to

quantify degradation were heat stable salts such as acetates, formates, glycolates, and oxalates, which were analyzed using ion chromatography.

Oxidation experiments were performed by sparging compressed air into amine solutions with and without 0.25 mol CO<sub>2</sub>/mol amine. The solutions were agitated and kept at a temperature of 80 °C for 28 days. The amines used by Dow were not further purified and probably contain a significant amount of dissolved iron.

When the total concentrations of anions in each solution were plotted against time, oxidation resistance increased in the order: 30% DEA > 50% MDEA > 30% MDEA > 50 % DGA > 20% MEA for oxidation without CO<sub>2</sub> (Figure 2.8).

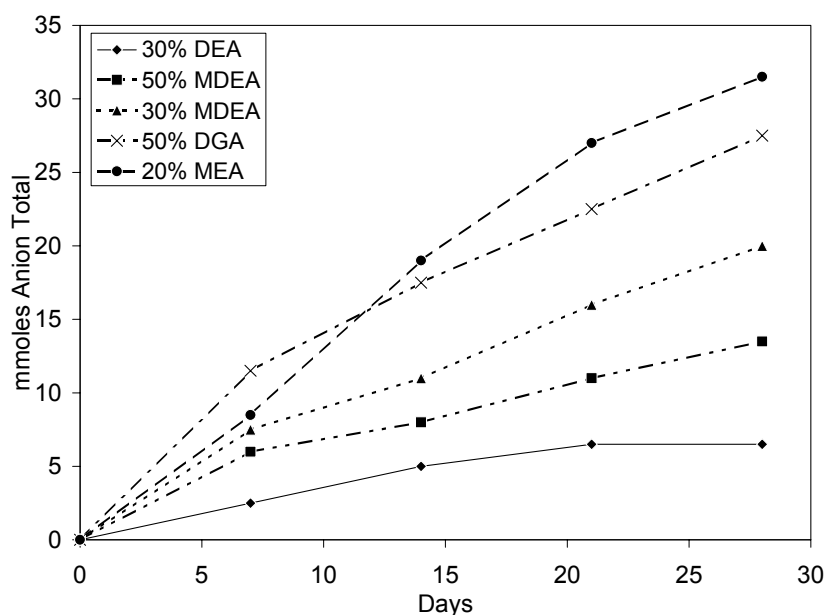


**Figure 2.8** Comparison of Total Anions Measured for Unloaded Amines (Rooney, 1998)

With CO<sub>2</sub> loading of 0.25, the oxidation resistance increased in the order: 30% DEA > 50% DGA > 20% MEA > 50% MDEA > 30% MDEA. See Figure 2.9.

The rate of anion formation in 20 wt % of unloaded MEA is 3.3 mM/hr which is three times greater than the rate of 1.1 mM/hr in 20 wt % loaded MEA. The total anions is less for all the amines they tested when CO<sub>2</sub> is present compared to when CO<sub>2</sub> is not present leading to the conclusion that CO<sub>2</sub> decreases the oxidation of amines.

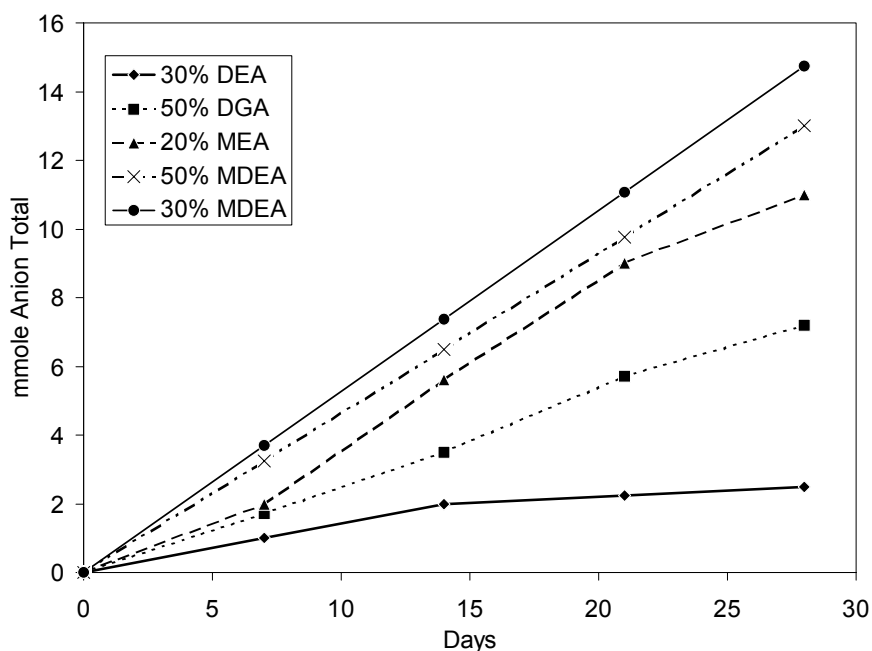


**Figure 2.9** Comparison of Total Anion Measured for 0.25 mole CO<sub>2</sub>/mole Amines (Rooney,1998)

The scheme in Figure 2.10 was proposed to account for the presence of all the anions observed in this study. This mechanism could be applied to any alkanolamine. Also, it was noted that although the acid form of acetic, formic,

glycolic, glyoxalic, and oxalic acids are shown in Figure 2.10, each of these anions are almost completely ionized to the amine heat stable salt in basic solutions.

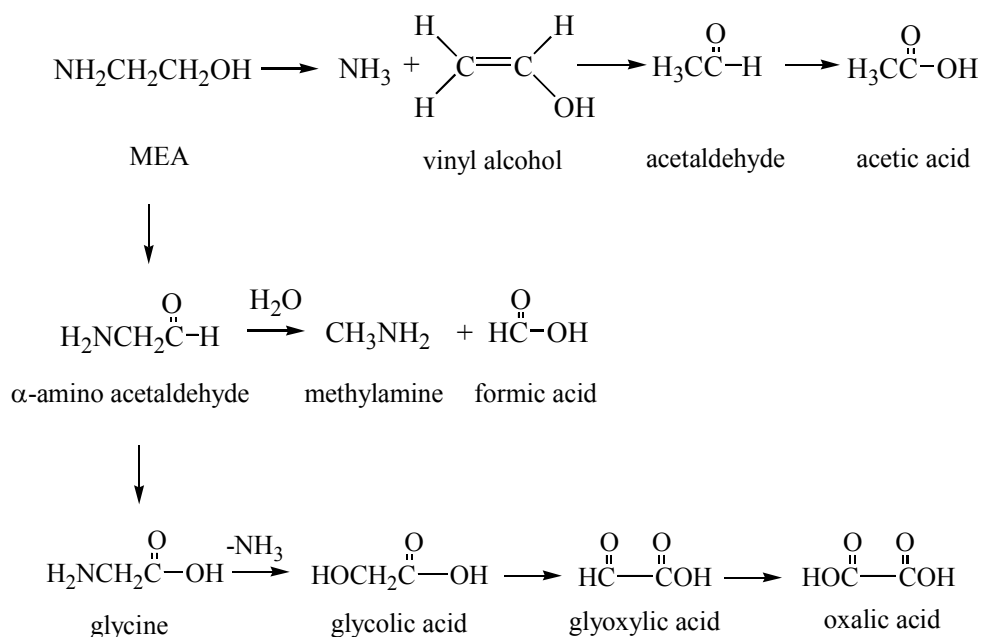


**Figure 2.10** Oxidation of MEA (Rooney, 1998)

## 2.3 Chapter Summary

This chapter reviews key mechanisms and studies involving alkanolamine degradation which are directly applicable to oxidation of monoethanolamine. Important conclusions are as follow:

- Amine oxidation is mediated by free radicals and metals
- $\text{NH}_3$  and formaldehyde are the major products of MEA oxidation
- Iron can be an important oxidation catalyst in our system

## Chapter Three

### Experimental Methods and Procedures

This chapter describes the details of the experimental setup, which includes the sparged reactor along with the supporting equipment used to control and measure experimental variables. Analytical methods for gas phase and liquid phase analysis will be presented. Finally, the chapter provides the method of data reduction.

#### 3.1 Overall Flow Diagram

Figure 3.1 shows the overall flow diagram and the experimental setup.

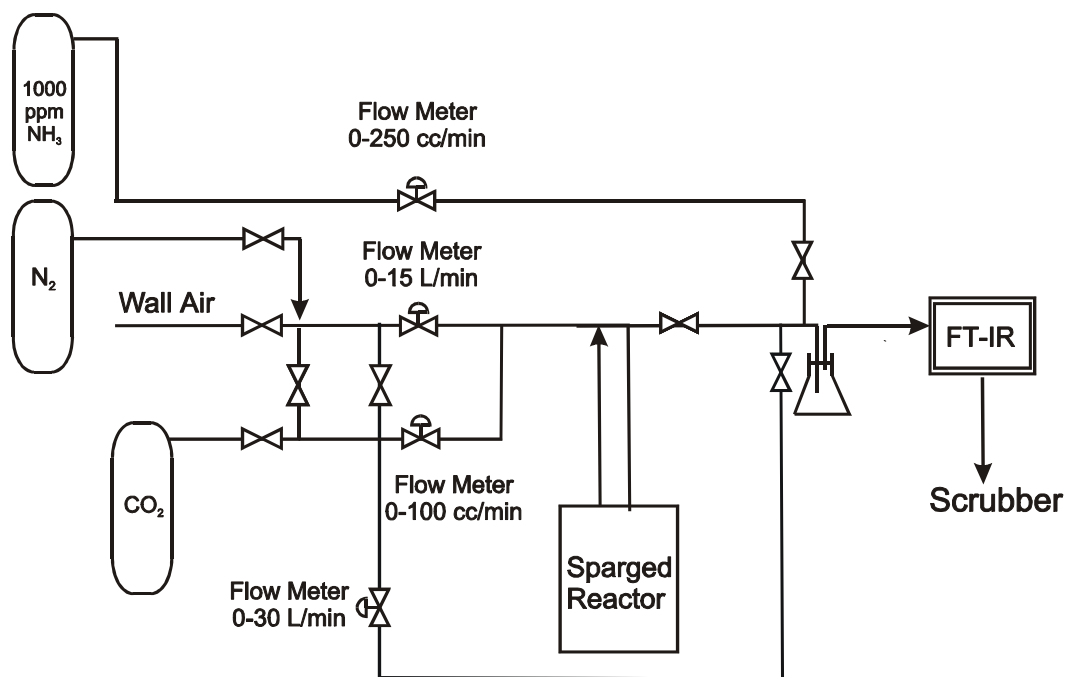


**Figure 3.1** Experimental Flow Diagram for MEA Oxidation

The flow system was capable of sparging  $\text{N}_2$ , air, air with a fixed percent  $\text{CO}_2$ , and pure  $\text{CO}_2$  into the reactor depending on the conditions of the experiment. The system operated in a batch mode for the liquid phase. The exit gas from the reactor was diluted with either air or  $\text{N}_2$  to eliminate water condensation in the tubing leading to the FT-IR analyzer. This system also allowed for convenient ammonia calibration via bypassing the reactor and delivering a known concentration of  $\text{NH}_3$  directly to the analyzer. All gases were sent to a knockout flask before reaching the FT-IR, after which they were sent to the scrubber.

### 3.2 Sparged Reactor

All experimental data were collected in the sparged reactor. Figure 3.2 shows the reactor in relation to its supporting equipment and its gas path. It is a jacketed reactor made of a smaller glass cylinder inside a larger one. The medium flowing between the inner wall of the outer larger cylinder and the outer wall of the smaller cylinder was 30% ethylene glycol / 70% water.

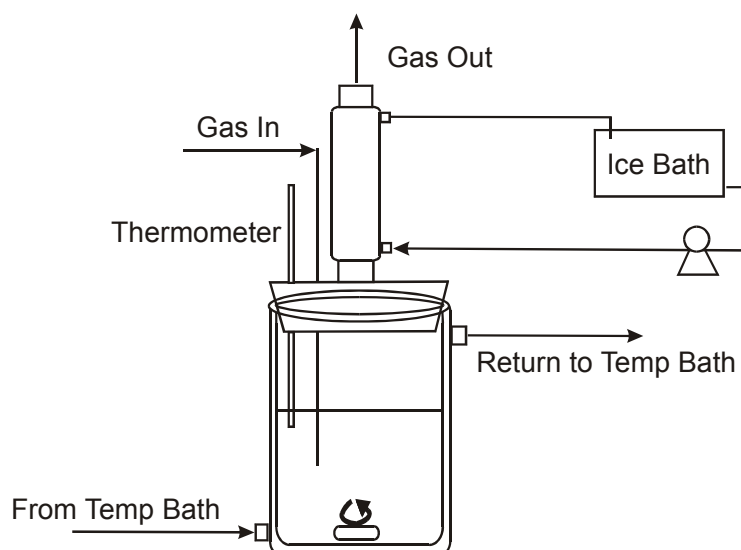


**Figure 3.2** Reactor Schematic Diagram



The schematic diagram of the reactor and its dimensions is provided in Figure 3.3. The reactor was 16.5 cm in height and had an internal diameter of 8 cm and an external diameter of 11 cm. This corresponded to an internal cross-sectional area of  $5.0 \times 10^{-3} \text{ m}^2$  ( $50 \text{ cm}^2$ ). The total volume for the reactor was  $8.29 \times 10^{-4} \text{ m}^3$  (0.829 liters), of which the maximum liquid capacity was  $7.04 \times 10^{-4} \text{ m}^3$  (0.704 liters) due to the dimensions and protrusion level of the rubber stopper.

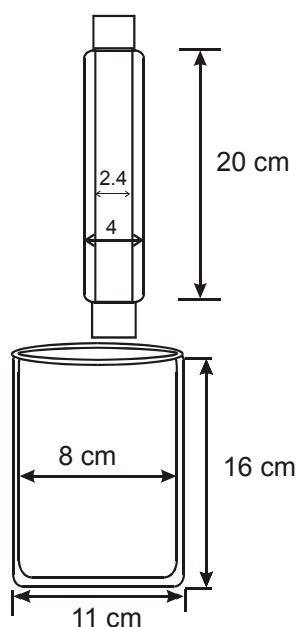


**Figure 3.3** Reactor and Condenser Dimensions

A condenser was connected to the reactor to remove water vapor in the exit gas. The dimensions of the condenser are also shown in Figure 3.3.

The condenser was connected to the reactor via a rubber stopper. The rubber stopper also had ports for inlet gas sparger, thermometer, and injection/withdrawal of samples. A schematic for the top view of the rubber stopper is shown in Figure 3.4.

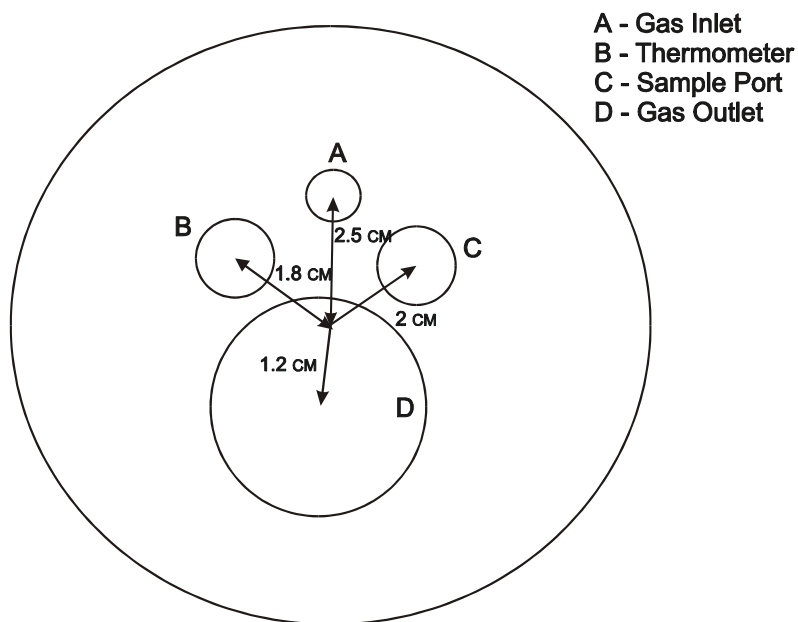


**Figure 3.4** Reactor Top Plate Configuration and Dimensions

### 3.3 Supporting Equipment

This section provides the details of other supporting equipment used for experimental data collection.

All the tubing carrying source gases (air, N<sub>2</sub>, or CO<sub>2</sub>) into the reactor were 1/4" polyethylene with the maximum operating temperature of 150 °F. The sparger used to introduce reaction gases into the reactor was 1/4" OD stainless steel, protruding the half depth of the solution. The tubing carrying exit gas to the analyzer was 1/2" OD teflon. From the analyzer, the exit gas was sent to a scrubber through Tygon 3606 tubing.

Ethylene glycol/water mixture flowed through 3/8" reinforced PVC tubing between the temperature bath/circulator (MS LAUDA®) and the jacketed reactor. Ice water was circulated between condenser and ice bath using a Cole-Parmer

MasterFlex (Model 7520-00) peristaltic pump, equipped with QuickLoad Pump Head (Model 7021-20) through 1/4" ID Tygon tubing.

Miscellaneous other equipment included a Corning magnetic stir plate for liquid phase agitation. A K-type thermocouple (Model 2170A-K) was taped to the outer wall of the condenser, and temperature was displayed on an Omega Digital Thermometer.

### 3.4 Source Gases

Most of the oxidation experiments were performed with house air. Nitrogen was supplied from a liquid nitrogen cylinder, and pure CO<sub>2</sub> was supplied from another cylinder. Calibration ammonia was a blend of 1000 ppm of NH<sub>3</sub> in N<sub>2</sub>. The discharge pressure of NH<sub>3</sub> was 40 psig, CO<sub>2</sub> was 40 psig, N<sub>2</sub> was 150 psig, and air was 80 psig. The flow rates of these gases were regulated using Brooks mass flow meters/controller. Each flow meter was calibrated using nitrogen or house air.

Details of the source gas used to collect experimental data are provided in Table 3.1. The calibration results, applicable ranges, and configuration data for the flow meters are provided in Table 3.2.

**Table 3.1** Gas Cylinder Used for Experimental Data Collection

Gas	Manufacturer	Cylinder Date	Analysis	Cylinder Number	Miscellaneous Notes
NH <sub>3</sub> in N <sub>2</sub>	Praxair	7-29-99	1000 ppm (± 1%)	CC109060	2000 psig @70°F 135 ft <sup>3</sup> CGA Outlet 705

**Table 3.2** Calibration Data for Mass Flow Meters and Controller

Flow Meter	Calibration Equation	R <sup>2</sup>	Range	Gas	Model	Serial Number
100 SCCM	SCCM=108.81(%)-1.6192	1	50-90%	N <sub>2</sub>	5850E	9103HCO37044/4
250 SCCM	SCCM=257.43(%)-5.6278	0.9999	15-90%	N <sub>2</sub>	5850C	9310HCO38404/2
15 SLPM	SCCM=16245(%)-160.65	0.9999	10-60%	N <sub>2</sub>	5850E	9310HCO38402
30 SLPM	SCCM=29738(%)-189.50	0.9997	10-50%	N <sub>2</sub>	5850E	9203HCO37104

### 3.5 Reagent Preparation, Storage, and Disposal

The LCI (Low Chloride Iron) grade monoethanolamine used in all experiments was produced by Huntsman (Date 11/9/99, Tank Lot 613311). Refer to Table 3.3 for specific analysis and assays on MEA. The original stock solution was refrigerated at 4°C. Concentrations of MEA solutions were conveniently expressed in units of molal (mole MEA / kg water). The solutions were prepared gravimetrically, and parafilm was used to prevent oxidation by room air prior to loading the reactor. MEA solutions were disposed into the proper amine waste container. All other reagents and their corresponding assays are provided in Table 3.4.

**Table 3.3** Assays for LCI MEA

Analysis	Result	Units
Monoethanolamine	99.97	Wt%
Chloride	< 0.5	ppm
Iron	0.02	ppm
Sulfate	1	ppm
Water	0.06	Wt%

**Table 3.4** Reagent Specifications

Reagent	Manufacturer	Formula Weight	Assay	Lot Number
Bicine	Fisher Scientific	163.17	99+%	A014372601
Glycine	EM Science	75.07	98.5%	39141937
EDTA	EM Science	372.24	99.0%	38139842
FeCl <sub>3</sub> ·6H <sub>2</sub> O	Mallinckrodt	270.30	99.4%	5029N01621
FeSO <sub>4</sub> ·6H <sub>2</sub> O	Fisher Scientific	278.02	99.5%	201392500
KMnO <sub>4</sub>	Mallinckrodt	158.03	99.6%	7068N52608
Formaldehyde	Mallinckrodt	30.03	37.7%	5016N46B00
H <sub>2</sub> O <sub>2</sub>	Mallinckrodt	34.01	31.0%	5240N15A01

### 3.6 Batch Mode Operation

All experimental data were collected while operating in a batch mode for liquid phase. At the start of each experiment, a background with water was taken at the same conditions as the actual experiment to zero out any water interference during the data acquisition process. Batch mode operation consisted of filling the reactor with 500 ml of MEA solution and sparging with 5L/min of air, N<sub>2</sub>, or air with 2% CO<sub>2</sub> through the 1/4" stainless stain sparger. The temperature of the water bath was set at 60°C keeping the temperature of the solution at 55°C throughout the experiment. The exit gas carrying the degradation product NH<sub>3</sub> as well as water vapor flowed through the ice condenser. It was then diluted with

16.5 L/min of dilution air or N<sub>2</sub> to eliminate any water condensation in the lines leading to the analyzer. A dilution factor of 4.3 eliminated any concern of physical adsorption or reactive adsorption of ammonia with the water in the lines. The gas exiting the analyzer was sent into a scrubber in the hood. Refer to Appendix A.2.2 for procedural details.

Ammonia calibration can be performed either before or after an experiment. It was usually performed after the end of an experiment. If calibration were performed before taking the background with water and if some ammonia were still remaining in the line, then the background acquired would have ammonia. This would zero out that ammonia signal and can cause significant error in the analysis. Ammonia concentrations were calibrated by blending the 1000 ppm standard ammonia with air to achieve the desired concentration, bypassing the reactor, and sending the mixture directly to the analyzer. The detailed calibration procedure is provided in Appendix A.1.2.

When running experiments with CO<sub>2</sub> loaded MEA solutions, it was necessary to first achieve the desired CO<sub>2</sub> loading. This was done by sparging pure CO<sub>2</sub> into the MEA solution for 30 minutes in the reactor. The oxidation gas used was a mixture of pure CO<sub>2</sub> in air to keep the loading constant throughout the entire experiment.

Aqueous solutions of chemical reagents were injected through the sampling port into the reactor while data acquisition was occurring without introducing any undesirable disturbances to the system. Injection was done with a syringe equipped with a stainless steel needle.

### **3.7 Analytical Methods**

Only the gas phase  $\text{NH}_3$  concentration was analyzed. The analyzer provided continuous and instantaneous measurement of  $\text{NH}_3$  concentration throughout the entire run of the experiment.  $\text{CO}_2$  loaded MEA solution was sampled at the beginning and the end of the experiment to check for  $\text{CO}_2$  loading. pH measurements were also made at the end of the experiment at 25 ° (Appendix A.2.2).

#### **3.7.1 Gas Phase Analysis by FT-IR Spectroscopy**

Gas phase analysis was performed using Fourier Transform infrared spectroscopy (FT-IR). This method of analysis had the advantage of greater precision in measuring gas phase concentrations by providing digital output. FT-IR analysis was conducted using a Perkin Elmer FT-IR spectrometer (Model Spectrum 2000, SN 41626) equipped with an Infrared Analysis, Inc. gas cell (Model G-5-22-V-AU, SN TA920911). Software used to collect and analyze data included Spectrum for Windows (by Perkin Elmer, version 1.00, 12 May 1995), and TR-IR for Windows (by Perkin Elmer, version 1.00, 7 May 1995). The FT-IR analyzer was calibrated for  $\text{NH}_3$  for each experiment. Detailed procedures of instrument operation are provided in Appendix A.1.

A typical FT-IR spectrum for  $\text{NH}_3$  is shown in Figure 3.5. Ammonia absorbs at two characteristic wavelengths  $930\text{ cm}^{-1}$  and  $970\text{ cm}^{-1}$ . It was determined that the peak at  $970\text{ cm}^{-1}$  was the most resolved and least interfered peak. Water vapor absorbs from  $4000\text{ cm}^{-1}$  to  $3500\text{ cm}^{-1}$  and from  $2000\text{ cm}^{-1}$  to  $1300\text{ cm}^{-1}$ , distant enough not to interfere with the  $\text{NH}_3$  peaks. Figure 3.6 is the overall spectrum for experiment 91600 at 364 minutes. It shows the  $\text{NH}_3$  peaks in

relation to the other peaks in the spectrum in a CO<sub>2</sub> loaded MEA solution. Notice that water peaks are negative due to the fact that there was more water in the background than in the MEA solution. The two peaks between 2400 cm<sup>-1</sup> and 2200 cm<sup>-1</sup> and the peak centered at 650 cm<sup>-1</sup> are due to CO<sub>2</sub>. The two peaks between 3350 cm<sup>-1</sup> and 3500 cm<sup>-1</sup> are characteristic of primary amines, and these peaks can be used to measure MEA volatility.

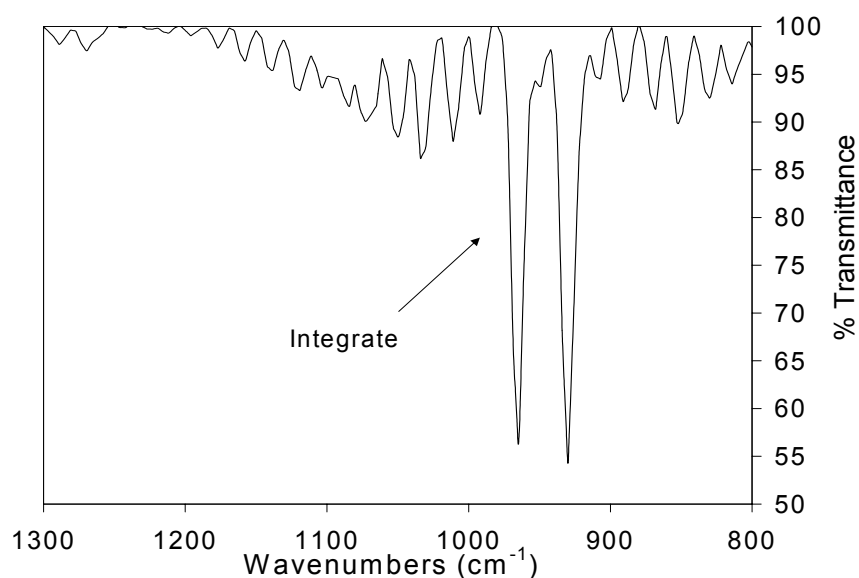


**Figure 3.5** FT-IR Spectrum for Ammonia



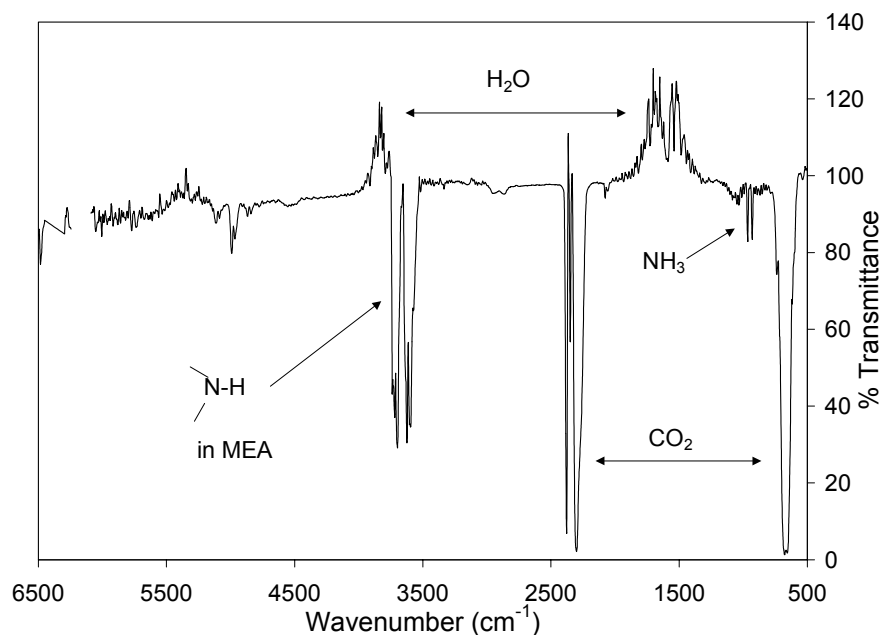
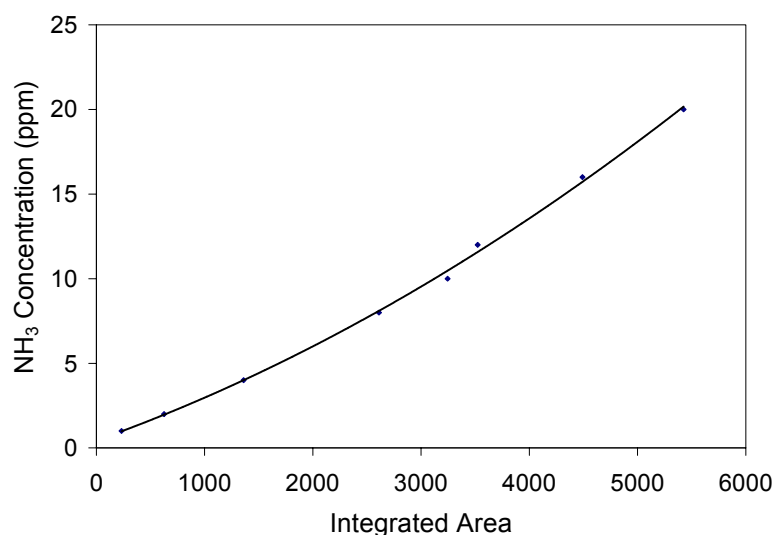


**Figure 3.6** FT-IR Spectrum for 7 m MEA with 0.4 mole CO<sub>2</sub>/mole MEA  
(Exp 91600, 364-365 minutes)

Integrating the area underneath this peak allows for a convenient determination of NH<sub>3</sub> concentration. When integrating this peak, or any peak on the FT-IR spectrum, it is imperative to choose a baseline that has no interference from the peak. If the baseline is chosen too close to the peak, it will move with the peak and yield concentration behaviors that are not intuitively correct. Usually a flat region on the spectrum adjacent to the peak of interest is chosen as the base line.

Notice that NH<sub>3</sub> also absorbs at various wavelengths from 1000 to 1300 cm<sup>-1</sup>. These peaks are not used to quantify concentration because in a typical MEA solution, MEA, formaldehyde, and NH<sub>3</sub> are all volatile and absorb from 1000 to 1300 cm<sup>-1</sup>. It becomes difficult, almost impossible, to resolve these peaks.

The analyzer can detect  $\text{NH}_3$  concentration as low as 1 ppm. The analyzer has a fairly linear range in the concentrations of  $\text{NH}_3$  that are typically encountered in experiments. An example of calibration is depicted in Figure 3.7.



$Y = M0 + M1x + \dots M8 x^8 + M9 x^9$	
M0	4.3708335e-1
M1	2.2833459e-3
M2	2.49605321e-7
$R^2$	0.998

**Figure 3.7** Ammonia Calibration Curve and Equation

This figure is a plot of the known  $\text{NH}_3$  concentration send to the FT-IR versus the integrated area for the peak at  $970 \text{ cm}^{-1}$ . For all  $\text{NH}_3$  peaks, it was determined that integrating from  $978$  to  $955 \text{ cm}^{-1}$  best accommodates the entire peak, and integrating from  $955$  to  $954 \text{ cm}^{-1}$  gives a constant and representative baseline. Subtracting the baseline from the peak area results in the values for the integrated area plotted in Figure 3.7.

### **3.7.2 CO<sub>2</sub> Infrared Analyzer**

The total CO<sub>2</sub> (free plus reacted) in the liquid phase was determined using a total carbon analyzer (Model 525) from Oceanography International Corporation. The principle of operation is as follows: the analyzer has an acid chamber with an injection port where one millimeter of 30-40 wt % phosphoric acid is injected. A liquid sample (50µl to 150 µl) is injected into the acid freeing the chemically reacted CO<sub>2</sub> and the free CO<sub>2</sub>. A nitrogen stream carries the total CO<sub>2</sub> to the infrared analyzer with a range of 0-0.25 % CO<sub>2</sub> volume basis. The analyzer is calibrated with 7 mM sodium carbonate solution. Variable volumes (10 to 200 µl) of the standard solution can be injected, and the output of the analyzer is recorded on a strip chart as peaks with varying heights. The CO<sub>2</sub> loading of an aqueous MEA sample is calculated as the ratio of total moles of CO<sub>2</sub> to the total moles of MEA.

## **3.8 Data Reduction and Analysis**

This section will discuss how raw data from the FT-IR analyzer is converted into useful information such as NH<sub>3</sub> concentration, NH<sub>3</sub> production rate, and total NH<sub>3</sub> produced.

### **3.8.1 Unsteady State Model**

The NH<sub>3</sub> concentration can be predicted using an unsteady state model. A material balance was done over the reactor and the condenser. The change in concentration of NH<sub>3</sub> in the liquid phase over time is equal to the rate at which NH<sub>3</sub> is produced minus the rate at which NH<sub>3</sub> is stripped ( $G y_c$ ).

$$\frac{d(Lx_R)}{dt} = R - Gy_c \quad (3.1)$$

$L$  = Total moles of liquid in the reactor

$x_R$  = Mole fraction of liquid phase  $\text{NH}_3$  in the reactor (ppm)

$R$  = Rate of  $\text{NH}_3$  production (mM/hr)

$G$  = Gas rate (mmole/hr)

This differential equation can be solved for the concentration of  $\text{NH}_3$  in the gas phase exiting the condenser which is the concentration sensed by the FT-IR.

$$y_c = \left( 1 - \left( 1 - \frac{G \cdot y_i}{R} \right) \cdot e^{-\frac{GK_R t}{L(1+y_w/K_c)}} \right) \frac{R}{G} \quad (3.2)$$

$y_c$  = mole fraction of gas phase  $\text{NH}_3$  exiting the condenser (ppm)

$K_R$  =  $y_{\text{NH}_3}/x_{\text{NH}_3}$  at 55 °C (reactor temperature)

$K_c$  =  $y_{\text{NH}_3}/x_{\text{NH}_3}$  at 10 °C (condenser temperature)

$y_w$  = mole fraction of water in the reactor (55 °C)

$y_i$  = Concentration dissolved  $\text{NH}_3$  in the original MEA

Multiply both sides of equation 3.2 by  $G$ , and divide both sides by the total volume of the solution. On the left hand side,  $y_c$  times  $G$  divide by volume gives mole of  $\text{NH}_3$ /L-hr, which will be referred to as the instantaneous rate of  $\text{NH}_3$  production ( $R_i$ ). On the right hand side,  $R/L$  also has the units of mole of  $\text{NH}_3$ /L-hr can be denoted as  $R_s$  for steady state rate rate.

$$R_i = \left( 1 - \left( 1 - \frac{G \cdot y_i}{R} \right) \cdot e^{-\frac{GK_R t}{L(1+y_w/K_c)}} \right) R_s \quad (3.3)$$

The instantaneous rate approaches the steady state rate as  $t$  approaches infinite. Assuming that  $R_s$  is not time-dependent, in the limit that  $t$  approaches infinite,  $dR_i/dt$  is zero, and  $R_i$  is equal to  $R_s$ .

The time it takes to reach this steady state rate is indicated by the time constant in equation 3.3. Note that the time constant depends on  $G/L$ ,  $K_R$ , and  $K_C$ , and typical values of the time constant are around one hour. The physical meaning of this time constant is essentially the time required to strip the  $NH_3$ .

### 3.8.2 Raw Data Manipulation

An example of raw data generated with the FT-IR is shown in Figure 3.8. The figure plots the integrated area underneath the  $970\text{ cm}^{-1}$  peak against time in minutes. Time is expressed in minutes because the instrument scans a spectrum every minute according to the prior program settings.

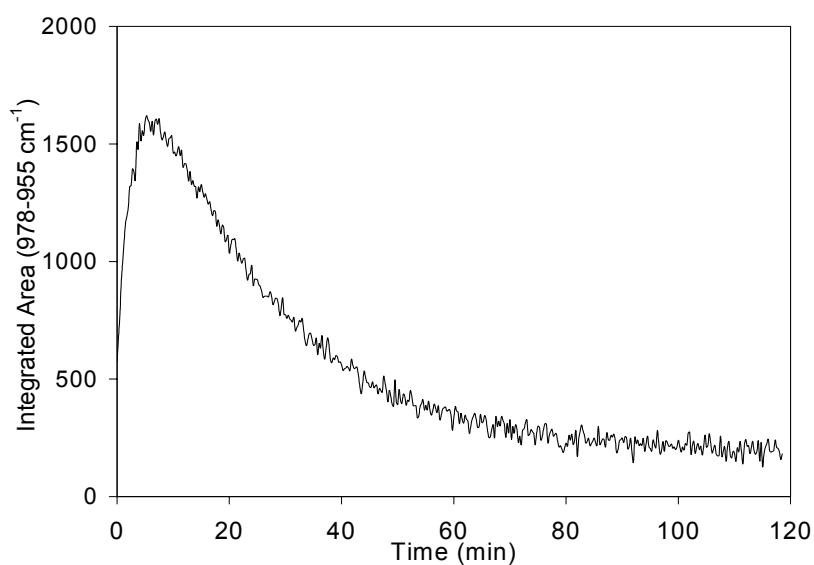


**Figure 3.8** FT-IR Raw Data

The  $\text{NH}_3$  calibration equation is used to convert integrated areas into concentrations in ppm. Parts per million in concentration units can be converted into the instantaneous rate with units of mM/hr simply by multiplying by the gas rate and dividing by the volume to obtain the unsteady state rate or instantaneous rate of  $\text{NH}_3$ . Sample calculations are provided in Appendix A.2.2. All the manipulated raw data will plot this instantaneous rate of  $\text{NH}_3$  production against time (in hours). Refer to Figure 3.9 as an example.

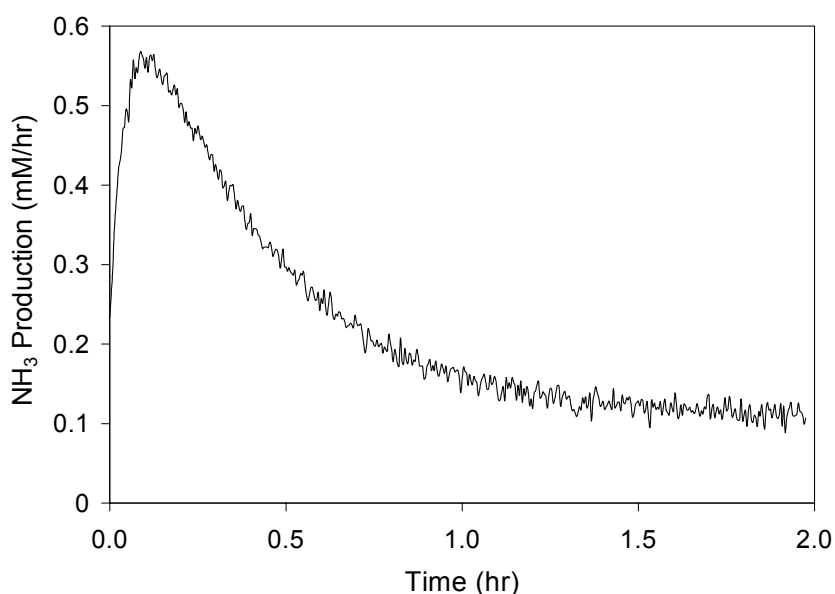


**Figure 3.9** Experiment 71700 Data for Unloaded 5 m MEA

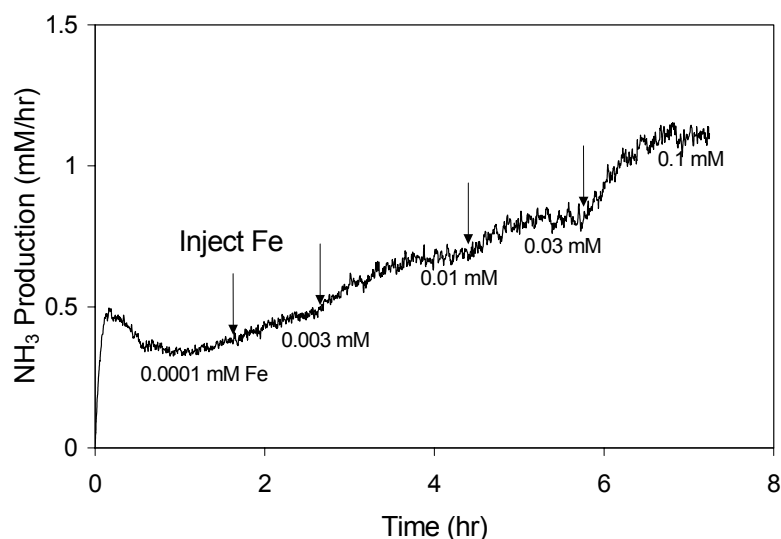
The unsteady state model presented in Section 3.8.1 predicts this behavior quite well. The two adjustable parameters are the steady state rate  $R_s$  and the initial concentration of dissolved ammonia  $y_i$ .

Figure 3.9 illustrates several key phenomena. In the first hour, air strips out the dissolved  $\text{NH}_3$  in the MEA solution until the rate becomes constant. The time it takes to reach this steady state rate is indicated by the time constant in Equation 3.3. Note that the time constant depends on  $G/L$ ,  $K_R$ , and  $K_C$ , and

typical values of the time constant are around one hour. This time constant is essentially the time required to strip the  $\text{NH}_3$ . The steady state rate of  $\text{NH}_3$  production reached in this experiment is 0.12 mM/hr.

### 3.8.3 Extrapolation of Steady State Rates

Frequently, one experiment provided information on several rates measured under different experimental conditions. Figure 3.10 illustrates an experiment where several steady state rates can be extrapolated. This experiment is the air oxidation of 7 m MEA with 0.4 mole  $\text{CO}_2$ /mole MEA at 55 °C. Ferric chloride is injected into the reaction in increasing concentrations after the previous reaction has reached steady state. The time of each iron injection along with the steady states associated with each iron concentration can be seen in Figure 3.10 and are tabulated in Table 3.5.



**Figure 3.10** Multiple Steady States with Increasing Ferric Concentrations in 7 m MEA with 0.4 mole  $\text{CO}_2$ /mole MEA

**Table 3.5** Multiple Steady-state Rates with 0.4 mole  $\text{CO}_2$ /mole MEA

Total Fe (mM)	Rate (mM/hr)
0.0001	0.35
0.003	0.48
0.010	0.68
0.030	0.81
0.100	1.11

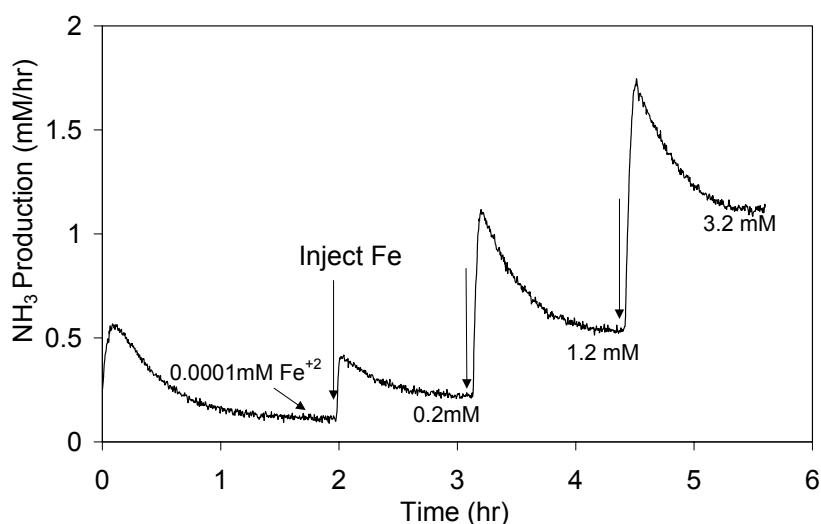


**Figure 3.11** Multiple Steady States with Increasing Ferrous Concentrations in 7 m Unloaded MEA

Under different experimental conditions, the instantaneous rate behavior of the reaction might differ; however, the steady state rates are obtained in the same manner. Figure 3.11 shows the unusual oxidation phenomenon with ferrous ion in unloaded MEA solution oxidized by air. Upon injection of ferrous sulfate,  $\text{NH}_3$  is produced instantaneously in solution and is stripped out in a period of one hour. A higher steady state is reached with each successive addition of iron. These steady state rates are tabulated in Table 3.6.

**Table 3.6** Multiple Steady-state Rates in Unloaded MEA



Total Fe (mM)	Rate (mM/hr)
0.0001	0.11
0.20	0.22
1.2	0.54
3.2	1.11

### 3.8.4 Extrapolation of Stoichiometry

The reaction of MEA with ferrous ion as presented by the data in Figure 3.11 exhibits a stoichiometric effect that can be quantified. In Figure 3.12 area

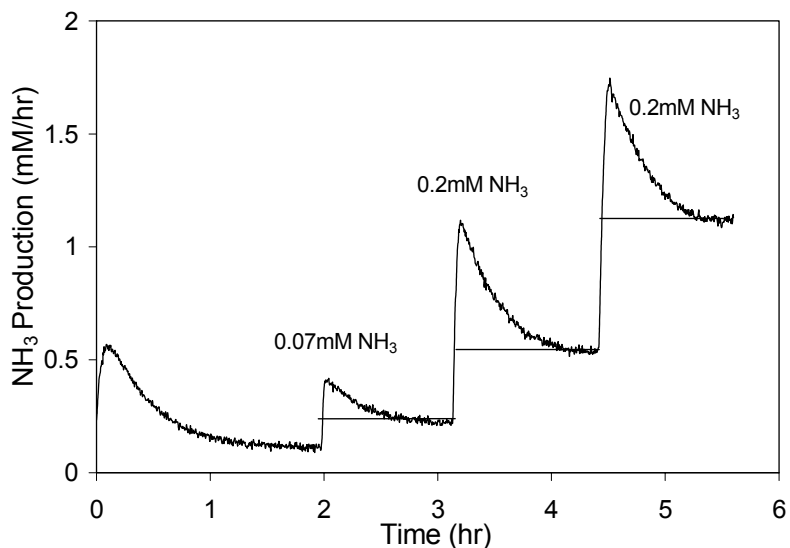


**Figure 3.12** Area of Integration for Determining Reaction Stoichiometry

underneath each triangle is integrated to obtain the total concentration of  $\text{NH}_3$  upon injection of a specific iron concentration. The reaction stoichiometry corresponding to the injected iron concentration can be determined. Table 3.7 shows the moles of  $\text{NH}_3$  produced by the moles of iron injected.

**Table 3.7** Ferrous Stoichiometry with Unloaded MEA

Injected Fe (mM)	NH <sub>3</sub> produced (mM)
0.2	0.07
1	0.2
2	0.2

## Chapter Four

### Experimental Results and Discussion

This chapter presents data on  $\text{NH}_3$  production measured in a sparged reactor apparatus where the gas phase  $\text{NH}_3$  composition was analyzed continuously. From the raw data, a steady state rate of  $\text{NH}_3$  production rate can be obtained. Rates measured under different sets of experimental conditions are compared. Oxidation rate dependence on iron concentration and additives are established. Lastly, rates measured in this study are compared to other studies of MEA oxidation studies.

#### 4.1 Experimental Conditions

Table 4.1 is a comprehensive list of experimental conditions studied in this work. All experiments were conducted at 55 °C to represent absorber

**Table 4.1** Experimental Conditions

MEA (m)	2.5 - 12 (13 - 42 wt%)
$\text{O}_2$ (mole fraction)	0, 0.21
$\text{CO}_2$ Loading/ pH <sub>(25°C)</sub>	0/12.7, 0/10.3, 0.4/10
$\text{Fe}^{+3}$ (mM)	0.0001 - 4
$\text{Fe}^{+2}$ (mM)	0.0001 - 3.2
EDTA (mM)	0 - 13
Bicine (mM)	0 - 100
Glycine (mM)	0, 75
Formaldehyde(mM)	0, 2
$\text{H}_2\text{O}_2$ (mM)	0, 1
Diethylethanolamine (mM)	0,100
$\text{KMnO}_4$ (mM)	0, 1

conditions. MEA concentrations were varied from 2.5 m to 12 m (13 to 42 wt %). ABB typically uses 15-20 wt % MEA, and Fluor Daniel uses 30 wt % with corrosion inhibitors added.

Most experiments were carried out with air, a few experiments were performed in nitrogen. Three MEA solution conditions were examined. Zero CO<sub>2</sub> loading which corresponds to a solution pH of 12.7, zero CO<sub>2</sub> loading with HCl added to get pH 10.3, and 0.4 CO<sub>2</sub> loading which corresponds to a pH of 10. In the first solution, most of the MEA is present as free MEA, whereas the second contains a mixture of free MEA as well as MEAH<sup>+</sup>. With a 0.4 CO<sub>2</sub> loading, MEA carbamate, MEAH<sup>+</sup>, and free MEA are all present. Data collected at 0.4 CO<sub>2</sub> loading are most representative of the actual degradation rates encountered in the absorber. The first two conditions of loading/pH are examined to understand the mechanisms of oxidation. Metals (Fe), oxidation catalysts (Fe, KMnO<sub>4</sub>, H<sub>2</sub>O<sub>2</sub>), potential oxidation inhibitors (EDTA, bicine, glycine, DMMEA), and degradation products (formaldehyde) were added.

## **4.2 Raw Experimental Data**

Raw data generates a plot of NH<sub>3</sub> production (mM/hr) versus time (hour). The x-axis represents the length of the run, while the y-axis represents the instantaneous rate of NH<sub>3</sub> production. All experiments are presented graphically. Each experiment is identified by the following conditions: MEA concentration, CO<sub>2</sub> loading/pH, and oxidizing gas. All of the experiments were performed at 55°C, with gas rate of 5L/min, dilution factor of 4.3, and solution volume of ~500 ml. The arrows indicate the exact point at which a chemical was injected into the reaction. The concentration of chemicals in the resulting solution as well as the time of injection is tabulated. Ten data points that best represent the entire

experiment are tabulated as well. These data include the high, medium, and low points on the graph and all the steady states values. The experiments are listed in chronological order in Appendix B.

### 4.3 Rate Data

The steady state rate of  $\text{NH}_3$  production ( $R_s$ ) can be determined ( $dR_i/dt = 0$ ) from these raw data. A detailed description of all the experiments, their conditions, and the steady-state rate and stoichiometry associated with each condition is shown in Table 4.2. Each experiment is identified by its date and defined by its conditions of MEA concentration,  $\text{O}_2$ ,  $\text{CO}_2$  loading, and final solution pH at  $25^\circ\text{C}$ . The additives and their *cumulative* concentrations in solution are tabulated along with their corresponding rates. Since the original MEA reagent contained 0.02 ppm of dissolved iron, the first steady state is actually the rate at the 0.02 ppm iron condition. The actual sequence of additions is shown from top to bottom in the *Additives* column. Since chemicals were added sequentially, any steady-state rate represents the rate at the *solution* condition at that point and not the condition that is listed in the preceding column. For instance, in experiment 071300 a rate of 0.13 mM/hr was obtained from oxidation of unloaded 5 m MEA (originally containing  $8.39\text{e-}5$  mM Fe) with air. 1 mM of  $\text{Fe}^{+3}$  was injected to this solution, and the rate of 0.13 mM/hr persisted. 1 mM of  $\text{Fe}^{+2}$  was added to the solution at this point, 6 mM EDTA was then injected into this solution shortly after, and the system was given time to reach steady state. A production rate of 0.33 mM/hr was obtained. This rate represents the rate of  $\text{NH}_3$  production in a MEA solution containing 1 mM  $\text{Fe}^{+2}$ , 1 mM  $\text{Fe}^{+3}$ , and 6 mM EDTA. See Figure 4.1.

**Table 4.2** Experiments at 55°C

Date	MEA (m)	O <sub>2</sub>	CO <sub>2</sub> Loading	Final pH <sub>25°C</sub>	Additives	Conc (mM)	Rate (mM/hr)
62700	2.5	Y	0	12.7	Fe <sub>initial</sub>	4.7E-05	0.10
62700	10	Y	0	12.7	Fe <sub>initial</sub>	1.4E-04	0.20
70700	5	N	0	12.7	Fe <sub>initial</sub> Ferric Ferrous KMnO <sub>4</sub> EDTA	8.4E-05 1 1 2 10	0 0 0 stoich = 0.97 0.27
71300	5	Y	0	12.7	Fe <sub>initial</sub> Ferric Ferrous EDTA	8.4E-05 1 1 6	0.13 0.13 - 0.33
71700	5	Y	0	12.7	Fe <sub>initial</sub> EDTA Ferrous Ferrous Ferrous	8.4E-05 5 0.20 1.2 3.2	0.11 - 0.22 0.54 1.11
71800	5	N	0	12.7	Fe <sub>initial</sub> EDTA Ferric Ferrous	8.4E-05 5 4 1	0 - 0 0
72000	5	Y	0	12.7	Fe <sub>initial</sub> (NH <sub>4</sub> ) <sub>2</sub> SO <sub>4</sub>	8.4E-05 1	0.12 stoich = 1.87
72600	5	Y	0	12.7	Fe <sub>initial</sub> EDTA Ferric	8.4E-05 5 1	0.12 - 0.20
81500	7	Y	0.4	9.85	Fe <sub>initial</sub> Ferrous	1.1E-04 1	0.37 2.06
81600	12	Y	0	13	Fe <sub>initial</sub> Ferrous	1.5E-04 1	0.21 0.39
90800	7	Y	0	12.7	Fe <sub>initial</sub> formaldehyde	1.1E-04 2	0.16 0.16
90900	7	N	0	12.7	Fe <sub>initial</sub> H <sub>2</sub> O <sub>2</sub>	1.1E-04 1.0E+00	0.00 2.06; stoich = 1
91000	7	Y	0.4	9.96	Fe <sub>initial</sub> Ferric	1.1E-04 1	0.37 2.32

**Table 4.2** *Continues*

Date	MEA (m)	O <sub>2</sub>	CO <sub>2</sub> Loading	Final pH <sub>25°C</sub>	Additives	Conc (mM)	Rate (mM/hr)
91300	7	Y	0.4	9.93	Fe <sub>initial</sub> Ferric EDTA	1.1E-04 0.20 4.45	0.40 1.77 1.06
91400	7	Y	0	11.57	Fe <sub>initial</sub> glycine Ferric	1.1E-04 75 1	0.16 0.23 0.30
91600	7	Y	0.4	10.05	Fe <sub>initial</sub> Ferric Ferric Ferric Ferric EDTA	1.1E-04 0.003 0.010 0.030 0.1001 13	0.35 0.48 0.68 0.81 1.11 0.86
92000	7	Y	0	10.27	Fe <sub>initial</sub> Ferric Ferric Bicine	1.1E-04 0.1 1 86	0.18 0.39 0.75 0.33
92200	7	Y	0.4	10.05	Fe <sub>initial</sub> Ferrous Ferrous Bicine Bicine Bicine	1.1E-04 0.01 1.0 1 10 100	0.36 0.94 1.70 1.64 1.29 0.80
100200	7	N	0.4	10	Fe <sub>initial</sub> Ferric	1.1E-04 1	0 0
100300	7	Y	0.4	10	Fe <sub>initial</sub> Ferric DEMEA	1.1E-04 1 100	0.37 1.77 1.65

Arrows point to the exact point of chemical injection while the steady states are labeled by the species present in solution that were responsible in establishing those rates.

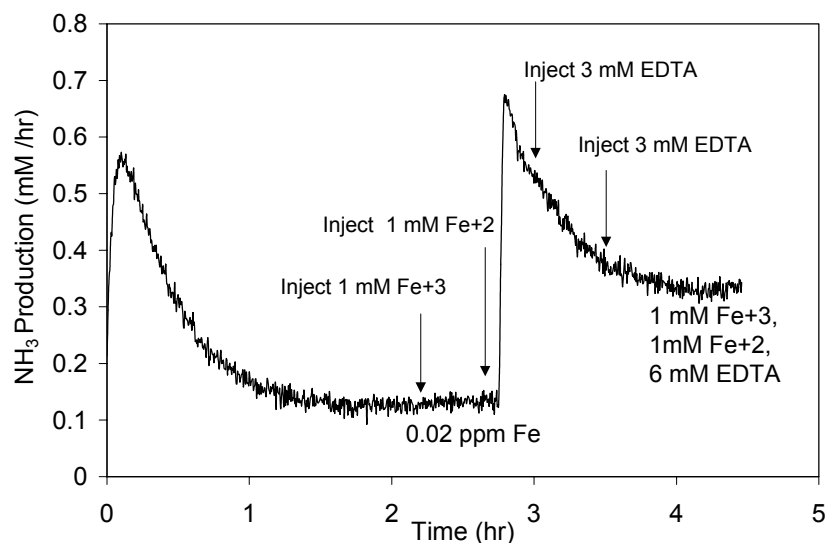


**Figure 4.1** Oxidation of Unloaded 5 m MEA

For experiments where chemicals were added in series of increasing concentrations, the table also provides the sequence of conditions. Experiment 92200 is an example of such an experiment. Figure 4.2 illustrates the times of chemical injection. Figure 4.3 illustrates the steady-state rates and the concentration of responsible species. Experiment 92200 began with 7 m MEA solution with 0.4 mole  $\text{CO}_2$ /mole MEA oxidized with air to yield a steady state rate of 0.36 mM/hr. 0.01 mM of  $\text{Fe}^{+2}$  was added, and a rate of 0.94 mM/hr was reached. The concentration of  $\text{Fe}^{+2}$  in the MEA was raised to a *total solution concentration* of 1 mM by injecting 0.99 mM  $\text{Fe}^{+2}$  into the reaction, and a rate of 1.7 mM was obtained. 1 mM bicine was added to this MEA solution containing 1 mM  $\text{Fe}^{+2}$ , resulting in a slightly decreased rate of 1.64 mM/hr. With a solution



concentration of 10 mM bicine and 1 mM  $\text{Fe}^{+2}$ , the steady state rate fell to 1.29 mM/hr. And lastly, a rate of 0.8 mM/hr was obtained with a solution bicine concentration of 100 mM and  $\text{Fe}^{+2}$  concentration of 1 mM.

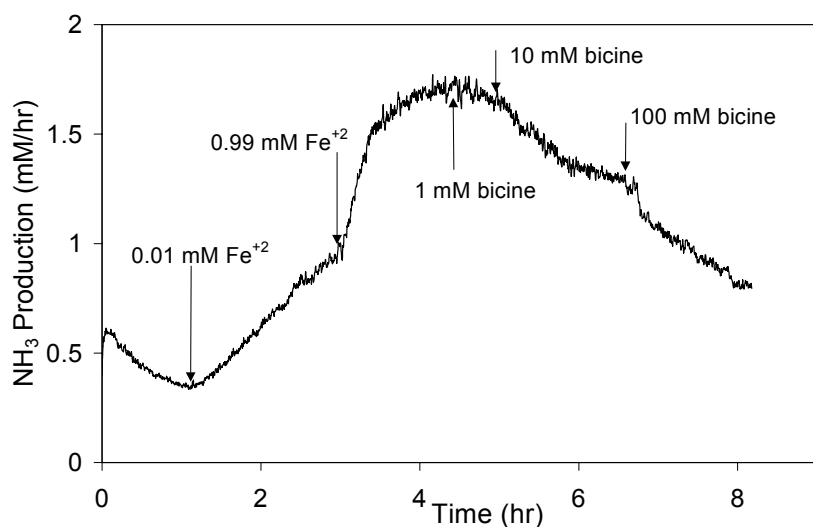


**Figure 4.2** Injection Times for Experiment 092200: Oxidation of 7 m MEA with 0.4 mole  $\text{CO}_2$ /mole MEA with Air

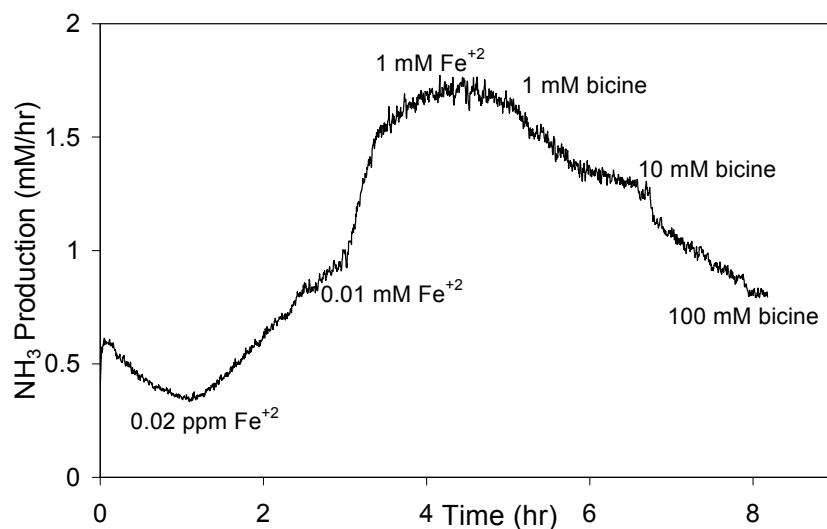


**Figure 4.3** Steady-state Rates for Experiment 09220

#### 4.4 Effect of Iron

The experimental data strongly support the conclusion that iron is an important catalyst in MEA oxidation. All of the iron data are summarized in Figure 4.4 where the rate of  $\text{NH}_3$  production is plotted as a function of iron concentration. All of these rates were measured in 7 m MEA at 55 °C. Five different series of data sets are shown. From top to bottom, rates measured for ferrous and ferric in 0.4  $\text{CO}_2$  loading/ pH 10 MEA are displayed in the uppermost curve, followed by ferric with unloaded, acidified MEA (pH 10.3), ferrous with unloaded / pH 12.7 MEA, and lastly ferric with unloaded / pH 12.7 MEA.

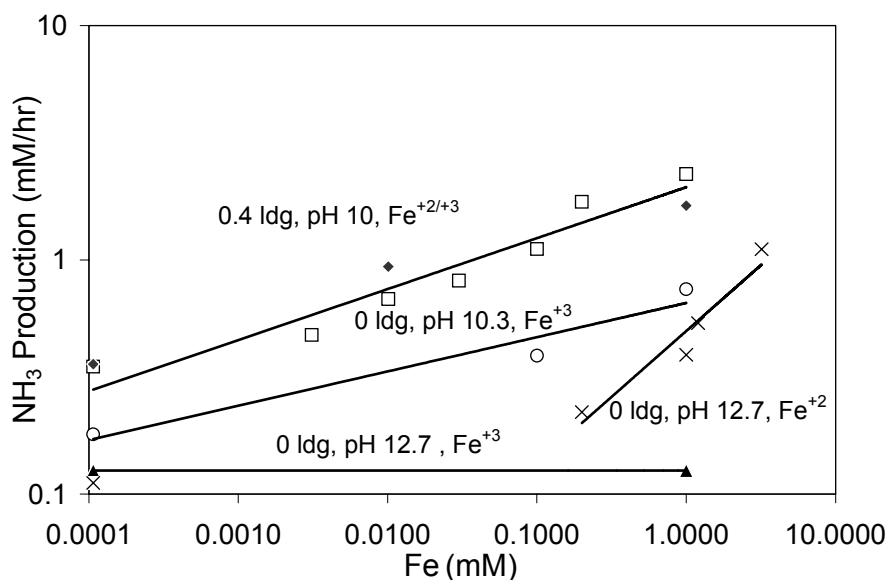


**Figure 4.4** Effect of Iron in 7 m MEA at 55 °C. ( $\square$   $\text{Fe}^{+2}$  and  $\blacklozenge$   $\text{Fe}^{+3}$ )

#### 4.4.1 Rates in CO<sub>2</sub> Loaded and Acidified MEA

With 0.4 moles of CO<sub>2</sub> /mole of MEA, the rate of oxidation increased a factor of five with the addition of 1 mM iron. The rate increased with ferrous or ferric concentration in the same manner. This behavior is consistent with the expectation that ferrous oxidizes rapidly to ferric in the presence of oxygen with rates around 100-200 mM/hr (Brown, 1987). Essentially all iron was present as ferric under these experimental conditions. The NH<sub>3</sub> production steady state rate behavior as a function of iron concentration can be described by Equation 4.1.

$$\text{Rate} = 0.36 \left( \frac{[\text{Fe}^{+3/+2}]}{0.0001} \right)^{0.2} \quad (4.1)$$

Where rate is in mM/hr and iron concentration is expressed in mM. Therefore, without introducing any additional iron into the MEA solution, the iron concentration is 0.0001 mM, and a steady state rate of 0.36 mM/hr was attained. Both ferrous and ferric data can be predicted by equation 4.1 up to 1 mM iron. It is clear from this data that as little as 1 ppm (0.01 mM) of iron in solution can cause the rate to increase a factor of three to 1 mM/hr.

When the pH of the unloaded MEA solution was decreased from 12 to 10.3 with the addition of 0.3 mole HCl/mole MEA, a similar rate behavior was observed with ferric. The only amine species present in this particular solution were free MEA and MEAH<sup>+</sup>. The steady state rate initially was lower than the rate in loaded solutions due to a number of reasons. First, the pH was higher and thus iron was less soluble. Second, MEA carbamate was not present as it is in loaded solutions. The carbamate species may be prone to oxidation. The oxidation rates observed in unloaded pH 10.3 MEA were three times smaller than the rates obtained with 0.4 mole CO<sub>2</sub>/mole MEA. Although these rate data were

collected with ferric, it is reasonable to expect that data with ferrous would follow the same trend.

#### 4.4.2. Rates in Unloaded MEA

In unloaded MEA, the steady-state rate corresponding to each ferrous concentration is labeled in Figure 4.5. The steady state rates can be linearly correlated with ferrous concentration.

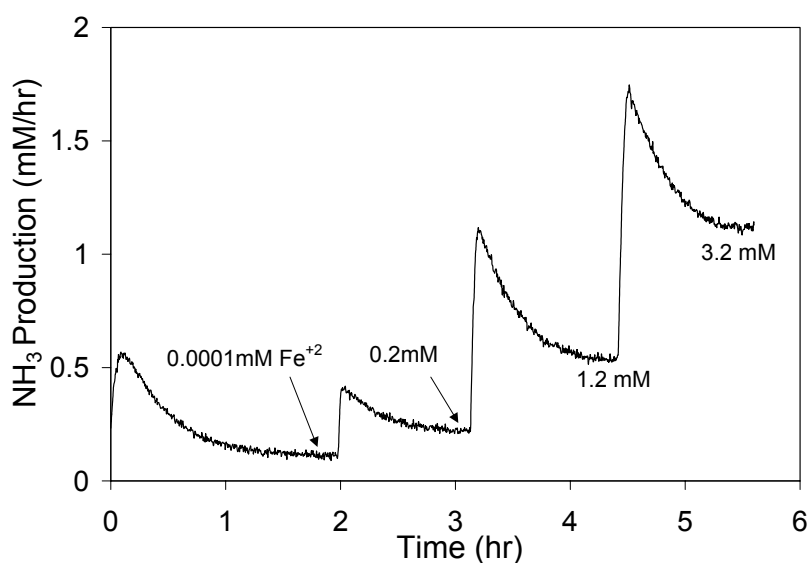


**Figure 4.5** Steady-state Rates in Experiment 71700: Oxidation of 5 m MEA, 0 CO<sub>2</sub> loading with Air

Figure 4.6 clearly illustrates the linear rate dependence on ferrous concentration and essentially plots the same data in Figure 4.4 on a linear scale.

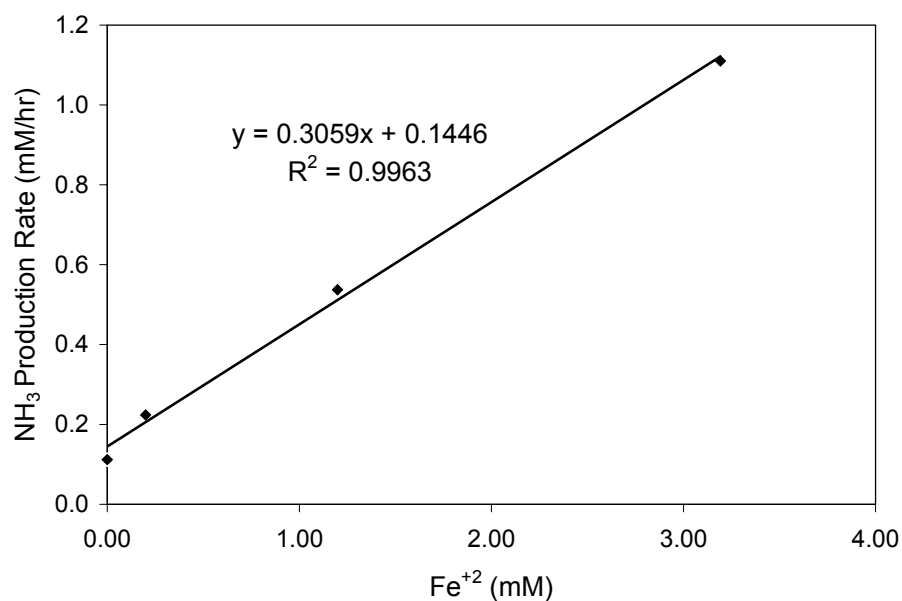


**Figure 4.6** Rate Dependence on Total Ferrous Concentration in Unloaded MEA

An unusual phenomenon occurred when ferric was used to oxidize MEA under condition of zero loading. The rate remained at the same steady state with the addition of ferric concentration over four orders of magnitude. A possible explanation is that ferric is not soluble at pH 12.7 and ferric hydroxide ( $\text{Fe}(\text{OH})_3$ ) precipitates under basic conditions seriously limiting the concentration of ferric ions in solution.

#### 4.4.3 Ferrous Stoichiometry in Unloaded MEA

The ferrous reaction stoichiometry can be derived from the data in Figure 4.7, where the integrated areas are shown.

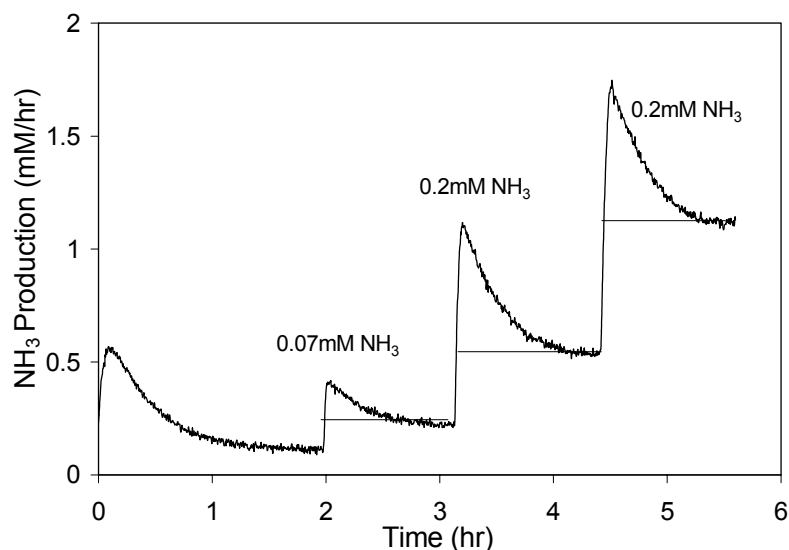


**Figure 4.7** Integration for Experiment 71700

Figure 4.8 shows the resulting stoichiometry as a function of the ferrous *added* (not total ferrous). The ratio of mole NH<sub>3</sub> produced per mole of Fe<sup>+2</sup> added ranged from 0.1 to 0.33.

This is consistent with the expected mechanism of iron oxidation presented in chapter two. Ferrous oxidizes to ferric in the presence of oxygen to produce the oxygen radical O<sub>2</sub><sup>•</sup> and the hydroxide radical OH<sup>•</sup>. O<sub>2</sub><sup>•</sup> is generated only when oxygen is present, but OH<sup>•</sup> can be generated when ferrous reacts with hydrogen peroxide (H<sub>2</sub>O<sub>2</sub>). If OH<sup>•</sup> is responsible for the oxidation of MEA, then 3 moles of ferrous produce 1 mole of OH<sup>•</sup> which can attack a mole of MEA to yield 1 mole of NH<sub>3</sub>. The stoichiometry consistent with this mechanism would range from 1/3 to smaller ratios depending on the efficiency of the reaction. It is intuitive that not all the OH<sup>•</sup> would react with MEA; it can react with more ferrous as suggested by the mechanism. The moles of NH<sub>3</sub> produced per mole of

ferrous decreased from 0.3 to 0.1 with each successive addition of ferrous suggesting that the reaction of ferrous with MEA was not always 100% efficient.

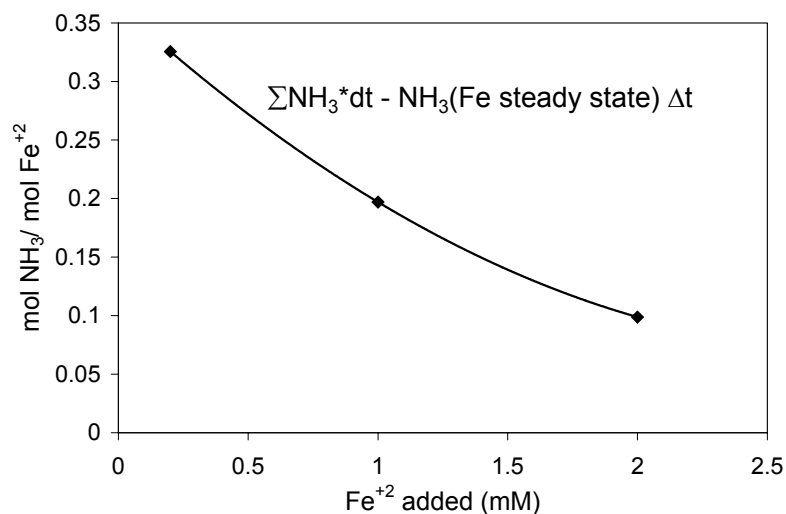


**Figure 4.8** Ferrous Stoichiometry in Unloaded MEA

To test the hypothesis of oxidation by  $\text{OH}^\bullet$ , an experiment was performed in  $\text{N}_2$ , thus precluding the presence of any  $\text{O}_2^\bullet$ . The oxidation rate of MEA with iron in the absence of oxygen was zero as seen in Exp 70700. As expected, the addition of ferrous into a solution of MEA in the absence of oxygen resulted in no  $\text{NH}_3$  being produced. When 1 mM hydrogen peroxide was introduced into this solution, 1 mM of  $\text{NH}_3$  was produced. Refer to Figure 4.9 for times of chemical injection as well as area under the peak integrated for total  $\text{NH}_3$  produced per 1mM  $\text{H}_2\text{O}_2$ . The only radical present in this solution was the hydroxide radical and it reacted in a one-to-one ratio with MEA to produce  $\text{NH}_3$ ; therefore, it is reasonable to conclude that  $\text{OH}^\bullet$  was directly involved in the attack of a MEA molecule.

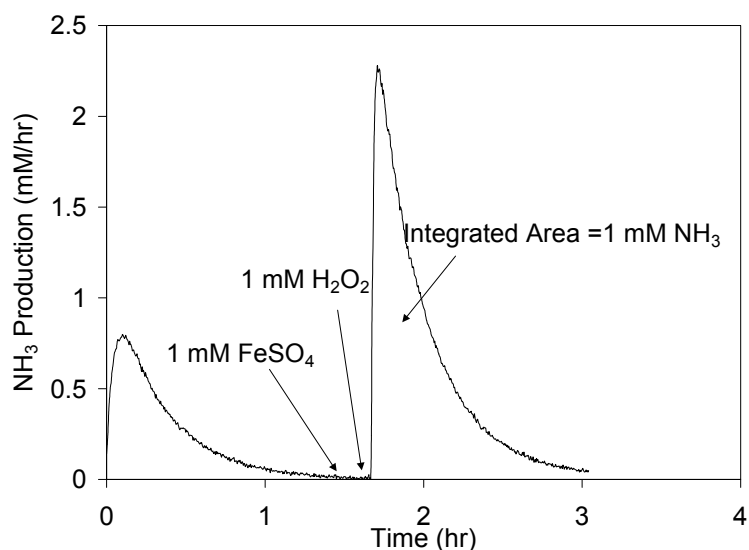


**Figure 4.9** Oxidation of 7 m MEA, 0 CO<sub>2</sub> Loading with N<sub>2</sub>

#### 4.5 Effect of CO<sub>2</sub> Loading

A dramatic increase in NH<sub>3</sub> production rate was observed in loaded compared to unloaded MEA solutions. This effect can be seen in the iron data. The steady-state rate in unloaded 7 m MEA solutions was consistently 0.16 mM/hr whereas the rate with 0.4 moles of CO<sub>2</sub>/mole MEA was 0.36 mM/hr. These rates are highly reproducible as seen in Table 4.2.

The effect of CO<sub>2</sub> loading on degradation suggests that the MEA carbamate species was more susceptible to oxidation than free MEA. An alternative explanation is that the low pH of the solution allowed more iron to stay in solution and catalyze oxidation.

Blachly and Ravner (1964) studied MEA oxidation by measuring NH<sub>3</sub> and peroxide production. The first important conclusion of this study was that in the absence of CO<sub>2</sub>, no degradation was observed. The addition of 1% CO<sub>2</sub> to the air stream simulating submarine atmospheric conditions resulted in almost



instantaneous degradation characterized by the production of ammonia and peroxides (Section 2.2.2).

CO<sub>2</sub> loading was observed to have an opposite effect on MEA oxidation, as well as oxidation of other amines, in the studies by Rooney et al., 1998 (Section 2.2.3). They concluded that CO<sub>2</sub> decreased the oxidation of amines, since the total anions (acetate, formate, glycolate) measured were less for all the amines they tested when CO<sub>2</sub> was present compared to when CO<sub>2</sub> was not present in solution.

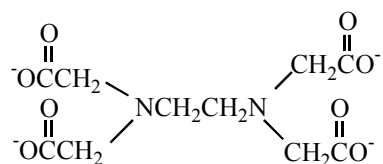
Oxidation rates have been quantified using different degradation products. Rooney observation of a decrease in the concentration of anions produced with CO<sub>2</sub> is not enough to conclude that the overall oxidation had decreased, especially if MEA oxidation clearly results in other degradation products that were not specifically examined by Rooney et al. Ammonia production increased in the presence of CO<sub>2</sub>, whereas anion production decreased. It can be seen from the MEA degradation mechanism proposed by Rooney et al. in Figure 2.10 that anions, such as acetate and formate, are further oxidation products of their aldehyde precursors. However, oxidation of MEA may produce NH<sub>3</sub> and aldehydes in the same step (fragmentation or hydrolysis) according to Figure 2.1. It is entirely possible that these aldehydes are stable species, and the anions can only be seen much later, after further oxidation has occurred. This is apparent in the Rooney study where some anions were detected in small quantities after 7 days, some were not even detectable within the course of their 28-day experiment. No glycolate or oxalate were detected in the oxidation of 0.25 CO<sub>2</sub> loading 30 wt % MEA with air. Table 4.3 lists the detected anion concentrations as a function of days. The detection limit for each anion was 10 ppm.

**Table 4.3** Oxidation Studies 20 wt % MEA with 0.25 mole CO<sub>2</sub>/mole MEA  
(Rooney et al., 1998)

Days	Acetate (ppm)	Formate (ppm)	Glycolate (ppm)
0	<10	<10	<10
7	<10	95	<10
14	22	265	<10
21	44	413	<10
28	60	498	<10

#### 4.6 Effect of EDTA

Ethylenediaminetetraacetic acid (EDTA) is a chelating agent. Its anion is present at high pH with the following structure:



It binds strongly and rapidly to metals as a result of multiple binding sites a single ligand. EDTA had been examined by Blachly and Ravner (1964) and determined to be an effective inhibitor of Cu<sup>+2</sup> oxidation of MEA. EDTA was not effective with ferrous and ferric.

Experiments with EDTA were performed in both loaded and unloaded MEA to determine its effectiveness in inhibiting oxidation. Figure 4.6 shows the effect of EDTA in 7 m MEA solutions with 0.4 CO<sub>2</sub> loading . The solid curve consists of rates measured in the absence of EDTA as a function of ferric concentrations. When 4.5 mM EDTA was injected into this solution containing 0.2 mM Fe<sup>+3</sup>, the steady state rate decreased 40% from 1.77 mM/hr to 1.06 mM/hr (See Exp 91300). When 13 mM EDTA was injected into a solution with 0.1 mM Fe<sup>+3</sup>, the steady state rate also decreased 40% from 1.11 to 0.86 mM/hr

(See Exp 91600). Thus upon the addition of more EDTA, no further effect was observed.

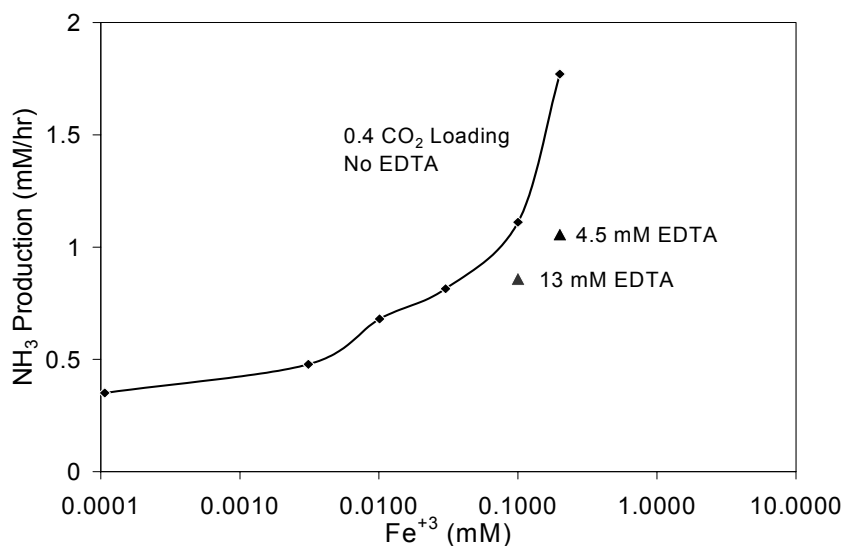


**Figure 4.10** Effect of EDTA in 7 m MEA with 0.4 mole  $\text{CO}_2$ /mole MEA

In unloaded MEA solutions, EDTA had a negligible effect on the oxidation rate. Comparing experiments 71300 (without EDTA) to 71700 and 72600 (with 5 mM EDTA), the rates with no additional ferrous were ~0.12 mM/hr in all three cases (Table 4.4).

**Table 4.4** Effect of EDTA in Unloaded 5 m MEA with No Additional Iron

Experiment	[EDTA] (mM)	Rate (mM/hr)
71300	0	0.13
71700	5	0.11
72600	5	0.12

As a matter of fact, not only was EDTA ineffective in unloaded MEA solutions, it was observed to even increase the rate of oxidation with ferric in unloaded solutions. Recall that in the unloaded MEA, ferric did not catalyze

oxidation as illustrated on the bottom curve on Figure 4.4. However, if EDTA is added to the solution prior to the ferric, the rate was observed to increase from 0.12 to 0.2 mM/hr as shown in Figure 4.11.

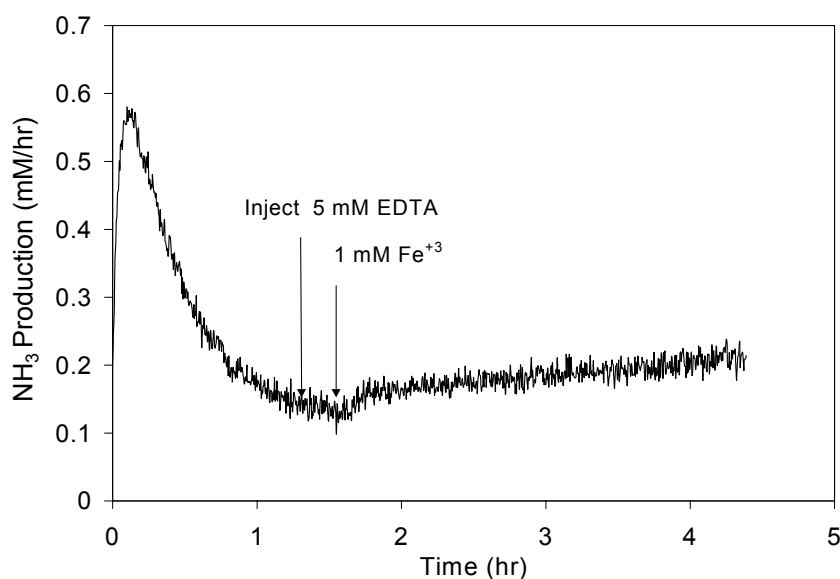
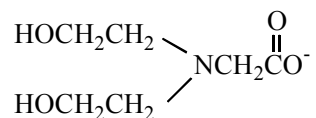


**Figure 4.11** Effect of EDTA in Unloaded MEA with 1 mM Fe<sup>+3</sup>

#### 4.7 Effect of Bicine

Bicine is a common name for the chemical compound N,N-Bis (2-hydroxyethyl)glycine. Bicine is a tertiary amine or just glycine with two ethanol groups attached to the nitrogen. At high pH, it is present in its anion form:



Bicine is a standard additive used by the U.S. Navy to minimize MEA degradation in submarines at a level of 1.5 wt% in 25 wt% MEA (Blachly and Ravner, 1964). Blachly and Ravner (1964) concluded in their study that bicine

acted as a peroxide scavenger and greatly reduced oxidation of MEA by both ferrous and ferric (Figure 2.7).

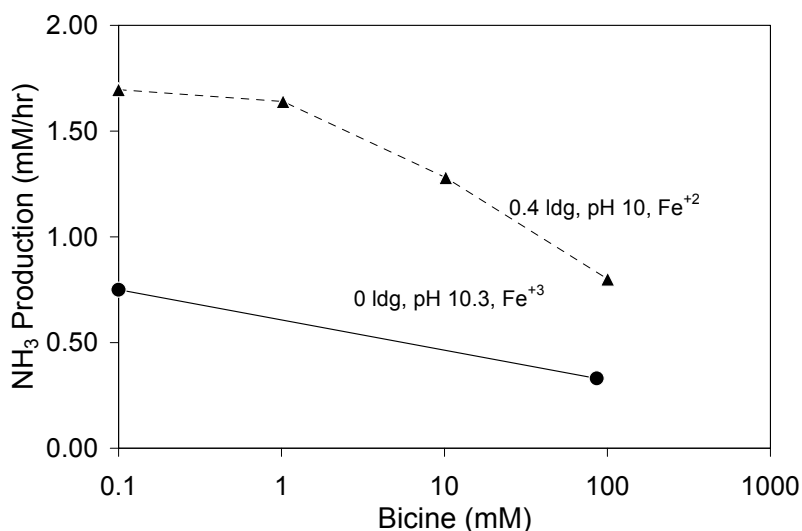


**Figure 4.12** Effect of Bicine in 7 m MEA with 1 mM Fe<sup>+2/+3</sup>

Figure 4.12 shows the effectiveness of bicine with 7 m MEA containing 1 mM ferrous or ferric. In both solutions (0.4 loading and pH 10.3/ 0 loading), a bicine concentration of 100 mM decreased the rate by a factor of two.

#### 4.8 Effect of KMnO<sub>4</sub>

Potassium permanganate caused MEA oxidation even in the absence of oxygen. Figure 4.13 shows data measured in unloaded 5 m MEA with N<sub>2</sub>. Neither Fe<sup>+2</sup> or Fe<sup>+3</sup> appeared to catalyze further oxidation without oxygen. The reaction of potassium permanganate with MEA had a stoichiometry of 0.97 mole NH<sub>3</sub>/mole KMnO<sub>4</sub>.

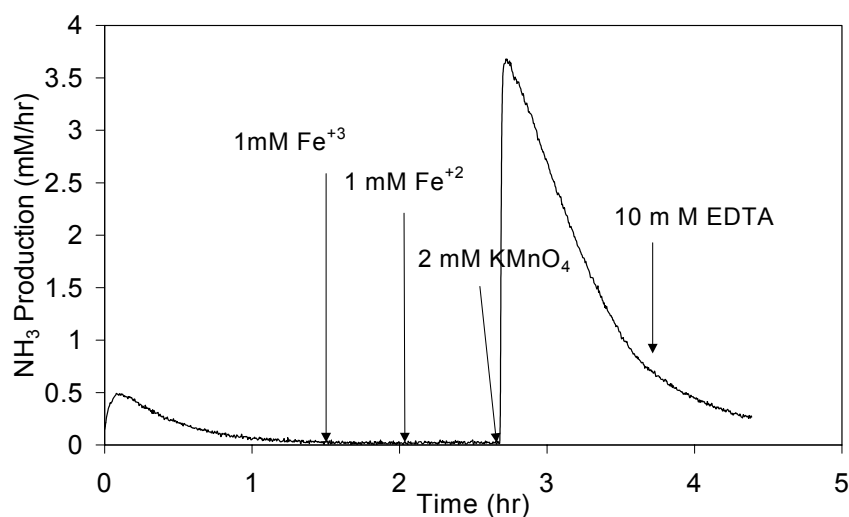


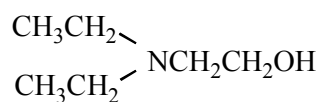
**Figure 4.13** Effect of KMnO<sub>4</sub> in Unloaded 5 m MEA with N<sub>2</sub>

#### 4.9 Other Additives

Bicine has been reported to exhibit corrosive properties in MEA solution, and it is relatively costly to utilize in large quantities. Additives that significantly reduce degradation are valuable to the process of CO<sub>2</sub> removal with MEA. A number of potential inhibitors including glycine, N,N-diethylethanolamine (DEMEA), and formaldehyde were studied. The structures of the first two are shown below. Formaldehyde is a product of MEA oxidation (Figure 2.1).



Glycinate



N,N-Diethylethanolamine

Glycine closely resembles bicine and also is similar in structure to MEA carbamate. It could exhibit degradation characteristics like MEA carbamate. An experiment was performed in unloaded MEA containing 75 mM glycine. Ferric was introduced into this solution since it does not catalyze further oxidation in

unloaded MEA/pH 12.7. The addition of glycine decreased the pH to 11.6 and caused more  $\text{NH}_3$  to evolve. The addition of ferric resulted in a slight increase ( $\sim 0.07$  mM/hr) from the steady state rate with glycine and MEA (Exp 91400). This experiment failed to mimic the effect of MEA carbamate. Ferric cannot cause MEA/glycine solution to degrade to the extent as it did in loaded MEA solutions where carbamate is present. A possible reason for the observed rate increase with ferric could be the lowering of pH due to glycine.

DEMEA is a tertiary amine with pKa of 9.82 (Christensen et al., 1969), similar to the pKa of bicine. Tertiary amines have been reported to inhibit degradation of primary and secondary amines (Kindrick et al., 1950). DEMEA is chosen because of its similarity to bicine in structure as well as pKa.

100 mM DEMEA was injected into a loaded MEA solution containing 1 mM ferrous. The rate dropped only  $\sim 7\%$ .

Lastly, an oxidation product, formaldehyde, was added to an unloaded MEA solution (Exp 90800). Formaldehyde appeared to absorb between 1250 and  $1000\text{ cm}^{-1}$ .  $\text{NH}_3$  and MEA both have characteristic absorption at that region of the spectrum. The sudden injection of formaldehyde into the system caused the ammonia peak at  $970\text{ cm}^{-1}$  to be skewed since the formaldehyde peaks directly adjacent to it increased in both height and width. This formaldehyde interference resulted in a dip in the  $\text{NH}_3$  profile. As formaldehyde was stripped from solution, the  $\text{NH}_3$  production rate returned to the consistent steady-state value of 0.16 mM/hr with 7 m MEA. Therefore, formaldehyde had no effect on the degradation of MEA.

#### 4.10 Effect of MEA Concentration

The effect of MEA concentration ( zero CO<sub>2</sub> loading) on rate is depicted in Figure 4.14. The rate increased a factor of two over a factor of five increase in MEA concentration. The dissolved iron content of LCl grade MEA was 0.02 ppm. More concentrated MEA solutions contain more dissolved iron and thus degraded faster than solutions containing less iron.

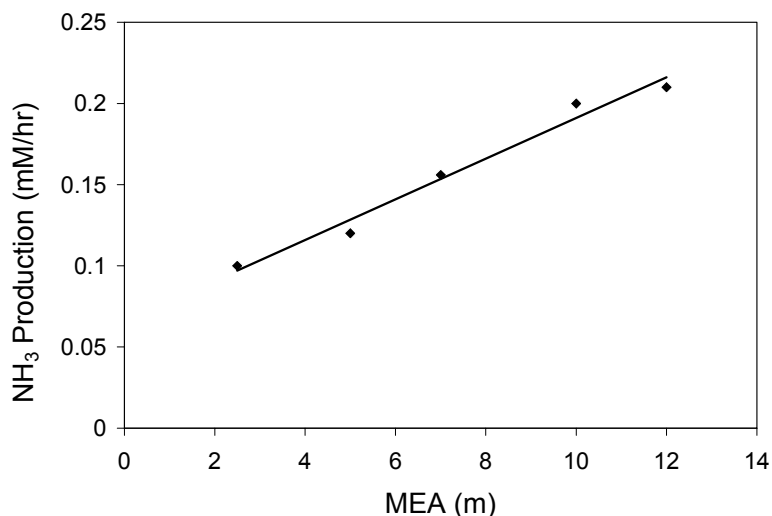


**Figure 4.14** Effect of MEA Concentration (0 CO<sub>2</sub> Loading, No Additional Iron, Air)

#### 4.11 Comparison with Other Studies

Rates of MEA degradation from this study can be compared to the rates obtained in past studies. The experimental conditions and the rates for MEA direct studies are summarized in Table 4.5.



**Table 4.5** Rate Comparison

Study	[MEA] (m)	T °C	CO <sub>2</sub> ldg / %CO <sub>2</sub>	Products Detected	Analytical Method	[Fe] (mM)	Rate (mM/hr)
This Work	7	55	0.4	NH <sub>3</sub>	FT-IR	0.0001	0.36
This Work	7	55	1% (air)	NH <sub>3</sub>	FT-IR	0.0001	0.16
This Work	7	55	1%	NH <sub>3</sub>	FT-IR	1	0.45
This Work	7	55	0.4	NH <sub>3</sub>	FT-IR	1	1.7
Blachly (1964)	5	55	1%	NH <sub>3</sub>	Titration	< 0.0001	0.14
Girdler (1950)	3	80	50%	NH <sub>3</sub>	Titration	0.5-1.0	0.3
Rooney (1998)	4	80	0.25	Anions	IC	*	1.1

\* Produced by Dow and used without further purification

As illustrated in Table 4.5, the MEA oxidation rates obtained in this study were comparable to the rates obtained in other studies. The main difference arose from the differences in experimental conditions as well as the experimental methods employed in each study. Blachly and Ravner studied oxidation in 1% CO<sub>2</sub>, which is equivalent to the air oxidation experiments conducted in this study. Their MEA iron concentration was not reported; however, the report did specify that all MEA used was redistilled and stored at 40°F in evacuated sealed vials until needed. Therefore, their iron content should be comparable to the iron content of the low metal grade MEA used in this study. The air oxidation rate with unloaded MEA in this study was 0.16 mM/hr which compared well with the Blachly and Ravner rate of 0.14 mM/hr.

The rate of 1.7 mM/hr obtained with 0.4 loading 7 m MEA with 1 mM Fe in this study was comparable to the rate of 1.1 mM/hr in 0.25 loading 4 m MEA obtained by Rooney. The differences should be greater due to the iron content of the MEA used in these studies. Since the two studies were detecting different degradation products, the results cannot be directly compared.

The rate of 1.7 mM/hr obtained in this study with 0.4 loading 7 m MEA with 1 mM Fe was significantly greater than the rate obtained in the Girdler study

with 50% CO<sub>2</sub> and 0.5-1.0 mM Fe. The latter rate compared better with the both the 0.4 loading MEA with 0.0001 mM Fe.

This work verified the inhibiting role of bicine on MEA degradation in the presence of iron (Blachly and Ravner, 1964). Figure 2.7 shows negligible degradation in MEA containing 1.5 wt% bicine and 0.5 mM iron. The effect of bicine was easily detected in this work where the rate dropped a factor of two shortly after its injection.

Blachly and Ravner (1964) concluded that EDTA (~ 40 mM) was less effective with 30 ppm (0.5 mM) of Fe<sup>+2</sup>. The oxidation rate was as high as 0.26 mM/hr for the first two days, and dropped to 0.08 mM/hr and persisted from day three until day six. In this work, a rate of 0.3 mM/hr was observed with 5 mM EDTA and 0.5 mM Fe<sup>+2</sup> in 5 m MEA oxidized by air .



## **Chapter Five**

### **Conclusions and Recommendations**

This chapter summarizes the important conclusions in the study of MEA oxidation by measuring  $\text{NH}_3$  production. This chapter also provides recommendations for future work needed to gain a better understanding of the oxidation reactions of MEA as well as other amine systems.

#### **5.1 Conclusions**

##### **5.1.1 Effect of $\text{CO}_2$ Loading**

Oxidation rates with 0.4 mole  $\text{CO}_2$ / mole MEA were two times faster than rates in unloaded solutions with no additional iron. This confirms the results of Blachly and Ravner (1964) who also measured production of  $\text{NH}_3$ . It disagrees with the results of Rooney et al. (1998) who measured the production of organic acids. The rate dependence on loading as well as the rate with a typical lean loading of 0.2 are left to be determined in the future.

##### **5.1.2 Iron in Loaded MEA**

Iron is an important catalyst in oxidation of MEA to  $\text{NH}_3$ . As little as 1 mM iron can increase the rate by a factor of five with 0.4 mole  $\text{CO}_2$ /mole MEA. The rate dependence on dissolved iron from 0.0001 to 1 mM is given by:

$$\text{Rate (mM/hr)} = 0.36 \times \left( \frac{[\text{Fe}^{+3/+2}]}{0.0001} \right)^{0.2}$$

In loaded solution, the rate depends on the total concentration of iron in solution, regardless of its oxidation state. In order to minimize oxidation of MEA, it would be necessary to decrease the iron content below 0.01 mM.

### **5.1.3 Iron in Unloaded MEA**

Without CO<sub>2</sub>, only ferrous ion catalyzes oxidation. Ferric does not appear to increase NH<sub>3</sub> production in unloaded solutions, possibly due to its solubility limit at high pH. The steady-state rate of NH<sub>3</sub> production depends linearly on ferrous ion:

$$\text{Rate (mM/hr)} = 0.306 [\text{Fe}^{+2}] + 0.145$$

In unloaded MEA solutions, the reaction stoichiometry ranges from 0.1 to 0.3 moles NH<sub>3</sub>/mole Fe<sup>+2</sup> added. Hydrogen peroxide reacts with MEA in the absence of O<sub>2</sub> to produce 1 mole NH<sub>3</sub>/mole H<sub>2</sub>O<sub>2</sub>. It can be concluded from these results that the hydroxide radical was responsible in the degradation of MEA to NH<sub>3</sub>.

### **5.1.4 Oxidants Other than Oxygen**

Neither Fe<sup>+2</sup> or Fe<sup>+3</sup> cause degradation to NH<sub>3</sub> without O<sub>2</sub> in loaded and unloaded MEA. However, some oxidants were able to oxidize MEA in the absence of O<sub>2</sub>. The reaction of H<sub>2</sub>O<sub>2</sub> or KMnO<sub>4</sub> with MEA rapidly produced NH<sub>3</sub>, and the reaction stoichiometry was determined to be 1 mole NH<sub>3</sub>/mole H<sub>2</sub>O<sub>2</sub> or KMnO<sub>4</sub>.

### **5.1.5 Oxidation Inhibitors**

The two effective oxidation inhibitors are bicine and EDTA. Both reduce MEA oxidation rate in loaded solutions. Bicine reduced the rate a factor of two in MEA containing 1 mM iron. EDTA reduced oxidation rate 20 to 40% in loaded MEA with ~0.2 mM iron. Commercial use of these inhibitors should consider potential adverse effects on corrosion.

## **5.2 Application to Acid Gas Treating**

Typical makeup rate in acid gas treating with 15-20 wt % MEA is 0.1 lb MEA/ton CO<sub>2</sub>. With 30 wt % MEA, the makeup rate is 1.5 lb MEA/ton CO<sub>2</sub>. The rich loading is 0.45, and the lean loading is 0.2. Assuming a liquid holdup of five minutes, the typical degradation rate is 7.4 mM/hr for 30 wt % MEA and 0.33 mM/hr for 15-20 wt% MEA.

The rate of oxidative degradation was 1.8 mM/hr with 0.4 loading in 30 wt % MEA containing 1 mM of iron at 55 °C. The higher makeup rate in commercial use of 30 wt% MEA may result from higher temperature carbamate polymerization.

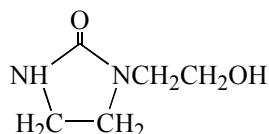
## **5.3 Recommendations**

Future study is recommended in the following areas:

- 1) Examine potential oxidation inhibitors for iron catalyzed MEA oxidation. Certain tertiary amines might be effective inhibitors when

blended with MEA. These may include bicine, EDTA, nitrilotriacetic acid (NTA), and MDEA.

- 2) Examine the effects of MEA degradation products on the oxidation rate. These can include degradation products formed via carbamate polymerization such as 1-(2-hydroxyethyl)-2-imidazolidone (HEIA) and N-(2-hydroxyethyl)- ethylenediamine (HEEDA).



1-(2-hydroxyethyl)-2-imidazolidone  
(HEIA)



N-(2-hydroxyethyl)-ethylenediamine  
(HEEDA)

- 3) Examine the effect of  $\text{Cu}^{+2}$  as a oxidation catalyst.
- 4) Study oxidation at stripper conditions of high temperature and 0.2 loading by oxidized metal ions such as  $\text{Fe}^{+3}$  and  $\text{Cu}^{+2}$ .
- 5) Examine rates at 0.2  $\text{CO}_2$  loading and quantify rate dependence on loading.
- 6) Apply this experimental method to investigate degradation characteristics of other amine systems. These include piperazine, alanine, and hindered amines such as amino-methyl propanol (AMP). This can be achieved with detection methods for formaldehyde and other volatile products.
- 7) Use the existing system to measure amine volatility.

## Appendix A

### Analytical Methods & Equipment Operating Procedure

#### A.1 FT-IR Spectroscopy Operating Procedures

This section discusses gas phase analysis for NH<sub>3</sub> using Perkin Elmer FT-IR spectrometer and software. Detailed procedures for using this equipment are provided by Chisolm (1999).

##### A.1.1 Start-Up Procedures

- Turn on the analyzer. Check that the green light is on, indicating that the laser is functioning
- Turn on the computer connected to the analyzer and start the Windows software
- Start the Spectrum for Windows software program
- Click the *Instrument* button in Spectrum to connect the software to the analyzer
- Click the *Initialize* button in Spectrum to initialize the software
- Click the *Align* button in Spectrum
  - Check that resolution is at 8 cm<sup>-1</sup>
  - Check that the gain is at 8.0
- Click the *Beam* button to make sure the it is connected to the left cell
- Click the Monitor button in Spectrum to check the energy level. An energy reading of ~ 600 is adequate; otherwise, the mirror needs to be realigned or cleaned



- Open the TRIR for Windows Program
- Click on the File/Open Method menu in the TRIR program. Select the PHCL method

### **A.1.2 NH<sub>3</sub> Calibration Procedures**

- Take air background with no NH<sub>3</sub>
  - 5L/min air into empty reactor (32.7% channel 1 & 100% channel 3)
  - 25L/min dilution air (83.3% channel 4)
  - Acquire FT-IR background by clicking Method/Background menu in the TRIR program. Overwriting the existing file is ok
  - Click Method/Start Run/Trigger menu in the TRIR program to start run
  - Hit the "A" key and left or right arrow keys to zoom in or out of the region on the x-axis
  - Hit the "A" key and up or down arrow keys to zoom in or out of the region on the y axis
  - Check that NH<sub>3</sub> peaks at 970 and 930 cm<sup>-1</sup> are absent
  - Acquire another background, then start run again
- Turn on NH<sub>3</sub> (1000 ppm standard) cylinder to ~20 psi
- Turn channel 2 to starting the first calibration value (24 %) and blend gas
- It will take five minutes to start detecting NH<sub>3</sub> (ammonia spectrum shown in Figure ), and wait for 5-7 minutes for each calibration concentration, record the time at each concentration step change

- Once peak reaches steady state, calibrate for the next concentration by adjusting the flow rates of NH<sub>3</sub> or dilution air or both (Table)
- F5 to halt the run
- Shutdown by turning NH<sub>3</sub> cylinder off and bleed NH<sub>3</sub> out of the lines
- In the TRIR program, click the View Results/Contour Section menu to view and save data.
- For each experiment, save a baseline contour section and a measurement contour section. Save the data as a chromatogram file in the C:\TRIR\Spectra directory on the hard drive. The baseline contour will account for any drift in the analyzer during the course of the experiment
- Baseline for NH<sub>3</sub> is taken from 955-954 cm<sup>-1</sup>, and peak is taken from 978-955 cm<sup>-1</sup>
- Once the baseline and measurement chromatogram files are saved, switch to the Spectrum for Windows software
- Open both the baseline and measurement chromatogram files within Spectrum for Windows
- Click on the *Auto X* and *Auto Y* buttons to automatically adjust the ranges
- Click on the *Diff* button to calculate the difference between the measurement and the baseline
- Close the baseline and measurement chromatograms, leaving only the difference chromatogram. This is a graph of integrated area versus time. See Figure A-1

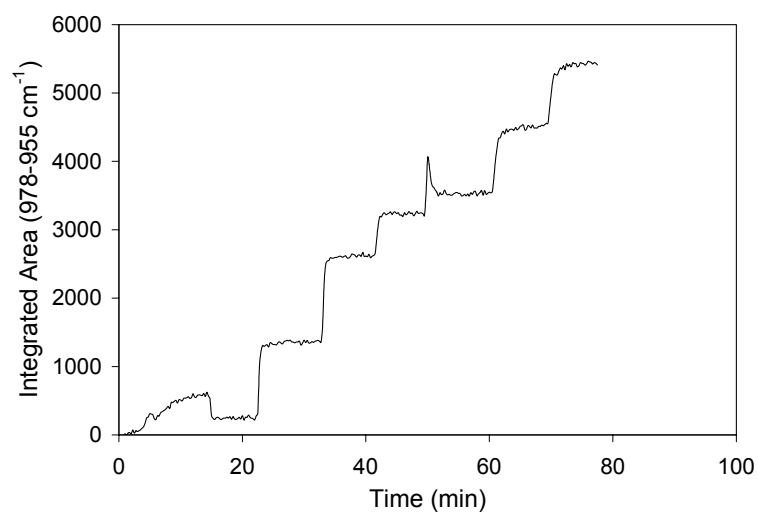


**Figure A-1** NH<sub>3</sub> Calibration Raw Data

- Save this difference file as a ASCII file for analysis in a spreadsheet program
- Knowing the times of each step change, obtain the calibration equation of concentration versus area. See example in Figure A-2

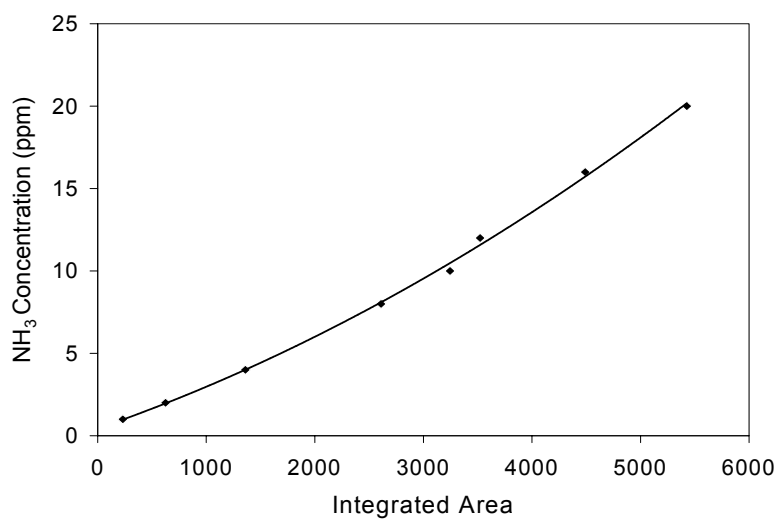


**Figure A-2** NH<sub>3</sub> Calibration Curve

**Table A-1**     $\text{NH}_3$  Calibration

ppm	Dilution Factor	Total Gas	Channel 4 % opening (Dilution air)	Channel 2 % opening ( $\text{NH}_3$ )
1*	1000	30	83.33	12
2*	500	30	83.33	24
3	333.3	30	83.33	36
4*	250	30	83.33	48
5	200	30	83.33	60
6	166.7	30	83.33	72
7	142.9	30	83.33	84
8*	125	20	50.00	64
9	111.1	20	50.00	72
10*	100	20	50.00	80
11	90.9	10	16.67	44
12*	83.3	10	16.67	48
13	76.9	10	16.67	52
14	71.4	10	16.67	56
15	66.7	10	16.67	60
16*	62.5	10	16.67	64
17	58.8	10	16.67	68
18	55.6	10	16.67	72
19	52.6	10	16.67	76
20*	50	10	16.67	80

\* indicate regularly calibrated concentrations

- Use this calibration equation to convert raw data (integrated area vs. time) into concentration versus time.

## **A.2    Experimental Procedures and Data Acquisition**

### **A.2.1    Solution Preparation**

- Prepare MEA solutions gravimetrically

- Load MEA solutions to desired loading by sparging pure CO<sub>2</sub> into the MEA solution in the reactor
- To reach a loading of 0.4, first sparge CO<sub>2</sub> for 35 minutes and check loading with CO<sub>2</sub> IR analyzer, then blend with unloaded MEA solution of the same molality
- Pour 500 ml prepared solution into a volumetric flask. This solution can be kept overnight without significant CO<sub>2</sub> desorption

### **A.2.2 Data Acquisition**

- Fill reactor with 300 ml of water
- Heat waterbath to 60 °C
- Fill condenser ice bath with ice water and turn on pump to fill condenser
- Do not allow the condenser temperature to rise above 13 °C; otherwise, either add more ice to the bath or increase the speed of the pump
- Flow air into the reactor and acquire background
- Start run and acquire data for 10 minutes to make sure there is no NH<sub>3</sub> present
- Halt run and acquire another background
- Dispose water and fill reactor with the appropriately prepared MEA solution
- Flow oxidation gas (air, air with 2% CO<sub>2</sub>, or N<sub>2</sub>) into the reactor and set valve to direct the flow dilution air to mix with the gas exiting the reactor

- Start run to acquire experimental data. A typical spectrum is shown on Figure 3.6.
- Zoom into the spectrum using "A" key and left or right arrow keys to 1200 to 900  $\text{cm}^{-1}$  region to view the  $\text{NH}_3$  peaks. Adjust the y-coordinate accordingly to view the height of the peak
- Wait 90 minutes for the first steady state with MEA and no additions. Subsequent steady states with each injection of a new chemical/concentration would take 90 to 120 minutes to reach.
- Inject chemical solutions using a plastic syringe with a 6" needle through the injection port. See Figure 3.4.
- F5 to halt the run
- Proceed to contour section both the peak (978-955  $\text{cm}^{-1}$ ) and the baseline (955-954  $\text{cm}^{-1}$ ) for  $\text{NH}_3$ , and acquire a difference file in Spectrum for Windows to enter into a spreadsheet program
- Calculate a rate in mM/hr of  $\text{NH}_3$  production for a given peak area:  
For a calibration equation of the form:  $Ax^2 + Bx + C$ ,  

$$\text{Rate(mM/hr)} = \frac{(As^2 + Bs + C) \times \text{dilution fact} \times \text{gas rate}}{\text{mL solution}}$$
- Check pH of the MEA using the pH meter
  - Let the solution to reach room temperature before measuring pH
  - Press *Calibrate* button to calibrate the pH meter with standard buffer solutions of pH 7, 4 and 10
  - Press *Measure* button to measure pH of solution

### A.2.3 Shut-Down Procedures

- Cut the gas flow into the reactor and the dilution gas

- Turn off waterbath pump, condenser pump, and stir plate
- Clean reactor and condenser with water
- Rinse the exit line with some acetone to rid any condensation/adsorption that might have occurred
- Dispose MEA solution in the appropriate amine waste container
- Turn off the main power switch for FT-IR

## **Appendix B**

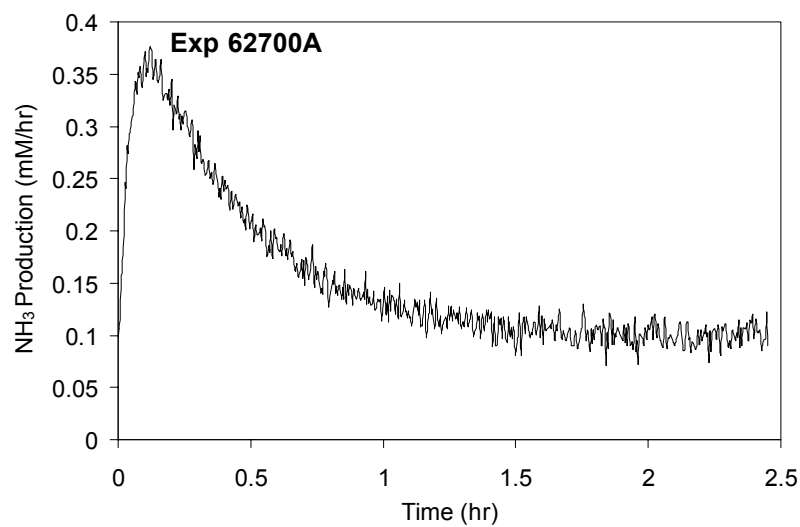
### **Experimental Data**

This appendix provides an archive of experimental data collected. Some of this data is presented as highlights in previous text, but the detailed data are contained here. The data are presented here without discussion, and they are organized chronologically. Each experiment is represented by a graph of  $\text{NH}_3$  production versus time. Graphs will illustrate the points of chemical injection. Integrations are performed to yield the total  $\text{NH}_3$  produced from a chemical injection. A table summarizing the details of the incremental additions of chemicals for each experiment is provided. Tabular data consisting of ten to twelve useful rates are also provided for each experiment.

All of these experiments were performed at 55°C with 5L/min of air or nitrogen sparged into 500 ml of MEA solution.

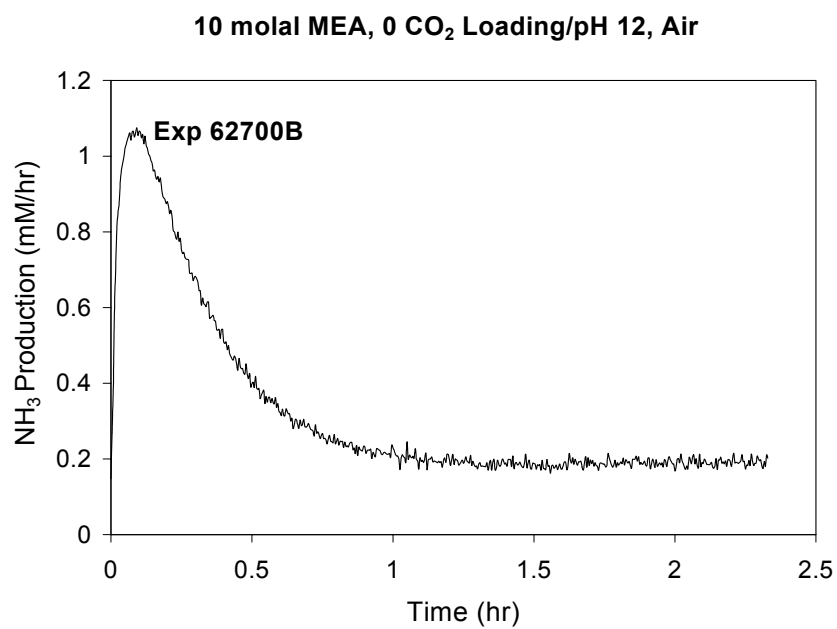


**2.5 molal MEA, 0 CO<sub>2</sub> Loading/pH 12, Air**



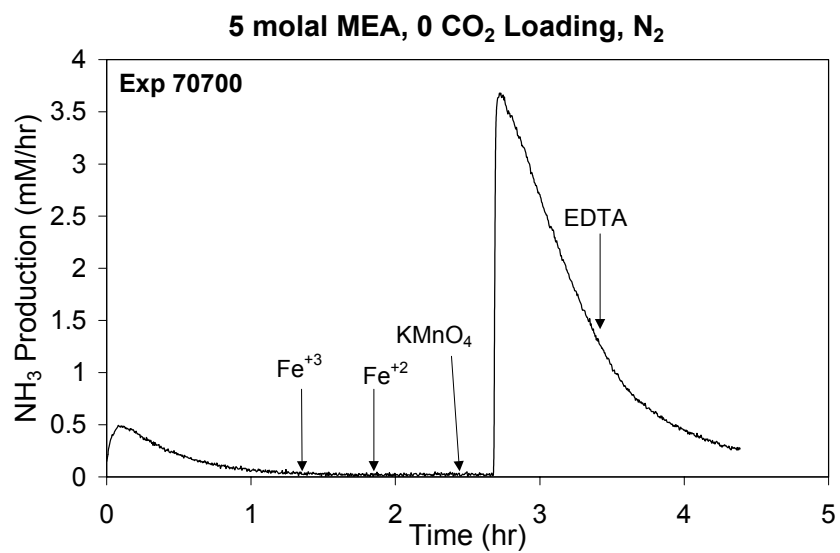
Time (hr)	NH <sub>3</sub> Production (mM/hr)
0.13	0.372
0.25	0.312
0.50	0.209
0.75	0.154
1.00	0.138
1.25	0.114
1.83	0.114
2.04	0.111
2.29	0.111
2.42	0.111

**Figure B-1** Experiment 62700A



Time (hr)	NH <sub>3</sub> Production (mM/hr)
0.10	1.053
0.25	0.754
0.50	0.399
0.75	0.267
1.00	0.229
1.32	0.180
1.70	0.182
2.00	0.180
2.26	0.183
2.32	0.181

**Figure B-2** Experiment 62700B

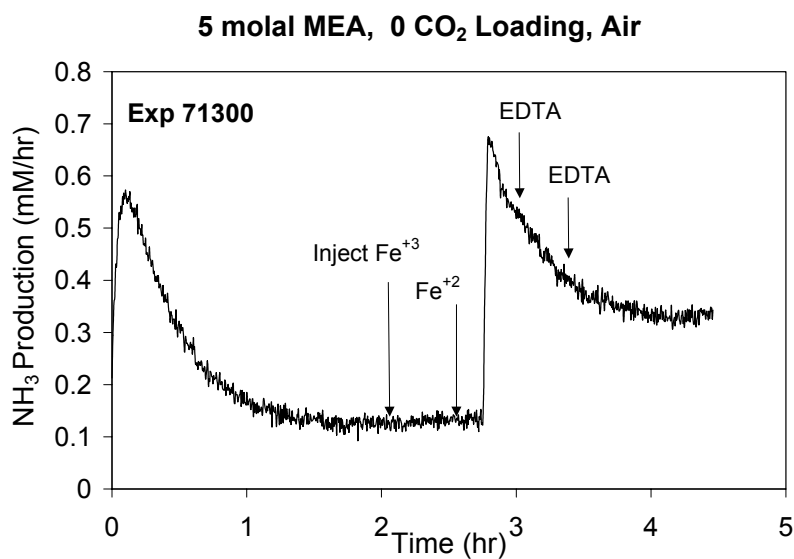


Reagent	Injected Conc. (mM)	Injection Time (hr)
FeCl <sub>3</sub>	1	1.50
FeSO <sub>4</sub>	1	2.00
KMnO <sub>4</sub>	2	2.67
EDTA	10	3.58

[KMnO <sub>4</sub> ] <sub>Injected</sub> (mM)	Mole NH <sub>3</sub> / Mole KMnO <sub>4</sub> injected
2	0.97

Time (hr)	NH <sub>3</sub> Production (mM/hr)
0.13	0.470
0.48	0.228
1.52	0.008
2.03	0.003
2.68	0.007
2.75	3.644
3.15	2.120
3.55	0.944
3.92	0.492
4.39	0.267

**Figure B-3** Experiment 70700

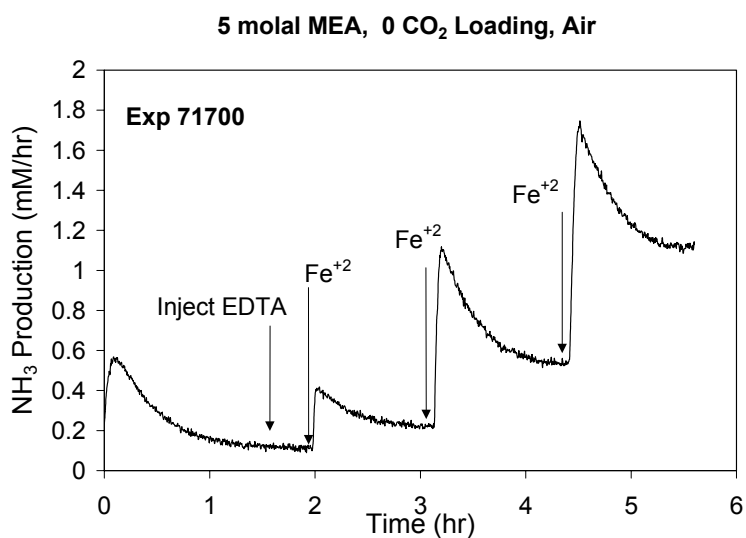


Reagent	Injected Conc. (mM)	Injection Time (hr)
FeCl <sub>3</sub>	1	2.25
FeSO <sub>4</sub>	1	2.75
EDTA	3	2.92
EDTA	3	3.33

[FeSO <sub>4</sub> ] <sub>Injected</sub> (mM)	Mole NH <sub>3</sub> / Mole FeSO <sub>4</sub> injected
1	0.124

Time (hr)	NH <sub>3</sub> Production (mM/hr)
0.13	0.569
0.50	0.321
1.29	0.133
2.00	0.132
2.75	0.139
2.82	0.665
3.08	0.504
3.43	0.402
4.02	0.338
4.46	0.343

**Figure B-4** Experiment 71300

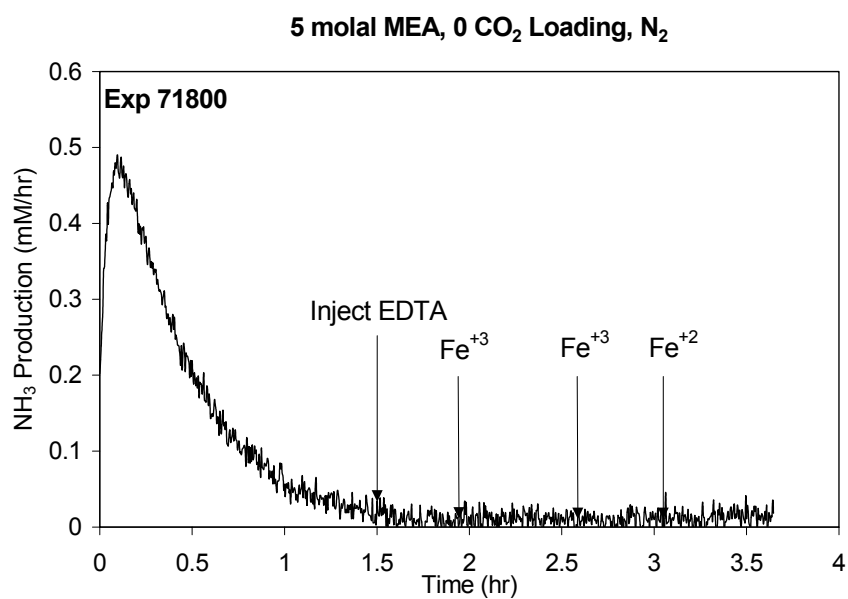


Reagent	Injected Conc. (mM)	Injection Time (hr)
EDTA	5	1.67
FeSO <sub>4</sub>	0.2	2.00
FeSO <sub>4</sub>	1	3.13
FeSO <sub>4</sub>	2	4.42

[FeSO <sub>4</sub> ] <sub>Injected</sub> (mM)	Mole NH <sub>3</sub> / Mole FeSO <sub>4</sub> injected
0.2	0.325643655
1	0.197042508
2	0.098779483

Time (hr)	NH <sub>3</sub> Production (mM/hr)
0.11	0.561
0.58	0.271
1.96	0.116
2.06	0.396
2.50	0.266
3.13	0.217
3.22	1.100
3.66	0.695
4.42	0.556
4.53	1.704
5.95	1.272
5.60	1.129

**Figure B-5** Experiment 71700

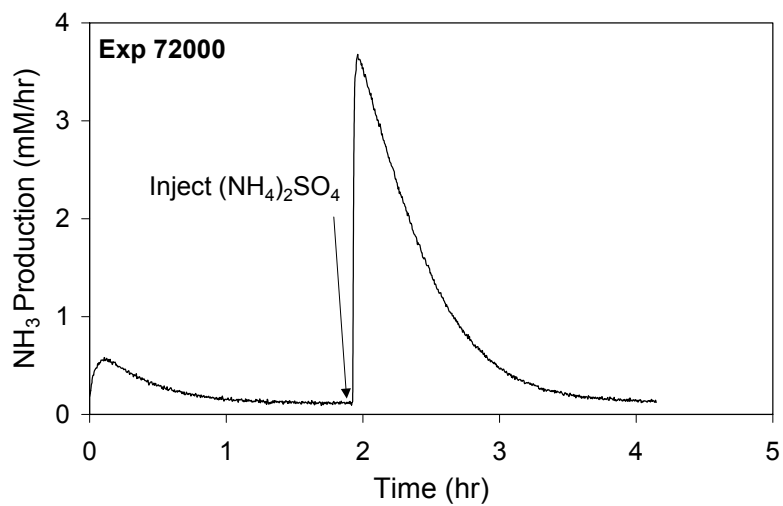


Reagent	Injected Conc. (mM)	Injection Time (hr)
EDTA	5	1.58
FeCl <sub>3</sub>	1	2.00
FeCl <sub>3</sub>	3	2.67
FeSO <sub>4</sub>	1	3.17

Time (hr)	NH <sub>3</sub> Production (mM/hr)
0.12	0.487
0.50	0.219
1.00	0.056
1.50	0.034
1.77	0.006
2.03	0.004
2.50	0.003
3.06	0.004
3.52	0.005
3.63	0.007

**Figure B-6** Experiment 71800

**5 molal MEA, 0 CO<sub>2</sub> Loading, Air**



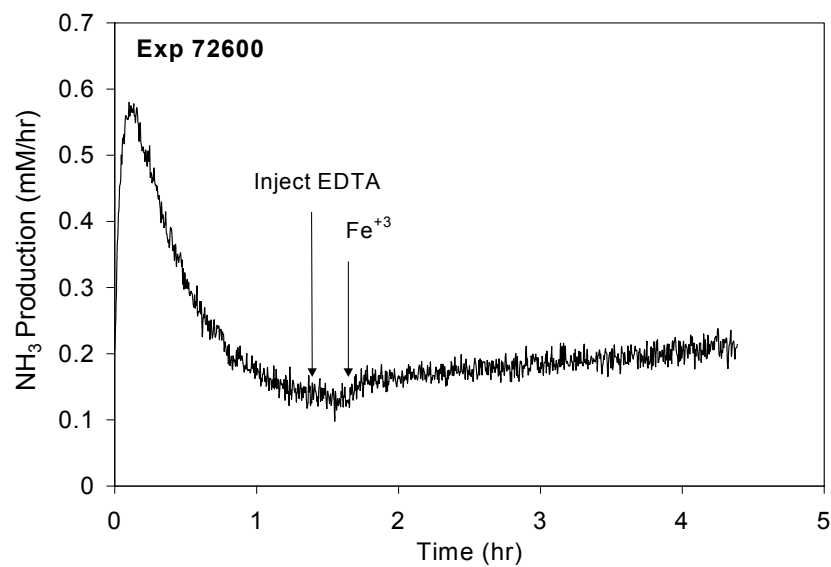
Reagent	Injected Conc. (mM)	Injection Time (hr)
(NH <sub>4</sub> ) <sub>2</sub> SO <sub>4</sub>	1	1.95

[(NH <sub>4</sub> ) <sub>2</sub> SO <sub>4</sub> ] Injected (mM)	Mole NH <sub>3</sub> / Mole (NH <sub>4</sub> ) <sub>2</sub> SO <sub>4</sub> injected
1	1.87

Time (hr)	NH <sub>3</sub> Production (mM/hr)
0.13	0.552
0.50	0.342
1.00	0.195
1.95	0.112
1.99	3.623
2.50	1.420
3.00	0.464
3.50	0.194
4.15	0.090

**Figure B-7** Experiment 72000

**5 molal MEA, 0 CO<sub>2</sub> Loading, Air**



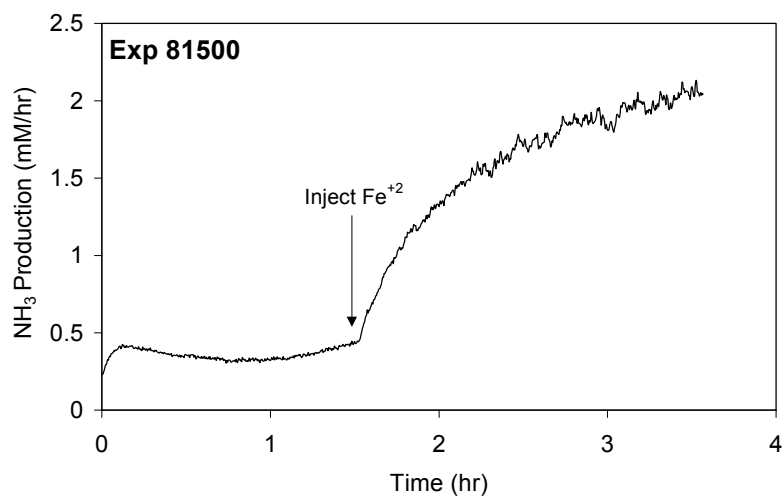
Reagent	Injected Conc. (mM)	Injection Time (hr)
EDTA	5	1.50
FeCl <sub>3</sub>	1	1.67

Time (hr)	NH <sub>3</sub> Production (mM/hr)
0.15	0.413
0.50	0.357
1.00	0.321
1.53	0.455
1.73	0.946
2.00	1.317
2.50	1.704
3.00	1.810
3.25	1.938
3.57	2.042

**Figure B-8** Experiment 72600



7 molal MEA, 0.4 CO<sub>2</sub> Loading, pH<sub>(25°C)</sub> 9.85, Air

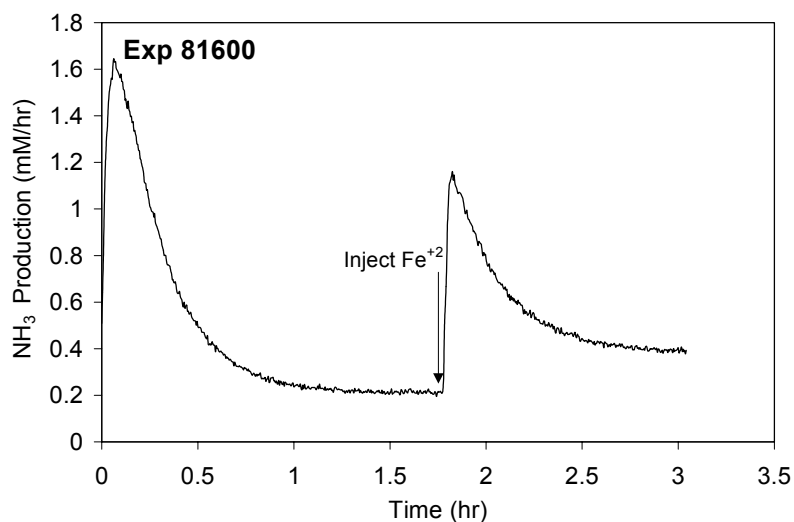


Reagent	Injected Conc. (mM)	Injection Time (hr)
FeSO <sub>4</sub>	1	1.53

Time (hr)	NH <sub>3</sub> Production (mM/hr)
0.08	1.605
0.28	0.980
0.50	0.495
1.00	0.236
1.78	0.219
1.83	1.146
2.06	0.693
2.65	0.421
2.81	0.395
3.04	0.393

**Figure B-9** Experiment 81500

12 molal MEA, 0 CO<sub>2</sub> Loading, Air



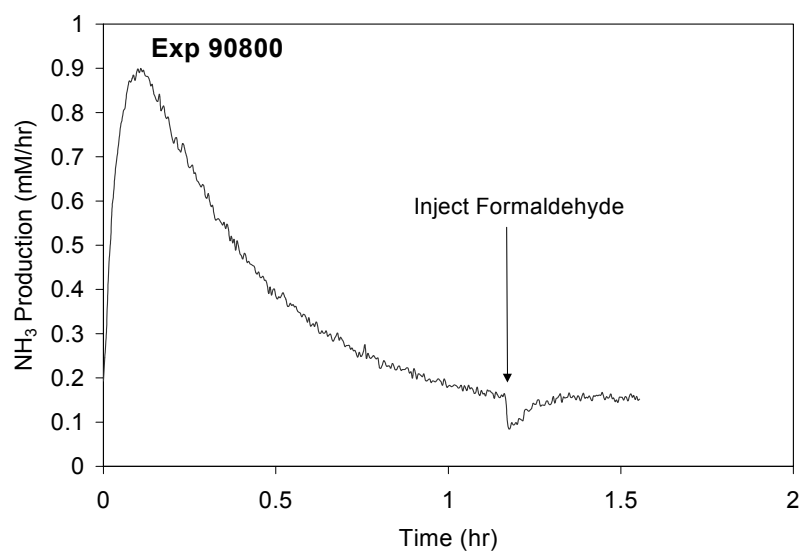
Reagent	Injected Conc. (mM)	Injection Time (hr)
FeSO <sub>4</sub>	1	1.78

[FeSO <sub>4</sub> ] <sub>Injected</sub> (mM)	Mole NH <sub>3</sub> /Mole FeSO <sub>4</sub> injected
1	0.213821717

Time (hr)	NH <sub>3</sub> Production (mM/hr)
0.15	0.572
0.50	0.312
1.00	0.168
1.67	0.139
1.83	0.168
2.10	0.164
2.50	0.182
3.00	0.196
3.50	0.190
4.39	0.214

**Figure B-10** Experiment 81600

**7 molal MEA, Air, 0 CO<sub>2</sub> Loading**

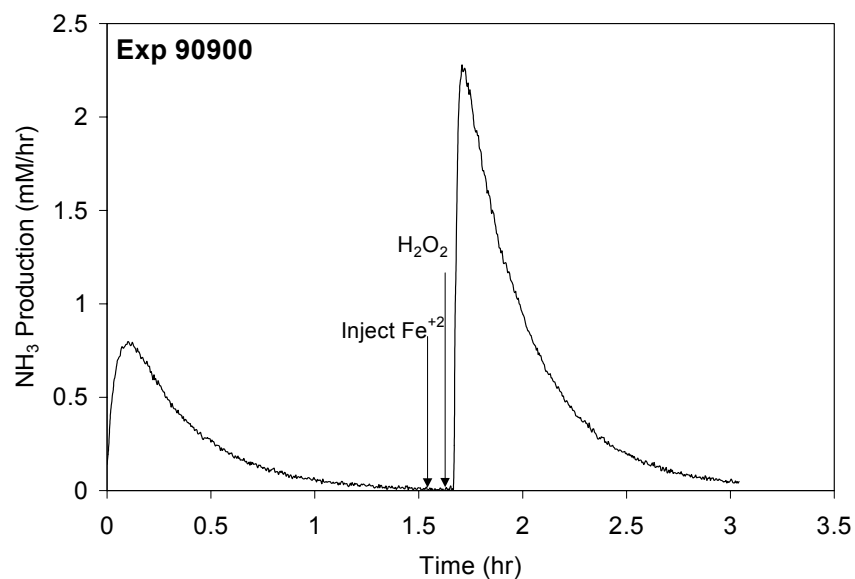


Reagent	Injected Conc. (mM)	Injection Time (hr)
Formaldehyde	2	1.17

Time (hr)	NH <sub>3</sub> Production (mM/hr)
0.12	0.884
0.25	0.675
0.50	0.385
0.75	0.251
1.00	0.181
1.17	0.148
1.18	0.085
1.27	0.138
1.40	0.157
1.55	0.152

**Figure B-11** Experiment 90800

**7 molal MEA, N<sub>2</sub>, 0 CO<sub>2</sub> Loading**



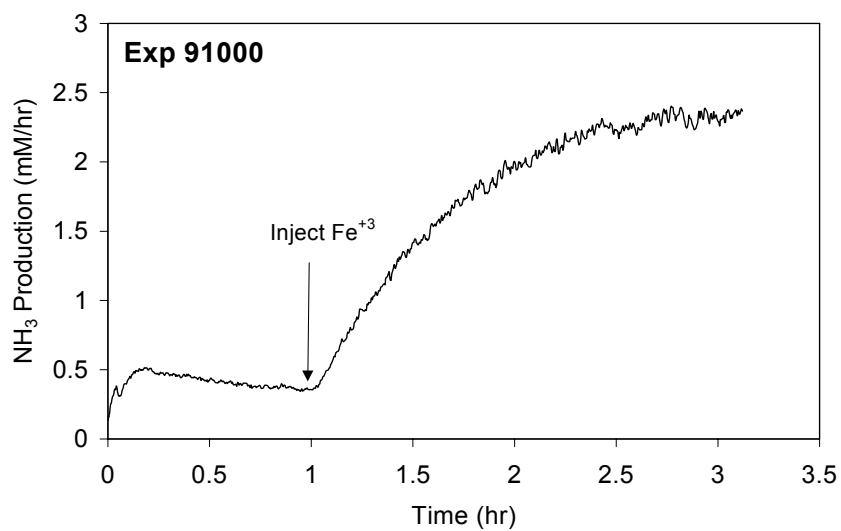
Reagent	Injected Conc. (mM)	Injection Time (hr)
FeSO <sub>4</sub>	1	1.58
H <sub>2</sub> O <sub>2</sub>	1	1.67

[H <sub>2</sub> O <sub>2</sub> ] <sub>Injected</sub> (mM)	Mole NH <sub>3</sub> / Mole H <sub>2</sub> O <sub>2</sub> injected
1	1.0

Time (hr)	NH <sub>3</sub> Production (mM/hr)
0.14	0.756
0.50	0.260
1.00	0.060
1.53	0.006
1.63	0.001
1.73	2.247
2.00	0.946
2.50	0.200
2.75	0.098
3.04	0.050

**Figure B-12** Experiment 90900

**7 molal MEA, 0.4 CO<sub>2</sub> Loading, pH<sub>(25°C)</sub> 9.96, Air**

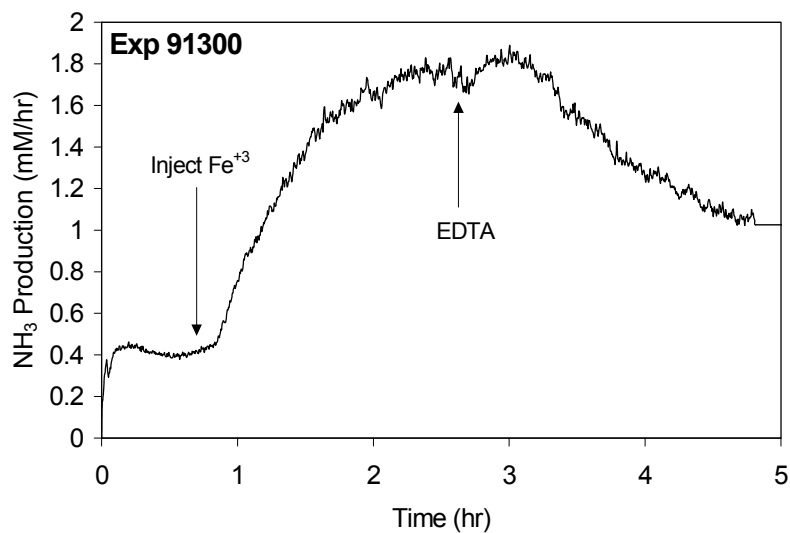


Reagent	Injected Conc. (mM)	Injection Time (hr)
FeCl <sub>3</sub>	1	1.00

Time (hr)	NH <sub>3</sub> Production (mM/hr)
0.16	0.493
0.50	0.422
1.00	0.354
1.25	0.934
1.50	1.419
1.75	1.739
2.00	2.003
2.25	2.209
2.50	2.232
3.12	2.367

**Figure B-13** Experiment 91000

7 molal MEA, 0.4 CO<sub>2</sub> Loading, pH<sub>(25°C)</sub> 9.93, Air

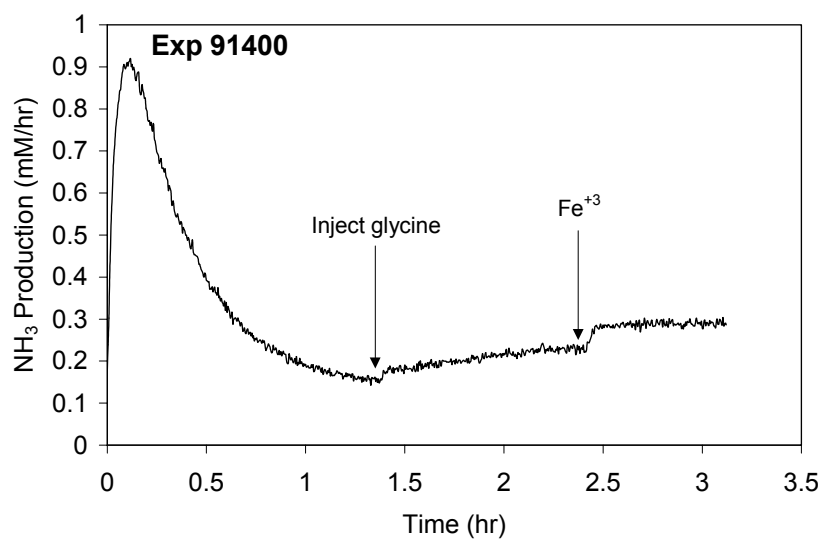


Reagent	Injected Conc. (mM)	Injection Time (hr)
FeCl <sub>3</sub>	0.2	0.83
EDTA	4.45	2.67

Time (hr)	NH <sub>3</sub> Production (mM/hr)
0.22	0.431
0.66	0.402
1.25	1.090
1.50	1.367
2.00	1.668
2.50	1.747
3.00	1.889
3.50	1.540
4.15	1.243
4.82	1.015

**Figure B-14** Experiment 91300

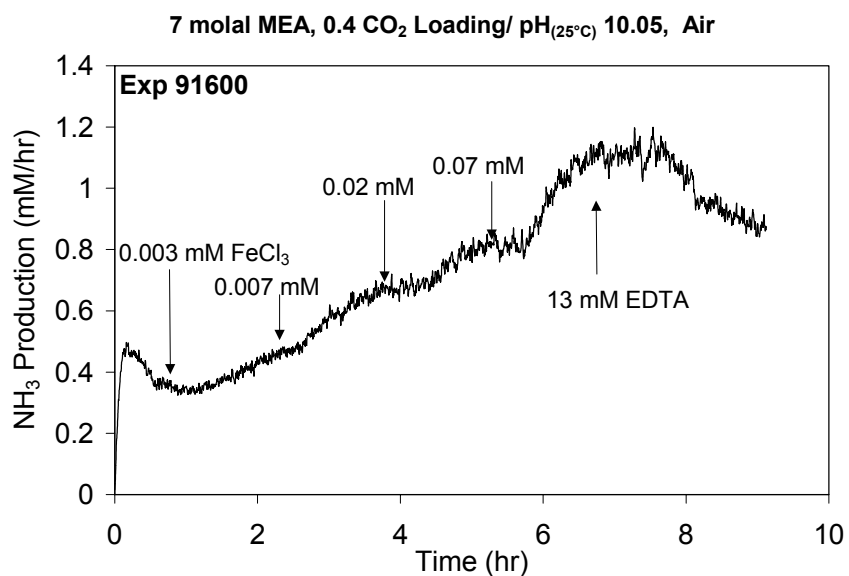
7 molal MEA, 0 CO<sub>2</sub> Loading/ pH<sub>(25°C)</sub> 11.57, Air



Reagent	Injected Conc. (mM)	Injection Time (hr)
glycine	75	1.383
FeCl <sub>3</sub>	1	2.416

Time (hr)	NH <sub>3</sub> Production (mM/hr)
0.11	0.914
0.50	0.393
1.00	0.192
1.39	0.162
1.43	0.183
2.00	0.218
2.42	0.226
2.48	0.282
2.75	0.203
3.12	0.287

**Figure B-15** Experiment 91400



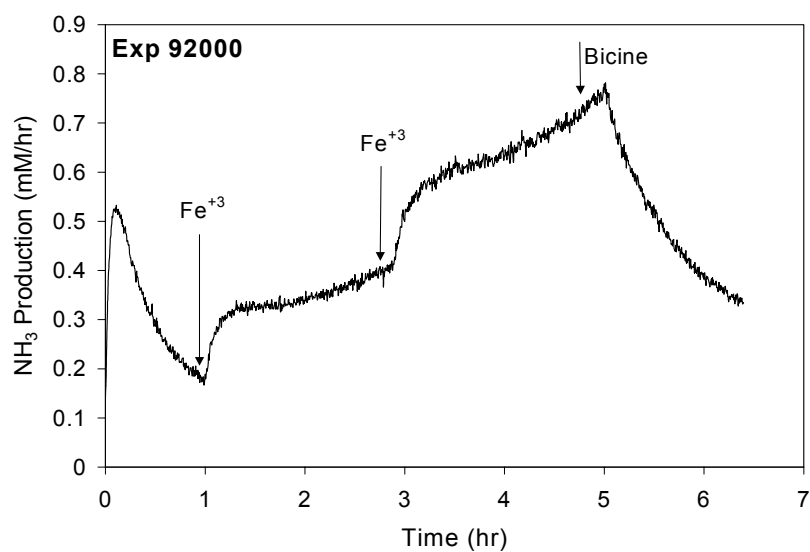
Reagent	Injected Conc. (mM)	Injection Time (hr)
FeCl <sub>3</sub>	0.003	1.00
FeCl <sub>3</sub>	0.007	2.67
FeCl <sub>3</sub>	0.02	4.33
FeCl <sub>3</sub>	0.07	5.83
EDTA	13	7.33

Time (hr)	NH <sub>3</sub> Production (mM/hr)
0.29	0.466
1.23	0.354
1.90	0.425
2.65	0.493
3.43	0.627
4.51	0.692
5.00	0.782
5.75	0.798
6.39	1.019
7.36	1.150
8.23	0.969
9.12	0.865

**Figure B-16** Experiment 91600



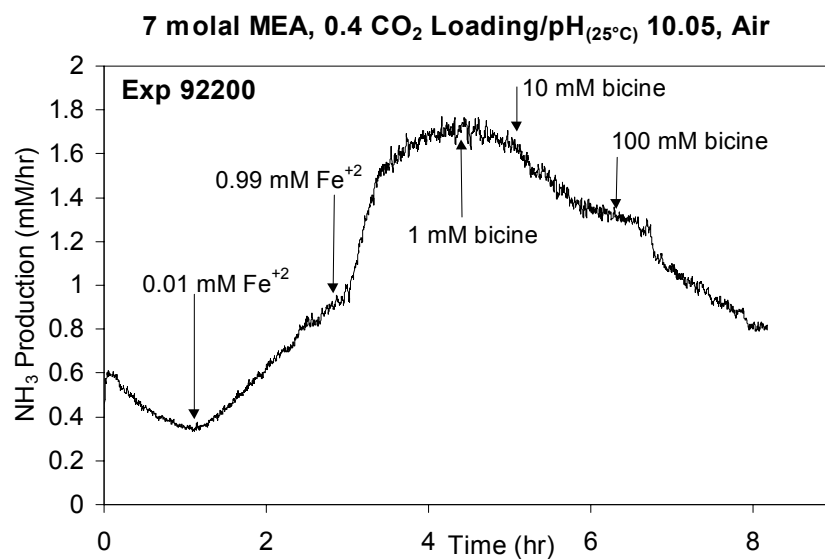
7 molal MEA, 0 CO<sub>2</sub> Loading/pH<sub>25</sub> c 10.27, Air



Reagent	Injected Conc. (mM)	Injection Time (hr)
FeCl <sub>3</sub>	0.1	1.00
FeCl <sub>3</sub>	0.9	2.85
Bicine	86	5.167

Time (hr)	NH <sub>3</sub> Production (mM/hr)
0.14	0.519
1.00	0.183
1.32	0.321
2.05	0.347
2.89	0.412
3.22	0.565
4.00	0.633
5.02	0.768
5.50	0.527
6.40	0.334

**Figure B-17** Experiment 92000

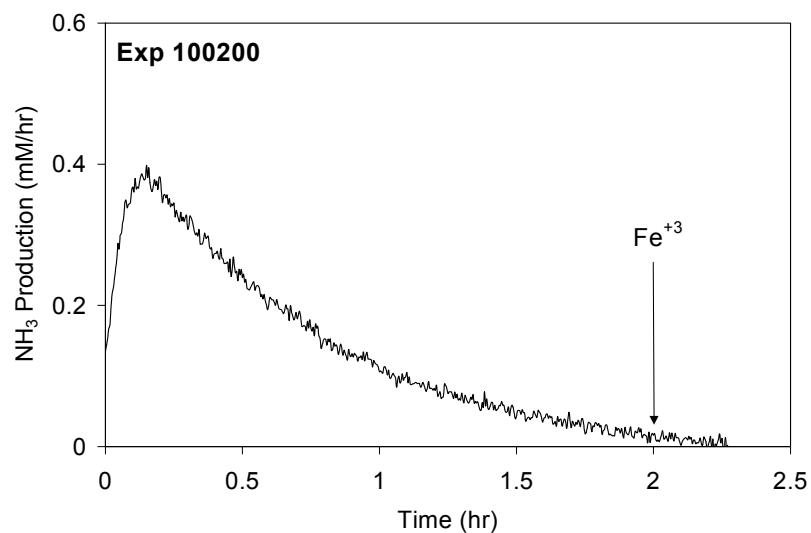


Reagent	Injected Conc. (mM)	Injection Time (hr)
FeSO <sub>4</sub>	0.01	1.3
FeSO <sub>4</sub>	0.99	3.025
Bicine	1	4.75
Bicine	9	5.167
Bicine	90	6.67

Time (hr)	NH <sub>3</sub> Production (mM/hr)
0.11	0.608
1.20	0.362
2.17	0.668
3.00	1.002
3.27	1.339
4.45	1.723
5.13	1.640
6.61	1.256
7.42	0.979
8.18	0.795

**Figure B-18** Experiment 92200

7 molal MEA, 0.4 CO<sub>2</sub> Loading/ pH<sub>(25°C)</sub> 9.96, N<sub>2</sub>

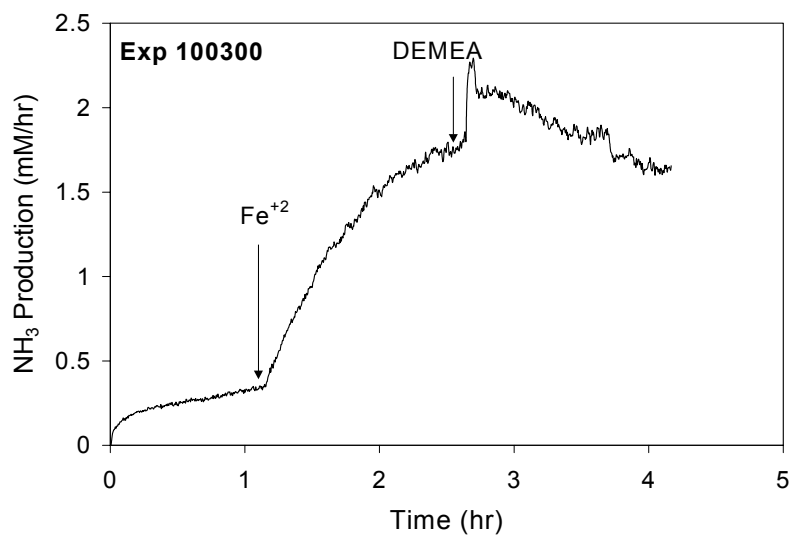


Reagent	Injected Conc. (mM)	Injection Time (hr)
FeCl <sub>3</sub>	1	2.00

Time (hr)	NH <sub>3</sub> Production (mM/hr)
0.16	0.395
0.25	0.345
0.50	0.239
0.75	0.167
1.00	0.106
1.25	0.075
1.50	0.043
1.75	0.018
2.00	0.016
2.27	0.002

**Figure B-19** Experiment 100200

7 molal MEA, 0.4 CO<sub>2</sub> Loading/pH<sub>(25°C)</sub> 10, Air



Reagent	Injected Conc. (mM)	Injection Time (hr)
FeSO <sub>4</sub>	1	1.167
DEMEA	100	2.6

Time (hr)	NH <sub>3</sub> Production (mM/hr)
0.14	0.175
0.53	0.253
1.16	0.362
1.50	0.971
2.00	1.496
2.61	1.760
2.70	2.279
3.20	1.948
3.78	1.719
4.17	1.656

**Figure B-20** Experiment 100300

## References Cited

Anbar, M., Neta, P., "A Compilation of Specific Biomolecular Rate Constants for the Reactions of Hydrated Electrons, Hydrogen Atoms and Hydroxyl Radicals with Inorganic and Organic Compounds in Aqueous Solutions," *Int. J. App. Rad. Isotopes*, **1967**, 18, 439-523,

Asmus, K.D., Bonifacic, M., "Radical Reaction Rates in Liquids: Carbon-Centered Radicals," *Landolt-Bornstein* Vol 13b, Springer-Verlag Berlin, 1984.

Audeh, C.A., Lindsay Smith, J.R., "Amine Oxidation. Part II. The Oxidation of Some Trialkylamines with Alkaline Potassium Hexacyanoferrate (III)," *J. Chem. Soc. (B)*, **1970**, 1280-1285.

Bacon, T.R., Dupart, M.S., Rooney, P.C., "Oxygen's Role in Alkanolamine Degradation," *Hydrocarbon Processing*, July **1998**, 109-113.

Blachly, C.H. and Raver, H., " Stabilization of Monoethanolamine Solutions in Carbon Dioxide Scrubbers," U.S. Naval Research Laboratory, Rept. 6189 (December 1964)

Blachly, C.H. and Raver, H., "Stabilization of Monoethanolamine Solutions in Carbon Dioxide Scrubbers," *J. Chem. Eng. Data*, **1966**, Vol 11, No. 3, 401-403.

Brown, E.R., Mazzarella, J.D., "Mechanism of Oxidation of Ferrous Polydentate Complexes by Dioxygen," *J. Electroanal. Chem.*, **1987**, 222, 173-192.

Chisholm, P.N., "Dry Absorption of Hydrogen Chloride and Sulfur Dioxide by Calcium-Based Sorbents from Humidified Flue Gas," Ph.D. Dissertation, Department of Chemical Engineering, University of Texas at Austin, 1999.

Christensen, J.J., Izatt, R.M., Wrathall, D.P., Hansen, L.D., "Thermodynamics of Proton Ionization in Dilute Aqueous Solutions. Part XI.  $pK$ ,  $\Delta H^\circ$ , and  $\Delta S^\circ$  Values for Proton Ionization from Protonated Amines at 25°," *J. Chem. Soc (A)*, **1969**, 1212-1223.

Cringel, D.C., Pearce, R.L., Dupart M.S., "Method for Maintaining Effective Corrosion Inhibitors in Gas Scrubbing Plant," U.S. Pat. 4,690,740, 1987.

Denisov, E.T., Mitskevich, N.I., Agabekov, V.E., "Liquid-Phase Oxidation of Oxygen-Containing Compounds," Consultant Bureau, New York, 1977.

Dennis, W.H., Hull, L.A., Rosenblatt, D.H., "Oxidation of Amines, IV. Oxidative Degradation," *J. Org. Chem.*, **1967**, 32, 3783-3787.

Ferris, J.P., Gerwe, R.D., Gapski, G.R., "Detoxication Mechanisms II. The Iron-Catalyzed Dealkylation of Tertiary Amine Oxide," *J. Am. Chem. Soc.*, **1967**, 89, 5370-5375.

Ferris, J.P., Gerwe, R.D., Gapski, G.R., "Detoxication Mechanisms III. The Scope and Mechanism of the Iron-Catalyzed Dealkylation of Tertiary Amine Oxide," *J. Org. Chem.*, **1968**, 33, 3493-3498.

Hall, W.D., Barron, J.G., "Solving Gas Treating Problems - A Different Approach," Presented at the Laurance Reid Gas Conditioning Conference, Norman, OK 1981.

Howard, J.A., Scaiano, J.C., "Radical Reaction Rates in Liquids: Oxy-, Peroxy- and Related Radicals, *Landolt-Bornstein* Vol 13d, Springer-Verlag Berlin, 1984.

Hull, L.A., Davis, G.T., Rosenblatt, D.H., "Oxidation of Amines. VII. Chemical and Electrochemical Correlations," *J. Phys. Chem.*, **1969**, 73, 2142-2146.

Hull, L.A., Giordano, W.P., Rosenblatt, D.H., Davis, G.T., Mann, C.K., Milliken, S.B., "Oxidation of Amines. VIII. Role of the Cation Radical in the Oxidation of Triethylenediamine by Chlorine Dioxide and Hypochlorous Acid," *J. Phys. Chem.*, **1969b**, 73, 2147-2152.

Hull, L.A., Davis, G.T., Rosenblatt, D.H., "Oxidation of Amines. IX. Correlation of Rate Constants for Reversible One-Electron Transfer in Amine Oxidation with Reactant Potentials," *J. Am. Chem. Soc.*, **1969c**, 91, 6247-6250.

Kindrick, R.C., Atwood, K., Arnold, M.R., "The Relative Resistance to Oxidation of Commercially Available Amines," Girdler Report No. T2.15-1-30, in "Report: Carbon Dioxide Absorbents," Contract No. NObs-50023, by Girdler Corp., Gas Processes Division, Louisville, KY, for The Navy Department, Bureau of Ships, Washington 25, DC (Code 649P), June 1, 1950a.

Kindrick, R.C., Reitmweier, R.E., Arnold, M.R., "A Prolonged Oxidation Test on Amine Solutions Resistant to Oxidation," Girdler Report No. T2.15-1-31, in

"Report: Carbon Dioxide Absorbents," Contract No. NObs-50023, by Girdler Corp., Gas Processes Division, Louisville, KY, for The Navy Department, Bureau of Ships, Washington 25, DC (Code 649P), May 25, 1950b.

Lee, Y.J., Rochelle, G.T., "Oxidative Degradation of Organic Additives for Flue Gas Desulfurization: Products, Kinetics, and Mechanisms," *Env. Sci. Tech.*, **1987**, 21, 266-272.

Lindsay Smith, J.R., Mead, L.A.V., "Amine Oxidation. Part VII. The Effect of Structure on the Reactivity of Alkyl Tertiary Amines towards Alkaline Potassium Hexacyanoferrate(III)," *J. Chem. Soc. Perkin II*, **1973**, 206-210.

Lindsay Smith, J.R., Mead, L.A.V., "Amine Oxidation. Part IX. Oxidation of Some Substituted Tertiary Alkylamines and Some N,N-dimethylphenethylamine with Potassium Hexacyanoferrate(III)," *J. Chem. Soc. Perkin II*, **1976**, 1172-1176.

Neta, P., Huie, R.E., Ross, A.B., "Rate Constants for Reactions of Inorganic Radicals in Aqueous Solutions," *J. Phys. Chem. Ref. Data.*, **1988**, 17, No. 3, 1027.

Pearce, R.L., Process for Removal of Carbon Dioxide from Industrial Gases, U.S. Pat. 4,440,731, 1984.

Pearce, R.L., Wolcott, R.A., Pauley, C.R., Process for the Recovery of CO<sub>2</sub> from Flue Gases, U.S. Pat. 4,477,419, 1984.

Rosenblatt, D.H., Hayes, A.J., Harrison, B.L., Streaty, R.A., Moore, K.A., "Oxidation of Amines. I. The Reaction of Chlorine Dioxide with Triethylamine in Aqueous Solutions," *J. Org. Chem.*, **1963**, 28, 2790-2794.

Rosenblatt, D.H., Hull, L.A., De Luca, D.C., Davis, G.T., Weglein, R.C., Williams, H.K.R., "Oxidation of Amines. II. Substituent Effects in Chlorine Dioxide Oxidation," *J. Am. Chem. Soc.*, **1967**, 89, 1158-1163.

Rosenblatt, D.H., Davis, G.T., Hull, L.A., Forber, G.D., "Oxidation of Amines. V. Duality of Mechanism in the Reactions of Aliphatic Amines with Permanganate," *J. Org. Chem.*, **1968**, 33, 1649-1650.

Russel, G.A. Peroxide Pathways to Autooxidation, p. 107-128 in *Peroxide Reaction Mechanism* ed. by J.O. Edwards, Interscience Publishers, New York, 1960.

Sajus, L., Seree De Roch, I. The Liquid Phase Oxidation of Aldehydes, p. 89-124 in *Comprehensive Chemical Kinetics, Vol 16, Liquid-Phase Oxidation*, Elsevier Scientific Publishing Co., Amsterdam, 1980.

Singh, V.N., Gangwar, M.C., Saxena, B.B.L., Singh, M.P., "Kinetics and Mechanism fo the Oxidation of Formaldehyde by Hexacyanoferrate (III) Ion," *Can. J. Chem.*, **1969**, 47, 1051-1056.

Stumm, W., Lee, G.F., "Oxygenation of Ferrous Iron," *Ind. Eng. Chem.*, **1961**, 53, 143-146.

Tamura, H., Goto, K., Nagayama, M., "Effect of Anions on the Oxygenation of Ferrous Iron in Neutral Solution," *Inorg. Nucl. Chem.*, **1976**, 38 113-117.

Ulrich, R.K., "Sulfite Oxidation under Flue Gas Desulfurization Conditions: Enhanced Oxygen Absorption Catalyzed by Transition Metals," Ph.D. Dissertation, The University of Texas at Austin, 1983.

Wolcott, R.A., Pearce, R.L., Pauley, C.R., "Process for the Recovery of CO<sub>2</sub> from Flue Gases, U.S. Pat. 4,624,839, 1986.



## **Vita**

Susan Chi was born on November 28, 1977 in Shanghai, China, the only child of Eric Chi and Sue Wang. She graduated from The Texas Academy of Mathematics and Science, a gifted program for high school students, in 1996 before attending The University of Texas at Austin. She graduated with Highest Honors with a B.S. in Biochemistry in 1998. Shortly after graduation, she was admitted on a full-fledged scholarship to Chemical Engineering graduate school at The University of Texas at Austin. Upon completion of her M.S. degree, she will begin her new job as a process engineer at MEMC Southwest in Sherman, Texas.

Permanent Address: 3111 Parker Lane #357  
Austin, TX 78741

This thesis was typed by the author.

